

DESIGN AND TESTING OF A MECHANICAL STRAIN EXTENSOMETER

by

Ahmet Fercan

B.S., Mechanical Engineering, Istanbul Technical University, 2003

Submitted to the Institute for Graduate Studies in
Science and Engineering in partial fulfillment of
the requirements for the degree of
Master of Science

Graduate Program in Mechanical Engineering

Boğaziçi University

2006

ACKNOWLEDGEMENTS

I would like to thank my advisor, Vahan Kalenderođlu, for his interest and technical support that made this thesis possible, and for his patience in correcting my scientific errors.

I would also like to thank İbrahim Mutlu for his skillful machining applications and advices in the university workshop.

Financial support from Genel Sistem Dizayn Inc. for purchase of the electronic devices of the extensometer is gratefully acknowledged.

Finally I would like to thank my father, my mother and my sister for their support, encouragement and understanding along this study.

ABSTRACT

DESIGN AND TESTING OF A MECHANICAL STRAIN EXTENSOMETER

This thesis' main aim is to conduct the creation of a mechanical extensometer with its all design levels including its necessary calculations, analysis, manufacturing, electronics and testing of it.

The most similar extensometers to the aimed design were investigated in literature and the key point decisions were made about the dimensions and structure. While doing this, essential calculations about predictable error analysis were made; contact force predictions were brought to a sufficient level. The extensometer body design was the initial level in design period. Those followed by the investigation of the possible sensors that could probably feature in the displacement measurement system. Among possible sensors which were presented in the thesis, LVDT was chosen to be used. That trailed by an LVDT selection phase to make decisions about the size, clearance, weight, stroke range and predictions about its behaviors within coordinate analysis when it was mounted on the arms. While those steps were being taken, the elevator of the measurement system is designed and manufactured. Moreover, the extensometer body construction followed that with aluminum 7075. Then the arm construction considering the cooperative elements, LVDT and contact elements was made. Then this followed by design and manufacturing of the calibration unit. The whole measurement system including this unit is constructed and the electronic installations are prepared and the calibration procedure is introduced step by step.

The thesis introduces the necessary calculations in a theoretical manner, the whole design and manufacturing periods, variations until the final design in a more practical way and finally the installations of the whole electronic equipment on the measurement system.

ÖZET

MEKANİK BİR EKSTANSOMETRENİN DİZAYNI VE TESTİ

Temel amacı mekanik bir ekstansometrenin ortaya çıkarılması olan bu tez yapılan gerekli hesaplamalar, analizler, imalat, elektronik aksam ve test gibi tüm dizayn evrelerini içermektedir.

İstenen tip bir ekstansometreye en benzer örnekler literatürde araştırılmış, boyutu ve yapısı ile ilgili önemli olan noktalar karara bağlanmıştır. Tüm bunlar yapılırken öngörülen hataların analizi yapılmış, temas kuvvetinin yeterliliği incelenmiştir. Ekstansometrenin gövde dizaynı tüm dizayn evresinin ilk bölümüydü. Bu bölümün en önemli kısmı ekstansometrenin alt ve üst kollarının şekillendirilmesiydi. Bunları, sistem içinde yer değiştirme ölçümünde kullanılması muhtemel olan sensörlerin incelenmesi izledi. Tezin içeriğinde tanıtılan olası sensörler arasından LVDT seçildi ve bunun ardından ebadı boşluğu, ağırlığı, strok aralığı ve koordinat analizi ile de kollar üzerine montajı sonrası davranışı ile ilgili öngörüler göz önüne alınarak LVDT seçimi yapıldı. Bu adımlar atılırken bir yandan da ölçüm sisteminin asansör bölümü dizayn edildi ve imalatı bitirildi. Alüminyum 7075 malzemesi kullanılarak ekstansometre gövdesi konstrüksiyonu baştan aşağı yapıldı. Yan elemanlar olan LVDT ve temas elamanlarına göre kolların konstrüksiyonu bitirildi. Bunun ardından kalibrasyon ünitesi imâl edildi. Bu ünite de dahil olmak üzere tüm ölçüm sistemi bitirilip elektronik sistemin montajı yapıldı ve kalibrasyon prosedürü adım adım açıklandı.

Tez teorik olarak gerekli hesaplamaları, pratikte ise tüm dizayn ve imalat aşamalarını, son dizayn aşamasına kadar olan varyasyonları ve son olarak da tüm elektronik teçhizatın kurulumunu açıklamaktadır.

TABLE OF CONTENTS

ACKNOWLEDGEMENTS	iii
ABSTRACT	iv
ÖZET	v
LIST OF FIGURES	viii
LIST OF TABLES	xiv
LIST OF SYMBOLS/ABBREVIATIONS	xv
1. INTRODUCTION	1
2. CONTACT FORCE (PUSHING FORCE)	4
3. GAGE LENGTH	8
4. SENSORS	9
5. INITIAL DESIGN AND DESCRIPTION OF THE SYSTEM	15
6. ERROR ANALYSIS	16
6.1. Gage Length Error	16
6.2. Independent Movement of Probing Arms	18
6.3. Uneven Transducer Air Gap	20
7. LVDT SELECTION	23
8. ARM DESIGN AND COORDINATE ANALYSIS FOR LVDT ELEMENTS	27
9. FINAL DESIGN OF THE ELEVATOR	42
9.1. Upper Base Plate	42
9.2. Lower Base Plate	45
9.3. Cap Plate	47
9.4. Shafts	49
9.5. Moving Plate	51
10. FINAL DESIGN OF THE EXTENSOMETER	53
10.1. Brackets	53
10.2. Chassis	56
10.3. Base Plate	58
10.4. Supporting Rods	60
10.5. Upper Arm	62
10.6. Lower Arm	65

10.7. Special Bolt with Low Pitch67
10.8. Core Connecting Rod69
10.9. Connecting Elements71
10.10. Additional Weights72
11. FINAL DESIGN OF THE CALIBRATION UNIT75
11.1. Base Plate75
11.2. Shaft78
11.3. Micrometer Carrier80
11.4. Micrometer82
12. JOINING ELEMENTS83
13. MANUFACTURING85
14. ELECTRONIC INSTALLATION99
15. CONCLUSION106
REFERENCES108

LIST OF FIGURES

Figure 2.1.	Schematic view of the extensometer	5
Figure 4.1.	Components of a traditional LVDT	11
Figure 4.2.	Output voltage with relation to the LVDT core position	13
Figure 4.3.	Variation of magnitude of the differential AC output voltage with core position	13
Figure 4.4.	DC output from electronics	14
Figure 6.1.	A schematic diagram illustrating slanted arms	16
Figure 6.2.	Possible tip designs for probing arms	16
Figure 6.3.	A schematic diagram illustrating lever arm ratio	17
Figure 6.4.	Independent arm angles	19
Figure 6.5.	A schematic diagram demonstrating the air gap	21
Figure 7.1.	LVDT selection - candidates for nomination	25
Figure 8.1.	Sectional view of MHR050	28
Figure 8.2.	Schematic demonstration of straight-unstepped arm mode	29
Figure 8.3.	Subcases of mode 1	31
Figure 8.4.	Schematic demonstration of stepped-pivoted before the step	32

Figure 8.5.	Subcases of mode 2	33
Figure 8.6.	Schematic demonstration of stepped-pivoted after the step	35
Figure 8.7.	Subcases of mode 3	36
Figure 8.8.	Arm design 1	37
Figure 8.9.	Possible positionings of contact element on arm	37
Figure 8.10.	Gage length with this arm mode	38
Figure 8.11.	Arm design 2	38
Figure 8.12.	Arm design 3	39
Figure 8.13.	Possible design of the rear portion of the arm	39
Figure 8.14.	Demonstration of core and the target points when $d1=7$ and $d1=5$ mm for 1:1 ratio	41
Figure 9.1.	3D view of upper the base plate	43
Figure 9.2.	Orthogonal projection of the upper base plate	44
Figure 9.3.	3D view of the lower base plate	45
Figure 9.4.	Orthographic projection of the lower base plate	46
Figure 9.5.	3D view of the cap plate	47
Figure 9.6.	Orthographic projection of the cap plate	48

Figure 9.7.	3D view of the shaft	49
Figure 9.8.	Orthographic projection of one shaft	50
Figure 9.9.	3D view of the moving plate	51
Figure 9.10.	Orthographic projection of the moving plate	52
Figure 10.1.	3D view of one bracket	54
Figure 10.2.	Orthographic projection of the bracket	55
Figure 10.3.	3D view of the chassis	56
Figure 10.4.	Orthographic projection of the chassis	57
Figure 10.5.	3D view of the base plate	58
Figure 10.6.	Orthographic projection of the base plate	59
Figure 10.7.	3D view of the supporting rod	60
Figure 10.8.	Orthographic projection of the supporting rod	61
Figure 10.9.	3D view of the upper arm	63
Figure 10.10.	Orthographic projection of the upper arm	64
Figure 10.11.	3D view of the lower arm	65
Figure 10.12.	Orthographic projection of the lower arm	66
Figure 10.13.	3D view of the special bolt	67

Figure 10.14. Orthographic projection of the special bolt	68
Figure 10.15. 3D view of the core connecting rod	69
Figure 10.16. Orthographic projection of the core connecting rod	70
Figure 10.17. 3D view of the connecting elements	71
Figure 10.18. Orthographic projection of the connecting elements.	71
Figure 10.19. 3D view of additional weight of the upper arm	72
Figure 10.20. Orthographic projection of additional weight of the upper arm	73
Figure 10.21. Assembly of the main extensometer body	74
Figure 11.1. 3D view of the base plate	76
Figure 11.2. Orthographic projection of the base plate	77
Figure 11.3. 3D view of the shaft	78
Figure 11.4. Orthographic projection of the shaft	79
Figure 11.5. 3D view of micrometer carrier	80
Figure 11.6. Orthographic projection of micrometer carrier	81
Figure 11.7. A photograph of the micrometer while it is on the shaft	82
Figure 12.1. Spring Loaded Plunger (SLP)	84
Figure 13.1. The lower base plate during milling process	85

Figure 13.2.	The upper base plate during milling process for its lateral faces	86
Figure 13.3.	The lower base plate after drilling and tapping processes	86
Figure 13.4.	The distances between the threaded holes on the lower base plate	87
Figure 13.5.	The upper base plate after machining processes	88
Figure 13.6.	Shafts of the elevator	88
Figure 13.7.	Moving plate before the slots are cut	89
Figure 13.8.	Cap plate	89
Figure 13.9.	Assembly of the elevating system	90
Figure 13.10.	The brackets	91
Figure 13.11.	The supporting rods	91
Figure 13.12.	Base plate of the extensometer	92
Figure 13.13.	Chassis	92
Figure 13.14.	Upper arm of the extensometer	93
Figure 13.15.	Lower arm of the extensometer	93
Figure 13.16.	Arms tips after the contact elements are mounted	94
Figure 13.17.	Contact elements are mounted by set-screws	94
Figure 13.18.	The special bolt	95

Figure 13.19. Assembly of brackets, rods and SLPs	96
Figure 13.20. Bracket tips after the assembly	96
Figure 13.21. The finalized extensometer without LVDT	97
Figure 13.22. The calibration unit	98
Figure 14.1. LVDT of the extensometer	99
Figure 14.2. Wiring of the LVDT	100
Figure 14.3. Views and dimensions of the module	100
Figure 14.4. Signal conditioner module	101
Figure 14.5. Wiring between LVDT, signal conditioner module and power supply .	101
Figure 14.6. Switching power supply	102
Figure 14.7. A photograph of the system from behind	104
Figure 14.8. A photograph of the system from left side	105
Figure 15.1. Possible gage points of the presently designed extensometer and a probable target extensometer design	107

LIST OF TABLES

Table 2.1.	Contact force variations with the inclination angle and sectional dimensions	6
Table 2.2.	Contact force variation of the finalized extensometer with inclination angle	7
Table 6.1.	Predicted GLE values %	18
Table 6.2.	Predicted eIMPA values %	20
Table 6.3.	Predicted eUTAP values %	22
Table 8.1.	Coordinates of the core in mode 1	30
Table 8.2.	Coordinates of the target body points in mode 1	32
Table 8.3.	Coordinates of the core in mode 2	33
Table 8.4.	Coordinates of the target body points in mode 2	34
Table 8.5.	Coordinates of the core in mode 3	35
Table 8.6.	Coordinates of the target body points in mode 3	36

LIST OF SYMBOLS/ABBREVIATIONS

C	Length of the rod lowering the core
C_u, C_a	Upper and lower length of the rod
d_1	Front length of the arm
d_2	Rear length of the arm
d_{Al}	Density of aluminum
D	Real distance between the arms
D^*	Perpendicular distance between the arms
ΔD	Sensor gap change
E_1, E_2	Voltages induced in the winding 1 and 2
E_{out}	Output voltage
F_c	Contact force
G	Differential distance between the arms on the specimen side
G_o	Distance between the arms on the specimen side
ΔG	Elongation of the specimen
ℓ	Length of the extensometer
L_o	Distance between the arms from the pivot points
L_o'	Decreased distance between the arms from the pivot points
P	Lever arm scale
r_t	Radius of the sensor head
W_a	Weight of the arms
W_b	Weight of the brackets and rods
Y	Length of the step until the pivot points
Z	Height of the arm step
δ	Gap change
δ	Change at the gage length

δ_i	Difference between real and perpendicular distance
θ	Inclination angle
ϕ	Slant angle
ϕ_1	Upper arm angle
ϕ_2	Lower arm angle
eIMPA	Error of maximum independent movement of probing arms
eUTAP	Error of uneven transducer air gap
GLE	Gage length error
LVDT	Linear variable differential transformer

1. INTRODUCTION AND RELATED STUDIES

Testing of materials, more specifically testing of mechanical properties of metals, polymers and ceramics has become widespread to collect engineering design data for design applications with various types of materials. Thus, strain and displacement measurements are major aspects of materials testing. Basically the problem and the main case encountered in strain measurements is to determine the displacement between two points, the bounds of the specific gage length, which are some distance apart.

The terms, stress and strain are the most used ones about deformation of solid materials. When the strain is not too large, the displacements are proportional to applied forces. The relation between the force and displacement depends also on the reference dimension [1].

There are a huge variety of physical methods, which have been employed to achieve the displacements on materials. From this point of view, extensometers, it can be said that they are rich in variety too. Recently optical and mechanical type extensometers are very common. Optical extensometers have an advantage of non-contacting. Unless non-contacting is inevitably a plus, the optical ones are not preferable because of their sophisticated systems and high costs [2]. On the other hand, they differ with their working environments. Temperature conditions have made high temperature, low temperature types appear [3]. There are even extensometers that are, for example, corrosion and submersible type.

According to the measurement purposes for which the extensometer is intended, different gage lengths can be utilized and different extensometers for those gage lengths can be obtained or designed and manufactured [3, 4].

When smaller deformations are the real cases to deal with, higher resolutions and accuracies are needed [5]. Moreover, long-term stability, especially in creep and fatigue tests, is an important aspect [2]. To suffice these requirements, a well-equipped extensometer is a real necessity. Because existing commercial resistance strain gages are

not as reliable as extensometers, if the main aim is to measure the displacement directly [6]. “Actually, strain cannot be directly measured, but displacement measuring devices called extensometers can calculate strain.” [7].

This thesis’ main aim is to conduct the creation of a mechanical extensometer with its all design levels including its necessary calculations, analysis, manufacturing and testing of it.

The most similar and related study on this prospect has been performed by Liu and Ding [2] in 1993 about a mechanical extensometer design. Liu and Ding designed a simple mechanical extensometer for high-temperature testing of ceramic materials. They also performed creep tests on round silicon nitride tensile specimens. Their design has a characteristic that it uses its own weight for contacting and its sensing element is a capacitive transducer. Experiments were conducted on round tensile specimens with a 25 mm reference gage length.

Liu *et al.* had performed a similar study [8] in 1988 on ceramic materials’ tensile and cyclic fatigue testing. Their next design [2] is a refined version of this design.

A paper prepared by Motoie *et al.* [9] gives information about the design and construction of a compact extensometer which utilizes from an LVDT. The design is made for investigation of the behavior of metals at high temperature. The contact is ensured by a spring-loaded clamp. It uses 3/8” of gage length for flat specimens. The LVDT is very similar with the model which was chosen to use in this thesis. The performance of the extensometer is judged to be quite successful.

An extensometer using an LVDT again which was designed for low-cycle fatigue tests on anisotropic materials at elevated temperatures has been represented by Raske and Burke [10] in 1978. Design is suitable for 5 mm diameter uniform-gage specimens. The construction met the contact force need with counter weights which are attached by nylon cords. This method seems a bit primitive for a recent design. It used a displacement magnification ratio of 2.5:1 and mentioned about the calibration technique that was performed.

Extensometers are very widespread not only at mechanical and civil engineering or metallurgy, but also at medical engineering and biomechanics. Boyd *et al.* [11] have prepared a good example of it in 2001 with their study on measuring mid-substance strain in bone during uniaxial compression. They designed a device which used a cantilever arm procedure instrumented by strain gages. They have designed a handcuff like structure to install three clip gage like extensometers together. Testing was performed on rubber and bone specimens.

Another extensometer by Perusek *et al.* [12] uses paired capacitive sensors which measures global bone strain due to bending, as well as compression or tension. It gives useful information about the air gap change calculations and angular displacements from which the error analysis and coordinate analysis for the sensor in this thesis benefit. Also it has been claimed that this design could be changed with small details to apply to other materials, like ceramics, metals and plastics, could let the reference gage length changes without difficulty.

While all these design variety was sometimes making things easier during noticing the possibilities, they also sometimes made it very hard to make decisions during designing and constructing the extensometer.

2. CONTACT FORCE (PUSHING FORCE)

To make the tips of the extensometer arms contact with the specimen without slipping, there is a need of force pushing the extensometer arms onto the specimen. That contact force is essential, because it is one of the main problems to obtain a sufficient contact between the extensometer and the specimen at the aimed contact points to reveal the slippage which could really affect the displacement measurements in a bad way. At the same way, while the extensometer is being positioned with the required contact force onto the specimen, applying an unnecessary and excessive force and pressure at contact points will be harmful for the security of the measuring goal, the specimen [13].

There is not an exact standard value in strain measurements for contact force values. It is depending and varying among different commercially used extensometers according to type and weight of the extensometer, the ambient temperature conditions which may change from minus-degree ($^{\circ}\text{C}$) temperatures to above 1000°C degrees and finally the material and shape of the specimen.

On the other hand, contact forces are gained by special spring configurations coupled with special contact points on the contact edges of the extensometer. Those springs may be spinning around the specimen generally for round specimens or clamping on the backside of the specimens generally for flat or plane specimens as attachment devices [14].

But during the initial design period, the proposed design for the extensometer did not include a spring. At the target design, the required contact force would be tried to attain by using its own weight. However, the force must not be at a fixed and constant value but must take values in respect of the measurement conditions and the user's necessity before and during the measuring stages until the most convenient amount is determined.

The mentioned contact (pushing) force would be only about the extensometer weight itself, inclination angle between the brackets and the ground surface and proportional to them [2].

At initial design phase, the shape of the extensometer was ready as shown in Figure 2.1 schematically, but the dimensions for all parts were not decided definitely. At that point;

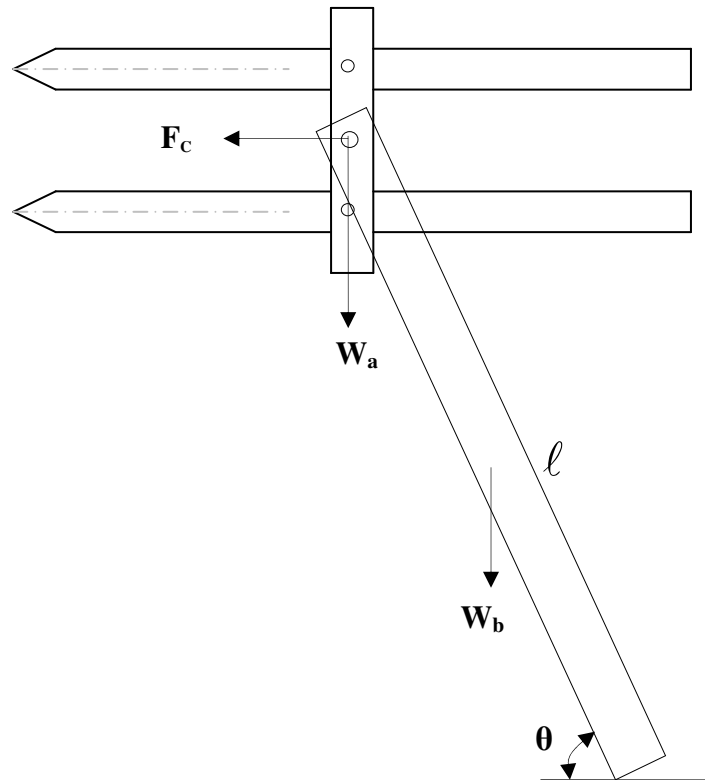


Figure 2.1. Schematic view of the extensometer

F_c : Contact force

ℓ : Length of the extensometer

W_a : Weight of the arms

W_b : Weight of the brackets (and rods)

θ : Inclination angle

$$F_c \cdot \ell \cdot \sin \theta = W_a \cdot \ell \cdot \cos \theta + W_b \frac{\ell}{2} \cdot \cos \theta$$

$$F_c \cdot \sin \theta = \left(W_a + \frac{W_b}{2} \right) \cdot \cos \theta \quad (2.1)$$

$$F_c = \left(W_a + \frac{W_b}{2} \right) \cdot \cot \theta$$

$$W_a = d_a \cdot V_a \quad d_a = d_b = d_{Al} = 2.7 \text{ g/cm}^3 = 0.0027 \text{ g/mm}^3$$

It could be seen that contact force is affected by the weight of the arms and the frame carrying them and half of the weight of the brackets carrying the frame. And the force is directly proportional to the cotangent of the inclination angle and it is given in Table 2.1.

Table 2.1. Contact force variations with the inclination angle and sectional dimensions

[1:1]		Contact Force (Pushing Force) [g] (x 1/2 per each arm)																	
8x10	d1	15°						30°						45°					
10x12	30	1107	1186	1286	1142	1222	1322	514	551	597	530	567	613	297	318	345	306	327	354
	40	1139	1219	1318	1190	1270	1370	529	566	612	552	590	636	305	327	353	319	340	367
12x12	50	1171	1251	1351	1239	1319	1418	543	581	627	575	612	658	314	335	362	332	353	380
12x15	60	1203	1283	1383	1287	1367	1467	558	595	642	597	634	681	322	344	371	345	366	393
15x15	70	1236	1315	1415	1336	1415	1515	573	610	657	620	657	703	331	352	379	358	379	406
	80	1268	1348	1447	1384	1464	1563	588	625	672	642	679	726	340	361	388	371	392	419
	90	1300	1380	1480	1432	1512	1612	603	640	687	665	702	748	348	370	396	384	405	432
	100	1332	1412	1512	1481	1560	1660	618	655	702	687	724	770	357	378	405	397	418	445
	d1	60°						75°						90°					
	30	171	184	199	177	189	204	79	85	92	82	88	95	0	0	0	0	0	0
	40	176	189	204	184	197	212	82	87	95	85	91	98	0	0	0	0	0	0
	50	181	194	209	192	204	219	84	90	97	89	95	102	0	0	0	0	0	0
	60	186	198	214	199	211	227	86	92	99	92	98	105	0	0	0	0	0	0
	70	191	203	219	207	219	234	89	94	102	96	102	109	0	0	0	0	0	0
	80	196	208	224	214	226	242	91	97	104	99	105	112	0	0	0	0	0	0
	90	201	213	229	222	234	249	93	99	106	103	109	116	0	0	0	0	0	0
	100	206	218	234	229	241	257	96	101	109	106	112	119	0	0	0	0	0	0

When commercially used extensometers are investigated, it was seen that the contact force is generally at about 100 grams per each arm.

For example, the slippage testing results of Albright and Annala [15] listed that MTS 632.54E-04 and MTS 632.54E-01 extensometer models had 100g of contact force per arm, however MTS 632.53E-04 had 300 g per rod. Other examples are available MTS 632.24-50 high temperature axial extensometer has again 100 g of contact force as well [14]. As these examples present, there is not an exact and fixed value for contact forces.

Table 2.2. Contact force variation of the finalized extensometer with inclination angle

		Contact Force (Pushing Force) [g] (x 1/2 per each arm)						
		d1	15°	30°	45°	60°	75°	90°
[1:1]	8x10	85	1485	689	398	230	107	0

3. GAGE LENGTH

Gage length is the distance between the arms of the extensometer contact points with the specimen where and in which the behavior of the specimen is followed. Gage lengths are also assorted. When there is a definite region on the specimen and if the extensometer is designed to measure the displacements at that region, for example a crack, then the gage length must be adjusted to follow that region from a distance as close as possible.

Although the extensometer is intended to be designed in a way that it could be used in many applications and specimen and that it would be multi-purpose one with its differential gage lengths and different contacting tips, the first aimed specimens to be inspected are the center-cracked tension specimens, M(T), that would be examined of the region near the crack from a most appropriate short gage length.

The intended extensometer is planned to make a design for the displacements near the crack of aluminum plane specimens during tension and fatigue tests. And the gage length is chosen to be 10 mm. The most similar example of extensometer as a reference for aluminum flat specimens is Motoie, Sakane and Schmidt's design [9] that is a cross-check for the gage-length selection. It's designed with a 3/8" (~9.5 mm) gage length.

4. SENSORS

An extensometer is a device which measures the change in the length within a specific gage length with the help of a suitable sensor that would be mounted onto the body of itself. Clip on extensometers are contacting type of extensometers which is planned to be designed.

Distance and displacement measurements are always hot and popular directions in engineering and industry. Displacement is a vector notifying the position changes of a certain point or a body with respect to a reference [16].

Extensometers are coupled by particular devices that are sensors sensing the elongation of the specimen by measuring the distance or displacement. These extensometers mostly carry strain-gages or LVDTs (linear variable differential transformers) or capacitive and inductive displacement sensors.

The first option was to use an LVDT. LVDTs convert a linear motion or displacement into a electrical signal and are in a large variety that they are manufactured from millionths of an inch to several centimeters [13].

Another strain sensing element is strain gage. It is made of a conductor or a semiconductor material and when it is contacted onto a measured specimen or a surface that is subjected to tension or compression, it also elongates or contracts. Thus the strain gage creates resistive changes under those conditions and this change on resistance makes sense on voltage by the use of Wheatstone bridges which combines two or four strain gages [6]. At several clip gage type extensometers the bridge is contacted and clamped on an elastic element which is then mounted on a suitable region of the extensometer [5].

When the excitation of the system takes place, the output voltage is a measure of strain sensed on the elastic element [17].

There are several types of strain gages. The oldest version is metal-wire strain gages which are not very common nowadays. Another type of them is metal-foil strain gages. They are very common, low-cost with development of mass production and in a huge variety of sizes. They are generally manufactured of copper-nickel, nickel-chromium or iron-chromium-aluminum alloys etc. [18].

One more solution for a possible strain sensing instrument is proximity sensor. These sensors are able to detect objects without any contact. Most common ones are inductive and capacitive sensors. The difference is that inductive sensors only detect metallic objects, but capacitive sensors detect all objects, metallic and non-metallic objects [19]. Since they are generally miniature, light-weight and low-cost sensors, it is advantageous to make use of them in small space applications. Conversely they are affected by other metallic and non-metallic materials near them which may change their inductance or capacitance.

But nevertheless it is better to utilize from an inductive displacement sensor only among the proximity sensors, because noise is a bigger deal in capacitive sensor applications. Since they are less affected environmentally, they are widely used and compact type sensors. They work in the principal of magnetic circuits. When there is a relative displacement between the conductor and a magnetic field, there will be an air gap change and a small air gap variation will serve a visible inductance change. This means a high increase in reluctance and decrease in the flux. Unless certain measurements are taken, there may be environmental effects which cause unwanted magnetic fields, currents and responses. The main precaution is magnetic shielding by using proper insulators to isolate the sensors in the measurement system [16]. An LVDT is an inductive sensor anyhow; however it's a more closed system including its own magnetic shields.

A common capacitive displacement sensor consists of two electrodes with capacitance. This capacitance is a function of the distance of those two electrodes most generally. But in a more detailed manner, capacitance is a function of distance between electrodes, the area of them and the permittivity of the dielectric between those electrodes. There is a drawback at capacitor usage, because the linearity is a problem. The output behaves non-linearly with respect to the distance and the sensitivity decreases as the electrodes become far away from each other. Non-contacting incremental displacements

can be measured by those types of capacitive sensors [20] when several signal conditioning measures are taken.

Structure and parts of an LVDT can be observed in Figure 4.1. LVDT consists of two main parts; the body of the coil assembly and the core. The body holds the coil assembly which contains one primary winding and two secondary windings at both sides of the primary winding. There are types of LVDTs that are working in the principle of half bridge contain only two windings and they are not as common as the ones with primary and secondary windings (full bridge) [21]. Those windings are in a magnetic shield and the outset layer is generally made of stainless steel to protect the inner magnetic relationship.

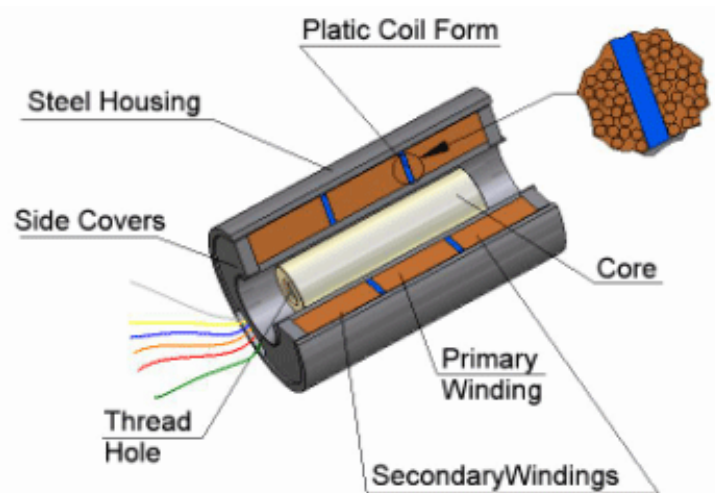


Figure 4.1. Components of a traditional LVDT [Singer Instruments]

The core is the active element of an LVDT. The movement of the core and the amount of this motion is essential thing to sense and measure. The core's material must be a magnetically permeable material [22]. The core must be free as much as possible and there should be enough clearance avoiding the possible undesired friction or contact between those two elements of LVDT [23].

Apparently it was realized that if it would be preferred to use a proper LVDT, it's a necessity to control the behavior of the core inside the bore of the body under the slight angular displacement conditions. Because when the arms of the extensometer turn around the pivoted points, the tip of the sensing side of the arm would not only move up and down

(vertically) but also perpendicularly. It is evident that this perpendicular motion among the two elements, the core and the coil body, would be an obvious danger for the measurement system within the principal of the freedom of the core and non-contacting relationship between them. That is why every possible condition must be investigated for the clearance inside the bore of LVDT. A possible contact could damage the core and also the measurement results because of the affected output signals.

An LVDT is electronically excited by alternating current from its primary winding and the output signal is collected from the secondary windings as differential AC voltage. This voltage is very proportional with the positioning and the displacement of the core element especially within the full stroke range of the LVDT. This output signal from the secondary windings is transformed to higher DC voltages that are much more meaningful to observe.

An LVDT's working principal is that it prepares an AC output whose magnitude is linearly proportional with the displacement of the core and a phase angle which is related to the core's midway position inside the body and the null point of the core [22].

Let the primary winding is W , and the secondary windings are w_1 and w_2 ; and W is excited with constant amplitude of AC voltage.

For example, when the core is displaced towards w_1 and it is further from w_2 , then the flux transmitted to w_1 and w_2 will be different, so that the voltage induced in w_1 and w_2 will differ as well. Then $E_1 > E_2$ and $E_{out} = E_1 - E_2$. The more the core gets near to w_1 or by w_1 's side; the more the voltage gets output value. Because E_1 is increased and E_2 is decreased.

The same principal is valid for the other winding. When the core is by the side of w_2 and further from w_1 , the flux transmitted to w_2 will be higher, at the same time the flux to w_1 will be less. At this case the differential output voltage value will be $E_2 - E_1$.

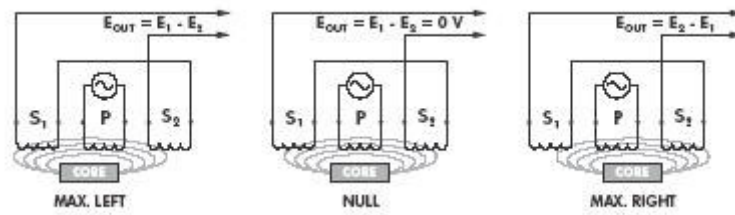


Figure 4.2. Output voltage with relation to the LVDT core position [22]

On the other hand, the transmitted flux on each winding, w_1 and w_2 , will be equal and so do the voltages induced in them; when the midpoint of the core is positioning at the midway level of the bore of the body. Then the output voltage, $E_{out} = E_1 - E_2 = E_2 - E_1 = 0$. These three cases are illustrated in Figure 4.2.

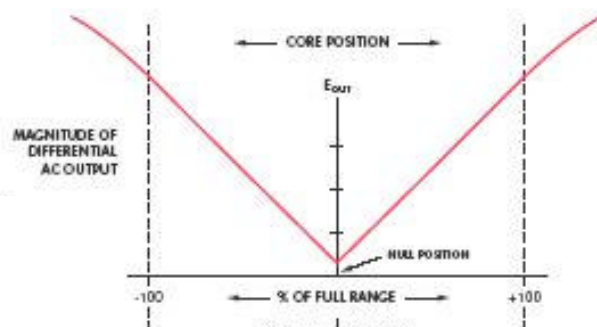


Figure 4.3. Variation of magnitude of the differential AC output voltage with core position [22]

Those three major cases show that the output voltage varies with the displacement of the core in respect of the null point of the LVDT as in Figure 4.3. Those output signals are also coupled with a phase angle and this phase angle only changes by 180 degrees, when the core passes the null point [23]. That shift is necessary to understand the position of the core with respect to the null point with the help of the support electronics.

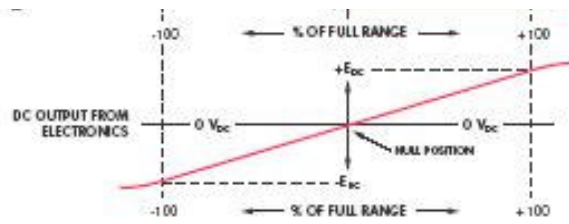


Figure 4.4. DC output from electronics [22]

The collected signals or the output voltage info have a special condition that they are linear inside the stated full range of the LVDT. This linearity continues in a poorer manner over that stated range as it is shown in Figure 4.4.

An LVDT is not enough by itself, but a supporting electronic element is essential to cooperate. Those elements are called as LVDT signal conditioning equipments. They are essential, because LVDT's need an AC power with a constant amplitude and frequency. Those signal conditioning equipments are sufficient to prepare the convenient excitation power. Another requirement for a well-organized measurement system is converting the low-level AC output signals into higher level DC signals with the addition of 180 degrees output phase shift information during the null point pass of the core. That will provide an output distribution with plus and minus signs. These are all benefits of and reasons to utilize from a signal conditioning equipment.

5. INITIAL DESIGN AND DESCRIPTION OF THE SYSTEM

The system is a combination of the extensometer itself and a lifting system of it.

The extensometer has basically a scissors-like design which is a combination of two lever- arms. The two lever arms are conically machined forming a sharp design at their edges to maintain a constant and unslipping contact with the specimen. Each arm is supported on its sides inside a rectangular frame chassis which is also attached to the upper part of two brackets. These brackets are supported at lower parts and attached to a base plate.

The rear end portions of the arms are instrumented electronically by a sensor. That sensor is chosen among LVDT, inductive transducer or an elastic element featured by strain-gage combinations.

The extensometer is supported on the base plate to the lifting system. The lifting system consists of two long circular shafts, a moving plate, and finally an upper, and a lower base plate. The base plate of the extensometer is attached to the moving plate of the lifting mechanism. With the help of adjustment of the height of this moving plate and the inclination angle of the extensometer brackets, the arms of the extensometer will rise and contact with the proper place on the specimen. That moving plate will move up and downwards along the circular shafts and those shafts will be attached to the upper base plate by bolts. Finally, the lower base plate will work as a track and the upper base plate - with shafts - will slide on lower base plate. Lower and upper base plates will be attached to each other by the help of four bolts. The lower base plate will be thick and large enough to serve as a heavy and unmoving base under the whole system.

The supporting elements are different types of bolts and screws. The whole system of the extensometer would be manufactured of aluminum 7075 with its good machinability, low density and sufficient strength.

6. ERROR ANALYSIS

6.1. Gage Length Error

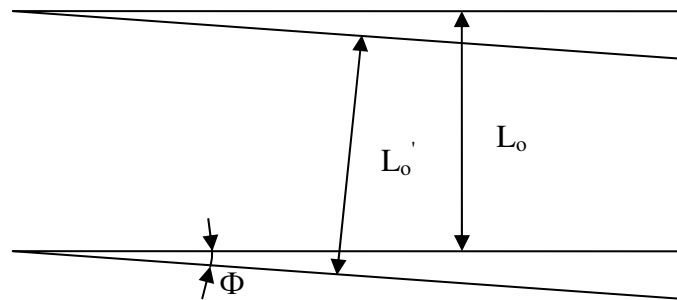


Figure 6.1. A schematic diagram illustrating slanted arms

Normally when the extensometer arms are installed in a way that it is planned theoretically; the distance between the arms on the specimen side is G_o , and the distance between the arms from the pivot points is L_o [2].

There could be different cases for G_o and L_o dimensions according to the tip design of the extensometer arms as illustrated in Figure 6.2. For example;

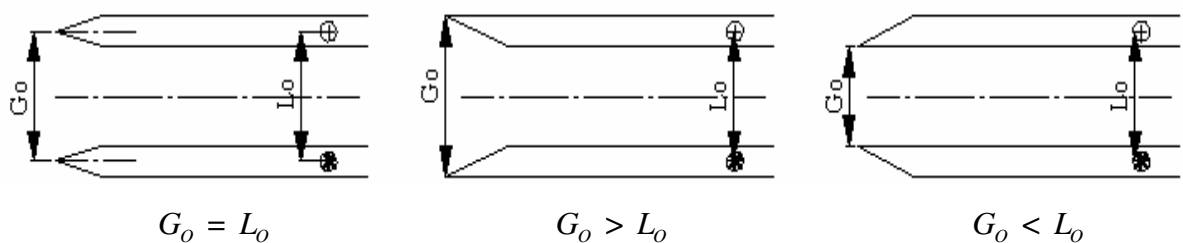


Figure 6.2. Possible tip designs for probing arms

All these cases are possible. At initial level let $G_o = L_o$. With the ideal positioning ($\phi=0$) when the arms are parallel to each other and horizontally, $G_o = L_o$.

It does not matter which type of sensor is used, calibration is inevitable. Because the output signals must be set to zero or reset before the measurement starts. When the two probing arms of the extensometer are parallel to each other, but slanted with an angle ϕ , L_o and sensor gap will slightly decrease as seen in Figure 6.1. If this slight change is δ , then;

$$\delta = L_o - L_o' = L_o \cdot (1 - \cos \phi) \quad (6.1)$$

According to the ideal case, the gap will decrease, and to reset the sensor, the gap must be increased, so the gage length must be decreased at that case.

δ' : change at the gage length (specimen side)

$$\frac{\delta'}{\delta} = \frac{d_1}{d_2} \quad (6.2)$$

and Figure 6.3 illustrates this as well.

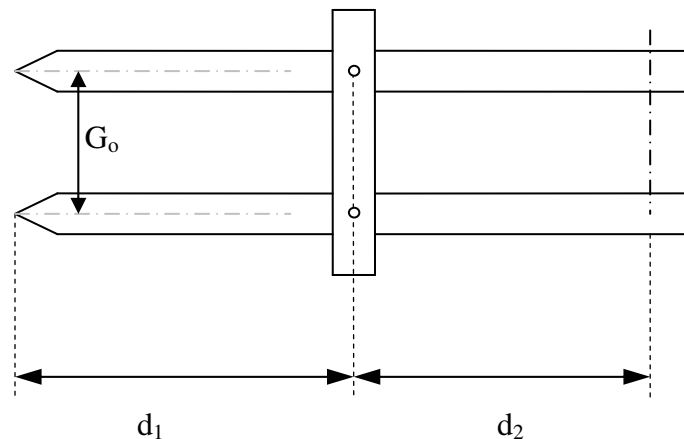


Figure 6.3. A schematic diagram illustrating lever arm ratio

When $d_1 = d_2 \Rightarrow \delta' = \delta$

The error caused by δ , namely the gage length error;

$$\frac{\delta}{G_o} = \frac{L_o(1 - \cos \phi)}{G_o} \quad (6.3)$$

If $L_o = G_o$

$$\frac{\delta}{G_o} = (1 - \cos \phi) = 100 \times (1 - \cos \phi) \% \quad (6.4)$$

The predicted errors are listed at Table 6.1 for different ϕ from (0° to 5°) and (d_1/d_2) values although it is impossible to reach to 5° .

Table 6.1. Predicted GLE values %

$\delta^*(d1/d2)/Go(\%)[GLE: \text{Gage Length Error}]$								
Φ	$\Phi(\text{rad})$	$Go=Lo$	δ	(d1/d2=1)	(d1/d2=1,1)	(d1/d2=1,2)	(d1/d2=10/12)	(d1/d2=0,8)
0	0,000	10	0,000	0,000	0,000	0,000	0,000	0,000
0,5	0,009	10	0,000	0,004	0,004	0,005	0,003	0,003
1	0,017	10	0,002	0,015	0,017	0,018	0,013	0,012
1,5	0,026	10	0,003	0,034	0,038	0,041	0,029	0,027
2	0,035	10	0,006	0,061	0,067	0,073	0,051	0,049
2,5	0,044	10	0,010	0,095	0,105	0,114	0,079	0,076
3	0,052	10	0,014	0,137	0,151	0,164	0,114	0,110
3,5	0,061	10	0,019	0,187	0,205	0,224	0,155	0,149
4	0,070	10	0,024	0,244	0,268	0,292	0,203	0,195
4,5	0,079	10	0,031	0,308	0,339	0,370	0,257	0,247
5	0,087	10	0,038	0,381	0,419	0,457	0,317	0,304

6.2. Independent Movement of Probing Arms

Since the specimen elongates and contract, the probing arms of the extensometer will move independently through testing. That will cause an angle for each arm. Let that angle be ϕ_1 for the upper arm and ϕ_2 for the lower arm.

For example, when the specimen elongates, the elongation ($\Delta G = G - G_o$) is proportional to the sensor gap change (ΔD).

$$\frac{\Delta D}{\Delta G} = \frac{d_2}{d_1} \quad (6.5)$$

There is a slight error, because a capacitive or an inductive displacement sensor measures the perpendicular distance, not the real gap [2]. If the perpendicular distance is referred as D^* and the real distance as D ; the error is $\delta_i = D - D^*$ and Figure 6.4 illustrates it schematically by a diagram.

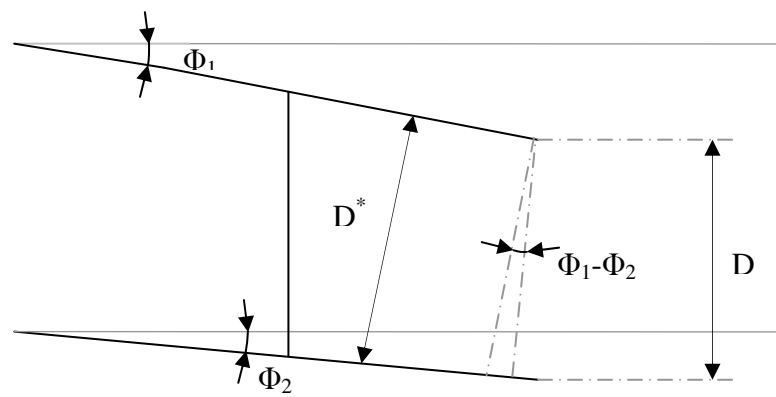


Figure 6.4. Independent arm angles

The error in percentage is;

$$\frac{\delta_i}{D} = \frac{(D - D^*)}{D} = 1 - \frac{D^*}{D} = 1 - \frac{\cos \phi_2}{\cos(\phi_1 - \phi_2)} \quad (6.6)$$

When ϕ_2 is zero, maximum error is introduced.

When ϕ_1 is zero, then minimum error is introduced.

If it is predicted that the extensometer's full strain range is $\pm 5\%$ and ϕ_2 is zero to get the maximum error, ϕ_1 can be expressed as;

$$\phi_1 = \arcsin \frac{\text{full strain range}(+) \cdot G_o}{d_1} \quad (6.7)$$

and $G_o = 10 \text{ mm}$

$$\phi_1 = \arcsin \frac{0.5}{d_1} \quad (6.8)$$

$$\frac{\delta_i}{D} = 1 - \frac{1}{\cos \phi_1} \quad (6.9)$$

and the variation is expressed in Table 6.2 below.

Table 6.2. Predicted eIMPA values %

$\delta_i^*/D(\%)$[eIMPA: Maximum Independent Movement of Probing Arms]										
		1%			3%			5%		
Go	d1	$\Phi 1(\text{rad})$	$\Phi 1(\text{deg})$	eIMPA	$\Phi 1(\text{rad})$	$\Phi 1(\text{deg})$	eIMPA	$\Phi 1(\text{rad})$	$\Phi 1(\text{deg})$	eIMPA
10	70	0,004	0,208	-0,0007	0,011	0,624	-0,0059	0,018	1,040	-0,0165
10	80	0,003	0,182	-0,0005	0,010	0,546	-0,0045	0,016	0,910	-0,0126
10	90	0,003	0,162	-0,0004	0,008	0,485	-0,0036	0,014	0,809	-0,0100
10	100	0,003	0,146	-0,0003	0,008	0,437	-0,0029	0,013	0,728	-0,0081
10	110	0,002	0,132	-0,0003	0,007	0,397	-0,0024	0,012	0,662	-0,0067
10	120	0,002	0,121	-0,0002	0,006	0,364	-0,0020	0,011	0,606	-0,0056
10	130	0,002	0,112	-0,0002	0,006	0,336	-0,0017	0,010	0,560	-0,0048
10	140	0,002	0,104	-0,0002	0,005	0,312	-0,0015	0,009	0,520	-0,0041
10	150	0,002	0,097	-0,0001	0,005	0,291	-0,0013	0,008	0,485	-0,0036
10	160	0,002	0,091	-0,0001	0,005	0,273	-0,0011	0,008	0,455	-0,0032
10	170	0,001	0,086	-0,0001	0,004	0,257	-0,0010	0,007	0,428	-0,0028
10	180	0,001	0,081	-0,0001	0,004	0,243	-0,0009	0,007	0,404	-0,0025

6.3. Uneven Transducer Air Gap

Independent motion of the arms results in an uneven air gap between the transducer and the plate [2] as in Figure 6.5. This condition affects the systems with inductive and capacitive sensors.

The expected error because of this property is approximately less than $\frac{1}{2} \cdot \left(\frac{\Delta D}{D^*} \right)^2$

where

$$\Delta D = D_{\max}^* - D_{\min}^* = D^* - D_{\min}^* \quad (6.10)$$

Within a full strain range of $\pm 5\%$, gage length of 10 mm and finally an air gap of $D^* \approx 0.5$ mm;

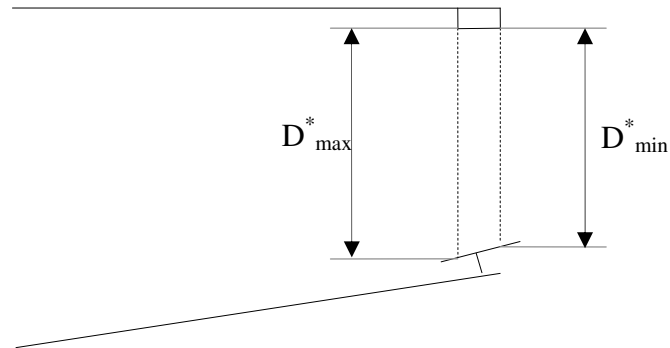


Figure 6.5. A schematic diagram demonstrating the air gap

r_t : radius of the sensor head

$$\frac{\Delta D}{r_t} = \frac{5\% \cdot 10}{d_1} = \frac{0.5}{d_1} \quad (6.11)$$

$$E_{UTAP} = \frac{1}{2} \cdot \left(\frac{r_t \cdot 0.5}{d_1 \cdot 0.5} \right)^2 = \frac{1}{2} \cdot \left(\frac{r_t}{d_1} \right)^2 \quad (6.12)$$

This property is represented with variations in Table 6.3.

Table 6.3. Predicted eUTAP values %

0,5*((rt*0,254)/(d1*1))^2)(%)[eUTAP: Error of Uneven Transducer Air Gap]											
		1%				3%				5%	
	1		1,5		1		1,5		1		1,5
d1	eUTAP	d1	eUTAP	d1	eUTAP	d1	eUTAP	d1	eUTAP	d1	eUTAP
70	0,0006	70	0,0014	70	0,0230	70	0,0517	70	0,3673	70	0,8265
80	0,0005	80	0,0011	80	0,0176	80	0,0396	80	0,2813	80	0,6328
90	0,0004	90	0,0009	90	0,0139	90	0,0313	90	0,2222	90	0,5000
100	0,0003	100	0,0007	100	0,0113	100	0,0253	100	0,1800	100	0,4050
110	0,0003	110	0,0006	110	0,0093	110	0,0209	110	0,1488	110	0,3347
120	0,0002	120	0,0005	120	0,0078	120	0,0176	120	0,1250	120	0,2813
130	0,0002	130	0,0004	130	0,0067	130	0,0150	130	0,1065	130	0,2396
140	0,0002	140	0,0004	140	0,0057	140	0,0129	140	0,0918	140	0,2066
150	0,0001	150	0,0003	150	0,0050	150	0,0113	150	0,0800	150	0,1800
160	0,0001	160	0,0003	160	0,0044	160	0,0099	160	0,0703	160	0,1582
170	0,0001	170	0,0002	170	0,0039	170	0,0088	170	0,0623	170	0,1401
180	0,0001	180	0,0002	180	0,0035	180	0,0078	180	0,0556	180	0,1250

Arm lengths are 170 mm which exposes that $d_1 = 85$ mm in the final design. All three types of potential errors around that value for 5% full strain range expose that they are negligible and an extensometer working on such principle is considered to be satisfactory for displacement measurements.

7. LVDT SELECTION

The most important criteria to be considered are availability, dimension (length and radius), weight, stroke range, type, core clearance and price while the most suitable LVDT is chosen. LVDTs are in huge variety, but also there are many specifications to pay attention.

The availability criterion was essential, because it was a requirement to try the product before using and purchasing it. Hence the most appropriate thing was to select an LVDT which had a distributor company in Istanbul. It would be beneficial to get information as well. An LVDT that is available in Istanbul would give chance to see, touch it and try its behavior out. To this end, it would be better to eliminate the ones without distributors not to face bad surprises.

From this point of view, the collected LVDTs were products of Solartron Metrology, Schaevitz, Applied Measurements and RDP Group. The LVDTs from these companies were candidates for nomination before considering the higher wishes.

Furthermore it does not mean that all models are reachable or you are free to select them when there is a distributor of that company. Sometimes there may be no agreements on some models which would be an appropriate solution for the extensometer design.

The second selection criterion was nominal stroke range of the LVDT. Nominal stroke range represents the displacement in both plus and minus direction in which the collected output would be in high linearity. The stroke range that could serve the need for the decided gage length must be at least ± 0.5 mm and must not be unnecessarily high. That ± 0.5 mm amount is determined in that way.

The gage length was decided before as 10 mm. The deflection of the extensometer which is being designed would not be approximately more than 0.5 mm in both positive and negative direction, since the predicted strain along the determined gage length would not be higher than 5% [9]. It means that the deflection could only be from +0.5 to -0.5 mm.

But it is better to be cautious and select an LVDT for more than that, for example two times of this deflection. So the most suitable selection was an LVDT that must not travel less than ± 1 mm and more than ± 2 mm, for instance. In that case, it was possible to eliminate the ones with ± 2.5 mm strokes or more than that. Because they generally travel around ± 1 mm, ± 1.27 mm (± 0.5 inch), ± 1.5 mm, ± 2.5 mm, ± 2.54 mm (± 1 inch) in lower stroke ranges.

Next step was to control and eliminate models with high dimensions and weights. During searches from catalogues and internet, it could easily be realized that the most appropriate ones are named as mini or miniature.

However they were all called in mini or miniature series, there were still at high variety of them. Possibly an easy remedy to see and compare the dimensions among each other was to draw them all and see the differentiation. They varied from 15 to 82 mm for height and from 6 to 21 mm for diameters of the body.

It truly came in handy to see them all in group on one piece of paper in Figure 7.1. The same variety was valid for the weights too. Moreover, some of them had lack of weight information, when their manuals and specification lists were examined; however this info was in fact essential for miniature measurement systems. Weight had variation from approximately 5 grams to 50 grams.

The next consideration step was type of the LVDT. There were two possible types to utilize in this extensometer design. One type was free. At free type models, the core moves inside the assembly freely without contacting the body. A frictionless movement is possible. The other type is spring-fitted or in other words, spring-loaded model. At those models, the transducer is featured by a spring which pushes the core to the end until the fully-extended position of the LVDT [24]. If a fixing component for the core is avoided, and if it is allowable for the core to press on a moving component in the system, the most suitable solution can be spring-fitted (spring-loaded) LVDTs.

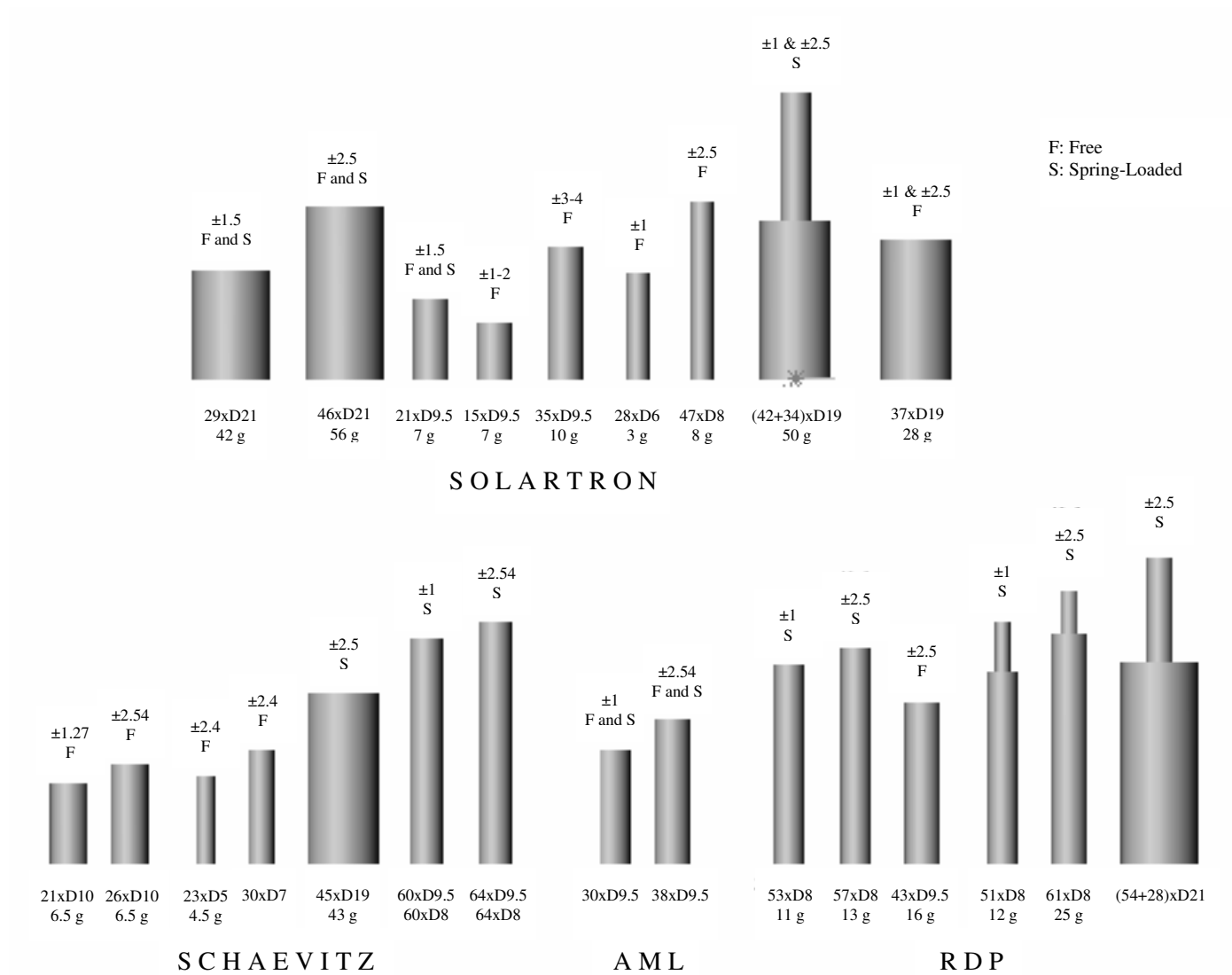


Figure 7.1. LVDT selection - candidates for nomination

In this design, force is also a considerable case and additional forces on the extensometer may result in a slipping problem. Hence the most useful choice was a free LVDT. In the futurework of the experiments, spring addition to the LVDT separately could be possible, if it was considered necessary.

The pricelist of all LVDTs was concealed deliberately, although the market prices for each were gathered before the best choice.

When all this selection steps were considered, the most suitable one for this design chain is Schaevitz's (now it is a company of Measurement Specialties) MHR050 model [25] with its light weight, dimensions, stroke and price at an acceptable level.

Weight: 6 g (body) + 0.4 g (core)

Dimensions: 20.3 mm (body length) × D 9.6 mm (body diameter)

12.7 mm (core length × D 2.75 mm (body diameter)

Nominal Linear Stroke Range: ± 1.27 mm (± 0.050 inch)

8. ARM DESIGN AND COORDINATE ANALYSIS FOR LVDT ELEMENTS

Since the arms will serve as a touching element or a fastener for separate touching elements and determine the displacements with a free rotary motion by the sense of the LVDT which is besides mounted on the arms, the most vital design considerations must be taken into account for a sensitive and accurate measurement.

At initial design stages, the plan was to machine one tip of each arm in a way that it would contact and push the specimen with a sufficient force and pressure not to face with a slippage problem. But the idea changed in the following design considerations on the basis that the arm tips would be fasteners for each thin and sharp contact elements.

Initially there were three basic cases that would possibly be the remedy for the arm design demand. And those three basic cases must be investigated within the change of coordinates. Because the arms would not move up and downwards on a line, but turn around particular points with a very slight angle, since they would be pivoted on them. This effect is only dangerous because friction, contact or a blow is likely to happen, unless the precautions starting with this coordinate analysis of the core and the specific interval of the bore of the body neighboring the core are taken. This is essential, because there is not a large clearance between them as it is expressed in Figure 8.1 with dimensions by a sectional view, which is a unique specialty for LVDTs. That is why their motion and limit coordinates must be under control.

Basically, the three possible cases are;

- 1) Straight – Unstepped
- 2) Stepped – Pivoted before the step
- 3) Stepped – Pivoted after the step

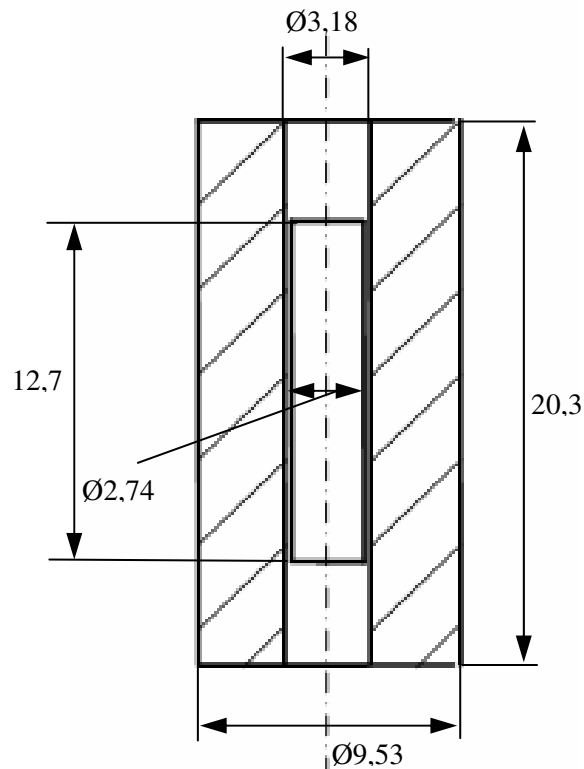


Figure 8.1. Sectional view of MHR050

Steps may be inevitable to make the LVDT fit between the two arms of the extensometer. Because there would not be an enough distance without a particular step when it is planned to mount the LVDT body to one arm and the core of it to the other arm. The preference is to fix the body to lower and the core to upper lever arm. Further, the three main cases branch out in Figure 8.2, Figure 8.4, Figure 8.6; and with subcases in Figure 8.3, Figure 8.5, Figure 8.7 according to the placement of the body on the lower arm.

First of all, the first main case is investigated separately for the coordinates of the lower arm and upper arm. Then it is followed by some constant numbers which represent the subcases for the placement of the body.

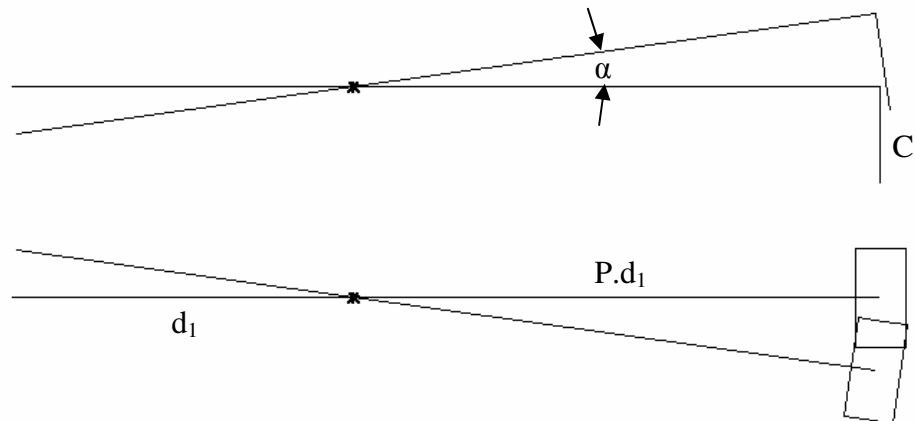


Figure 8.2. Schematic demonstration of straight-unstepped arm mode

The predetermined gage length was 10 mm. So the distance between two arms is 10 mm initially and the angle after a probable deflection for each arm is α . The case is explored in the direction that the specimen is contracted, so the specimen side tips deflect in a manner that they come closer to each other. Since the upper and lower arms are at different levels, the system needs a rod lowering the core to the midway of the body and the length of it is named to be C . The length of the arm from the tip on the specimen to pivot points is d_1 and from the pivot points to axis of the LVDT which is preferred to be joined is $P.d_1$. P is the lever arm scale. In this way, for every single unit displacement on the specimen side, would be measured by P times the same displacement on the rear LVDT side.

The simplest way to calculate the displacement in respect of the core's upper and lower top points and the body's target points which comes face to face with them at initial circumstance is to evaluate the initial x and y coordinates and the final x and y coordinates or the difference between them after a highest probable angular displacement for the arm. The subcases for this first, straight and unstepped main case are mounting the LVDT in a way that LVDT body's top surface is aligned with the top surface of the lower arm and that LVDT body's midpoint is aligned with the midpoint of the thickness of the lower arm. Before branching out for the subcases which only depends on the C variable, the general coordinate formulas for the core are (Table 8.1);

Table 8.1. Coordinates of the core in mode 1

X	P.d ₁ → P.d ₁ .cos α → C.sin α	P.d ₁ P.d ₁ .cos α + C.sin α
Y	-C ↑ P.d ₁ .sin α ↓ C.cos α	-C P.d ₁ .sin α - C.cos α

And the initial and final position coordinates are;

$$\mathbf{I. P.} (P.d_1 ; -C)$$

$$\mathbf{F. P.} ((P.d_1 \cdot \cos \alpha + C \cdot \sin \alpha) ; (P.d_1 \cdot \sin \alpha - C \cdot \cos \alpha))$$

Finally, the displacement of the core inside the body is

$$\mathbf{X} \Rightarrow P.d_1 \cdot \cos \alpha + C \cdot \sin \alpha - P.d_1 = P.d_1 \cdot (\cos \alpha - 1) + C \cdot \sin \alpha$$

$$\mathbf{Y} \Rightarrow P.d_1 \cdot \sin \alpha - C \cdot \cos \alpha + C = P.d_1 \cdot \sin \alpha + C \cdot (1 - \cos \alpha)$$

Assuming that the thickness of the arms would be minimum 6 mm, the two subcases could be evaluated by only changing the C values.

The key position is that α , which is necessary for the drafts of the possible limit position, can be calculated as follows, because it is predicted that the maximum displacement could be around 0,5 mm between the extensometer arms. Then half of it can be acceptable for one arm.

$$\frac{1}{2} \cdot \frac{0.5}{d_1} = \sin \alpha \quad (8.1)$$

$$\alpha = \arcsin \left(\frac{1}{2} \cdot \frac{0.5}{d_1} \right) \quad (8.2)$$

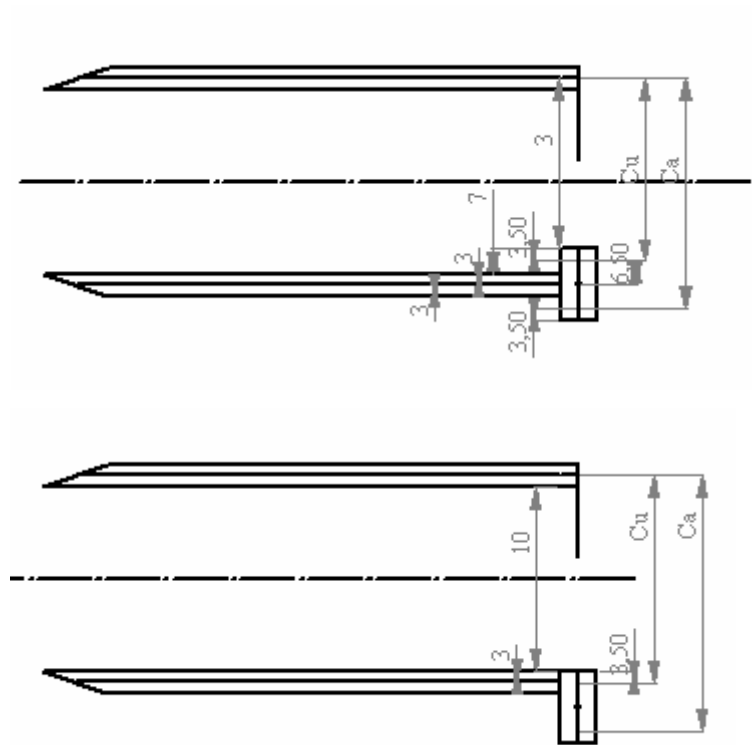


Figure 8.3. Subcases of mode 1

For example, for the subcases, assuming a 6 mm thickness for the arms, C_u and C_a values determines the upper and lower coordinates for the core.

$$H=3 \Rightarrow C_u = 9.5 \text{ \& } C_a = 22.5$$

$$H=10 \Rightarrow C_u = 16.5 \text{ \& } C_a = 29.5$$

When a similar group of calculations are reiterated, same type of data are gathered in Table 8.2 for the coordinates and displacements of the LVDT's target body points facing the upper and lower parts of the core initially.

Table 8.2. Coordinates of the target body points in mode 1

X	P.d ₁ → P.d ₁ .cos α ← C.sin α	P.d ₁ P.d ₁ .cos α - C.sin α
Y	-C ↓ P.d ₁ .sin α ↓ C.cos α	-C -[P.d ₁ .sin α + C.cos α]

The displacement of the body points is;

$$\mathbf{X} \Rightarrow P.d_1 \cdot \cos \alpha - C \cdot \sin \alpha - P.d_1 = P.d_1 \cdot (\cos \alpha - 1) - C \cdot \sin \alpha$$

$$\mathbf{Y} \Rightarrow C - [P.d_1 \cdot \sin \alpha + C \cdot \cos \alpha] = C \cdot (1 - \cos \alpha) - P.d_1 \cdot \sin \alpha$$

All those displacements and coordinates are valid for the central points. By using the information of the core and the channel in the body, it is possible to see the final positions with respect to different values of arm length.

Similar evaluations were made in Table 8.3 and Table 8.4 for the second main case, stepped and pivoted before the step, with three different subcases about the placement of the LVDT body. This time the only different additional variables are Z which represents the height of the step, Y length of the step until the pivot points and now the number of the subcases is three. Because by using a suitable step value, it is possible to make the LVDT fit from its base body surface too.

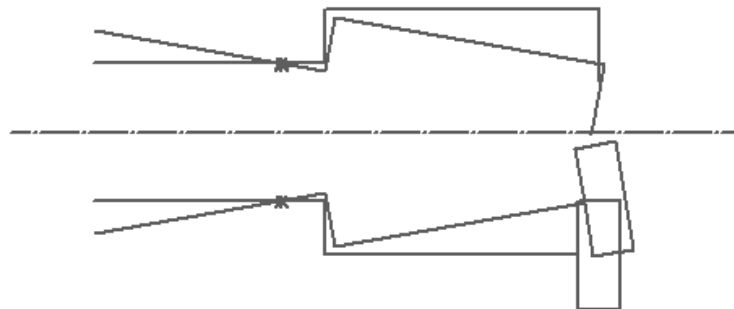


Figure 8.4. Schematic demonstration of stepped-pivoted before the step

Table 8.3. Coordinates of the core in mode 2

X	$P.d_1$ $Y.\cos \alpha - Z.\sin \alpha + (P.d_1 - Y).\cos \alpha + C.\sin \alpha$
Y	$Z - C$ $Y.\sin \alpha + Z.\cos \alpha + (P.d_1 - Y).\sin \alpha - C.\cos \alpha$

The displacement of the core inside the body is

$$\begin{aligned} \mathbf{X} &\Rightarrow Y.\cos \alpha - Z.\sin \alpha + P.d_1.\cos \alpha - Y.\cos \alpha + C.\sin \alpha - P.d_1 \\ &= P.d_1.(\cos \alpha - 1) + (C - Z).\sin \alpha \end{aligned}$$

$$\begin{aligned} \mathbf{Y} &\Rightarrow Y.\sin \alpha - Z.(1 - \cos \alpha) + (P.d_1 - Y).\sin \alpha + C.(1 - \cos \alpha) \\ &= P.d_1.\sin \alpha + (C - Z).(1 - \cos \alpha) \end{aligned}$$

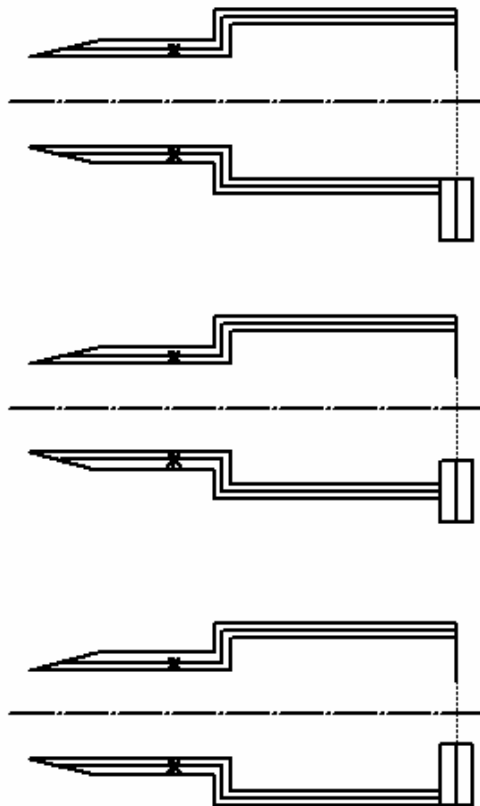


Figure 8.5. Subcases of mode 2

Table 8.4. Coordinates of the target body points in mode 2

X	P.d ₁ Y.cos α - Z.sin α + (P.d ₁ - Y).cos α - C.sin α
Y	- C - Z = - (Z + C) -Y.sin α - Z.cos α - (P.d ₁ - Y).sin α - C.cos α

The displacement of the body points is

$$\mathbf{X} \Rightarrow P.d_1 \cdot (\cos \alpha - 1) - (Z + C) \cdot \sin \alpha$$

$$\mathbf{Y} \Rightarrow -P.d_1 \cdot \sin \alpha + (Z + C) \cdot (1 - \cos \alpha)$$

The two main cases showed that as much as the distance between the arms increased by step length or gage length, the foreseen relation between the core and the body became worse and worse. That is why before the final design was shaped, that could be understood that the arm ends must be as near as possible to avoid a contact inside the LVDT.

This is obvious that α values are decreased when d_1 values are increased (Equation 8.2) as well.

In the third main case, the only difference from the second case is that the step is before than the pivot points and the coordinate evaluations are given in Table 8.5 and Table 8.6. This may considerably be a more efficient design since it was agreed on some contact elements which was going to be fixed on the arm tips.

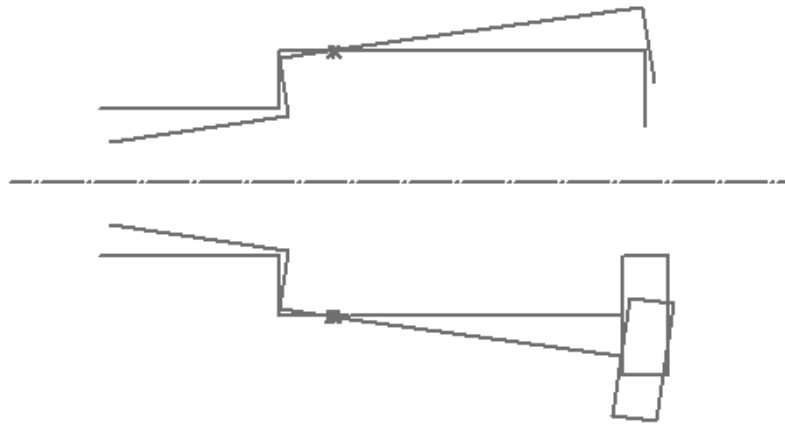


Figure 8.6. Schematic demonstration of stepped-pivoted after the step

Table 8.5. Coordinates of the core in mode 3

X	P.d ₁ P.d ₁ .cos α + C.sin α
Y	-C P.d ₁ .sin α - C.cos α

The displacement of the core inside the body is

$$\mathbf{X} \Rightarrow P.d_1(\cos \alpha - 1) + C.\sin \alpha = C.\sin \alpha - P.d_1(1 - \cos \alpha)$$

$$\mathbf{Y} \Rightarrow P.d_1.\sin \alpha + C.(1 - \cos \alpha)$$

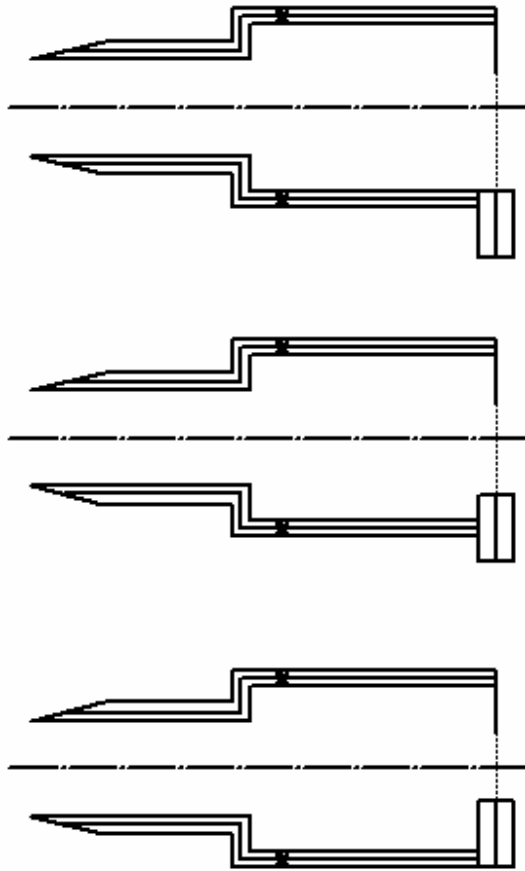


Figure 8.7. Subcases of mode 3

Table 8.6. Coordinates of the target body points in mode 3

X	P.d ₁ P.d ₁ .cos α - C.sin α
Y	-C -P.d ₁ .sin α - C.cos α

The displacement of the body points is

$$\mathbf{X} \Rightarrow P.d_1(\cos \alpha - 1) - C.\sin \alpha = -C.\sin \alpha - P.d_1.(1 - \cos \alpha)$$

$$\mathbf{Y} \Rightarrow -P.d_1.\sin \alpha + C.(1 - \cos \alpha)$$

The LVDT was considered to have an effective sensitivity, so the lever arm ratio was planned to be 1 (1:1).

Under all those possible conditions, the best possible arm designs are shaped to be as follows in Figure 8.8, Figure 8.9, Figure 8.10, Figure 8.11, Figure 8.12 and Figure 8.13.

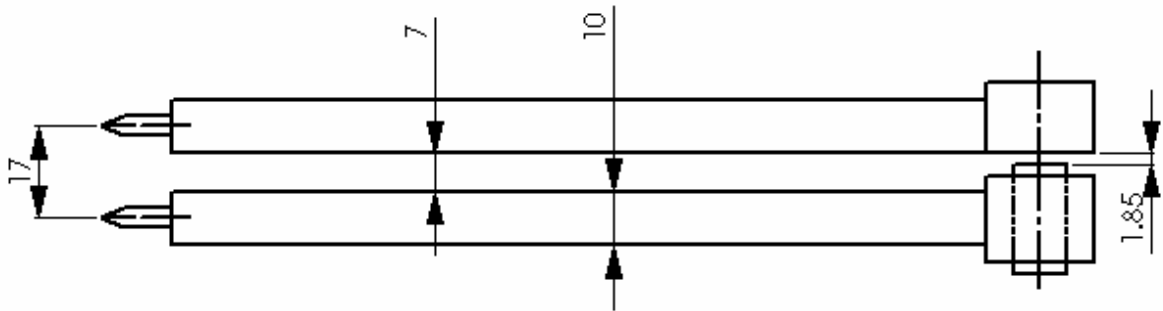


Figure 8.8. Arm design 1

During making the decision about the sharp contact elements, which would have a thickness around 3 mm, the best method was to remain an enough amount of thickness like 2 mm or to fix on the very center of the arm with a proper deepness. On the other hand, the arms are planned to have a sectional dimension like 8×10 , 10×10 or 10×12 .

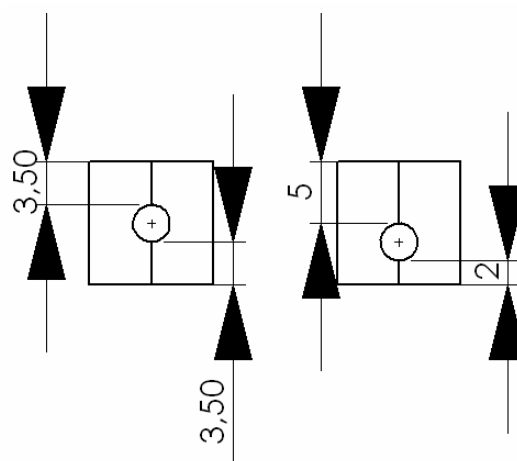


Figure 8.9. Possible positionings of contact element on arm

Not to bring the arms too near to each other, the second example is a better choice.

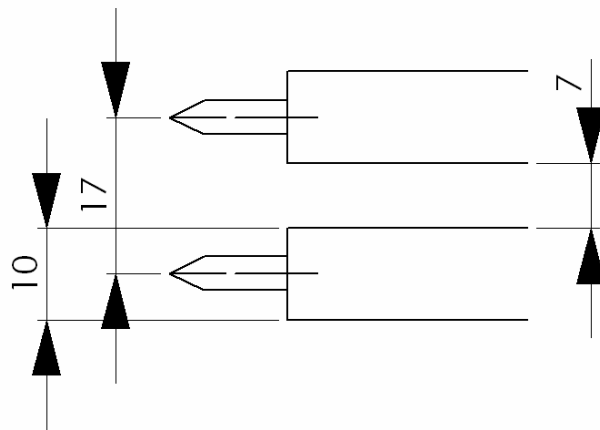


Figure 8.10. Gage length with this arm mode

But it did not seem to be possible to get a 10 mm gage length with this arm mode.

Second choice could be as follows;

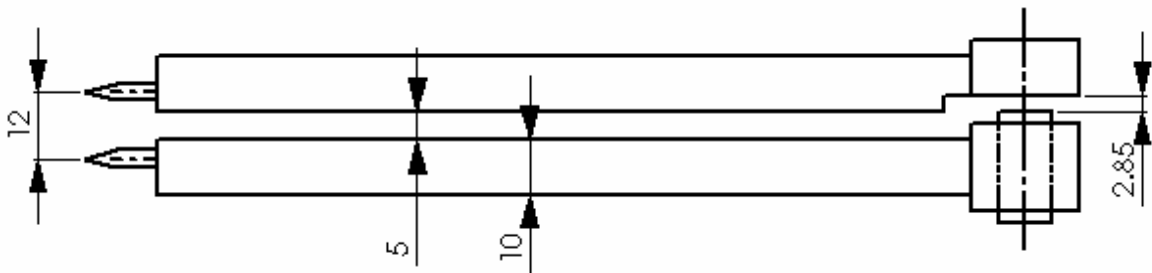


Figure 8.11. Arm design 2

This mode has an extra step at the rear side to make the arms come closer to each other which is only because of the necessity of getting a 10 mm gage length. But only a gage length with 12 mm could be obtained, and the rear side also has a complex and unwanted type of design.

The third choice was as follows;

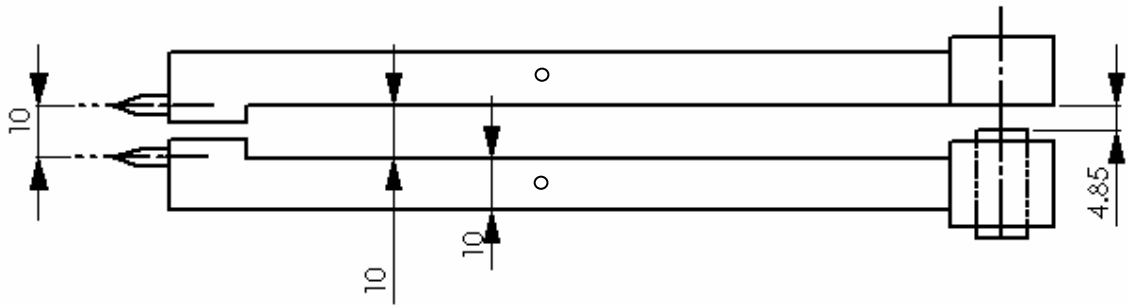


Figure 8.12. Arm design 3

It includes a projected tip to be able to supply a closer touch, closer areas for contact elements. The desired gage length is possible in that way and the projection must not be excessively high in length causing an inner contact which prevents to follow the specimen. In this mode of design, the rear ends of the arms would be the same as in the first choice.

Thus, the most appropriate arm design is the third mode with a 3.5 mm projection ahead.

The lower arm would carry the LVDT body inside. The best way was to hold the body's mid level at the same plane with the mid level of the rear portion of the lower arm. A small bolt would be enough to join, fix the position and prevent a possible motion of the body.

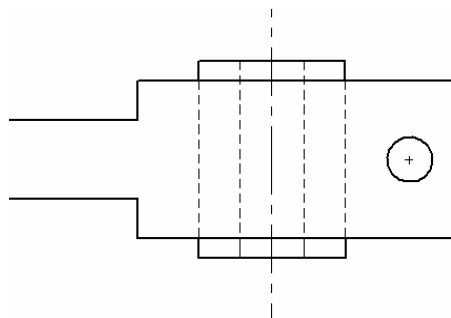


Figure 8.13. Possible design of the rear portion of the arm

At this condition, there would be a division with a larger section at the rear part with a hole all along this division to assemble the LVDT body and a slot which is featured by a bolt hole, with the addition of a screwed bolt the LVDT would be squeezed.

The upper arm would have to hold a rod and this rod would have to connect with the core. Schaevitz MHR050 LVDT has a core with a metric 2 thread inside. The product also can be coupled by an accessory of it, called core connecting rod. It was not possible, however, to reach this accessory in Turkey. The sole solution would be to prepare a rod with 2 mm diameter at a proper length and cut M2 thread on its one end. Besides an appropriate bolt which would hold that rod and whose pitch would be as small as possible would let us move the core sensitively with very little distances during calibration, before and after testing stage to prepare the instrumentation.

The analysis results exposes that using the arm mode three with an arm length of minimum 140 mm ($d_1 = 70$ mm) supplies a frictionless motion inside the LVDT and in this way the clearance is well enough. It is illustrated in Figure 8.14 for $d_1 = 70$ mm and 50 mm respectively.

Therefore with details, arm assembly includes two arms -upper and lower-, a special bolt to guide the core inside LVDT body and a rod connecting the core and the bolt.

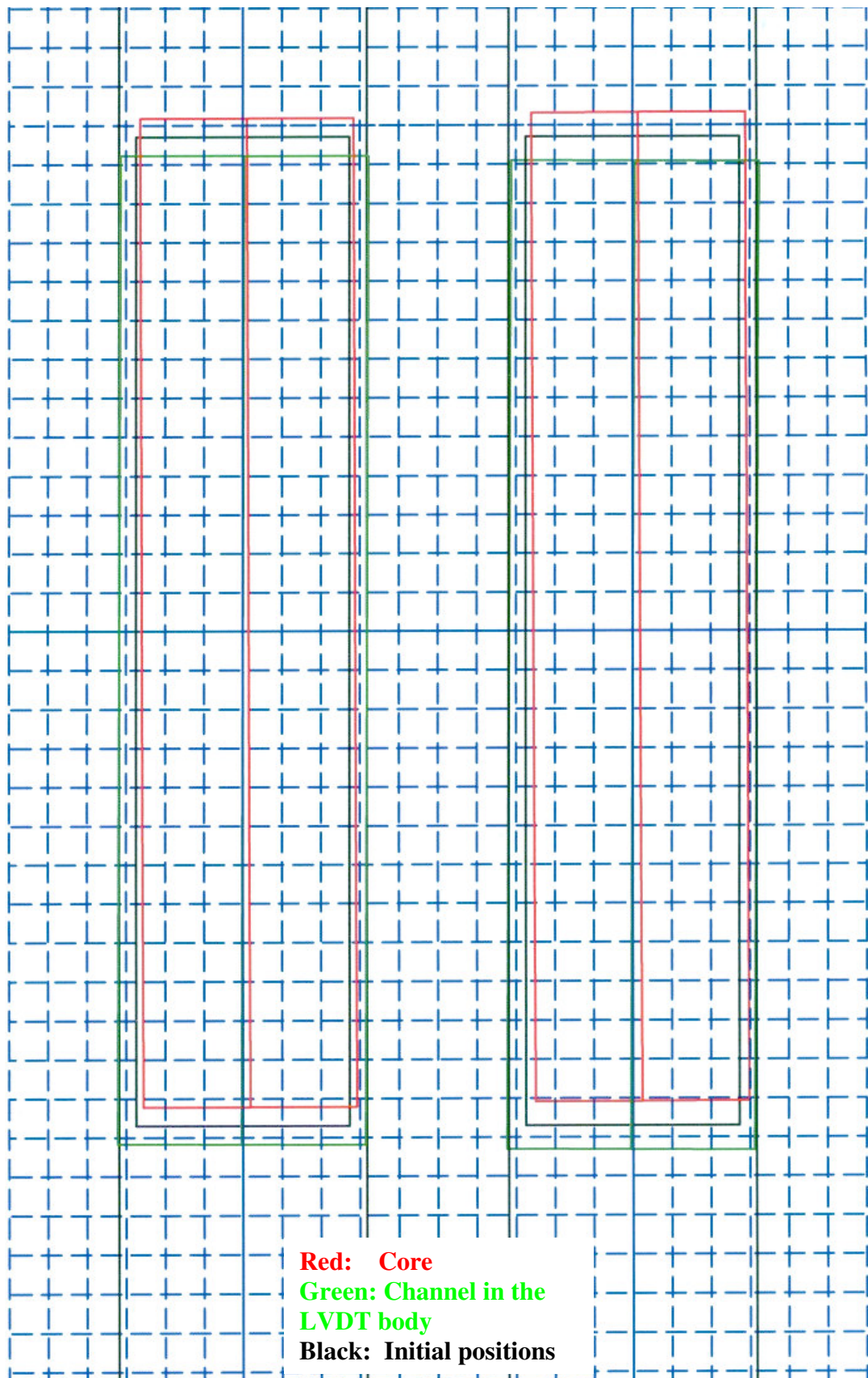


Figure 8.14. Demonstration of core and the target points when $d_1 = 70$ and $d_1 = 50$ mm for 1:1 lever arm ratio

9. FINAL DESIGN OF THE ELEVATOR

As it was discussed in the initial design section, the whole system consists of the elevator and the extensometer itself which are connected to each other.

The elevating system has a job that it serves to

- take the extensometer up and down,
- supply a heavy base to hold the system straight without an overturn,
- fix the system at a desired height,
- carry a rooted track to make a vertical linear motion possible,
- let the system make horizontal motions (forward, backward, left and right).

The elevating system consists of a heavy, large lower base plate at a proper thickness, an upper base plate relatively smaller than the lower base, a thinner cap plate to hold the shafts from top, two shafts to serve as a track, and a moving plate which includes the contact surface with the extensometer and several joining elements.

9.1. Upper Base Plate

Upper base (Figure 9.1 and Figure 9.2) is the part which contains the holes that the shafts are rooted and fixed inside; also it contains the bolt holes to attach itself to lower base plate. It is designed in a manner that all bolts which are in imbus style will be sunken with their heads.

The part is designed to have a 100 to 150 mm space between the shafts to install the extensometer in width. There must be an appropriate space to add the bolt holes attaching it to the lower base. Metric 6 bolts with sufficient height are appropriate for joining. The holes for shaft joining are special that they have diametrical steps for shaft, bolt and bolt head.

As a result, the part has overall dimensions of 210×80×35 mm. Four bolt holes are from end to end with 35 mm height including the sufficient cavities for sunken bolt heads. The shafts have a diameter of 25 mm. Diameter is decreased to 22 mm at the edges to release inside the plate with 15 mm length to provide a reference for an exact straightness and the shafts is supported from bottom by an M8 bolt for each. At these conditions, there is a 130 mm space to install the extensometer between two identical shafts.

The bolt holes are designed having intervals 180×60 mm. So it had to be adjusted in a way that 180 and 60 mm distances must be divisible by the distances between holes from center to center on the lower base plate.

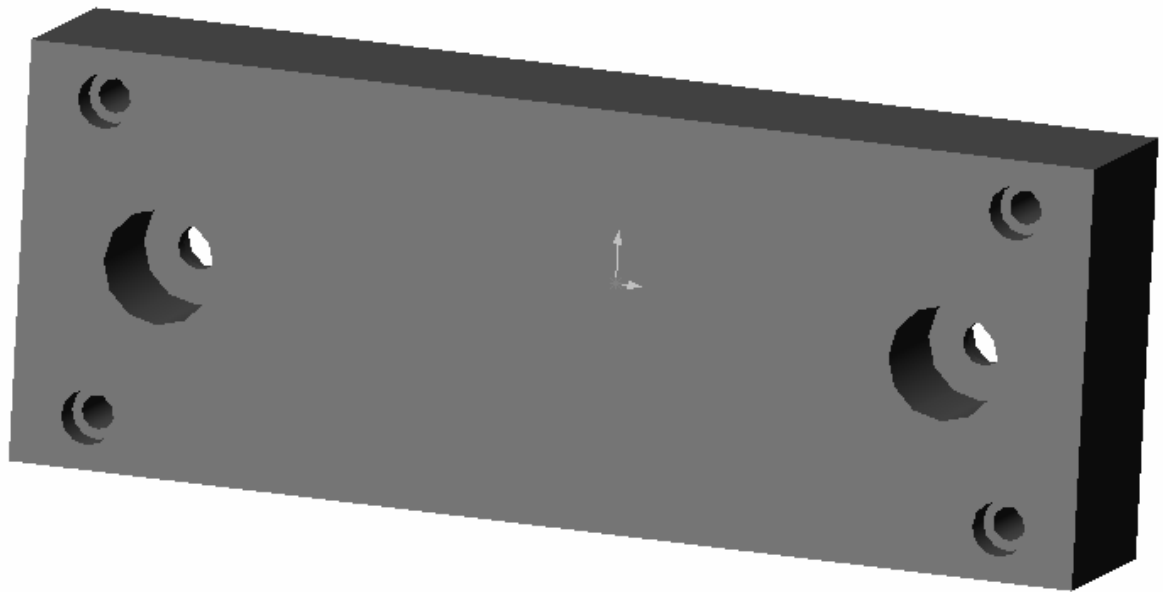


Figure 9.1. 3D view of upper the base plate

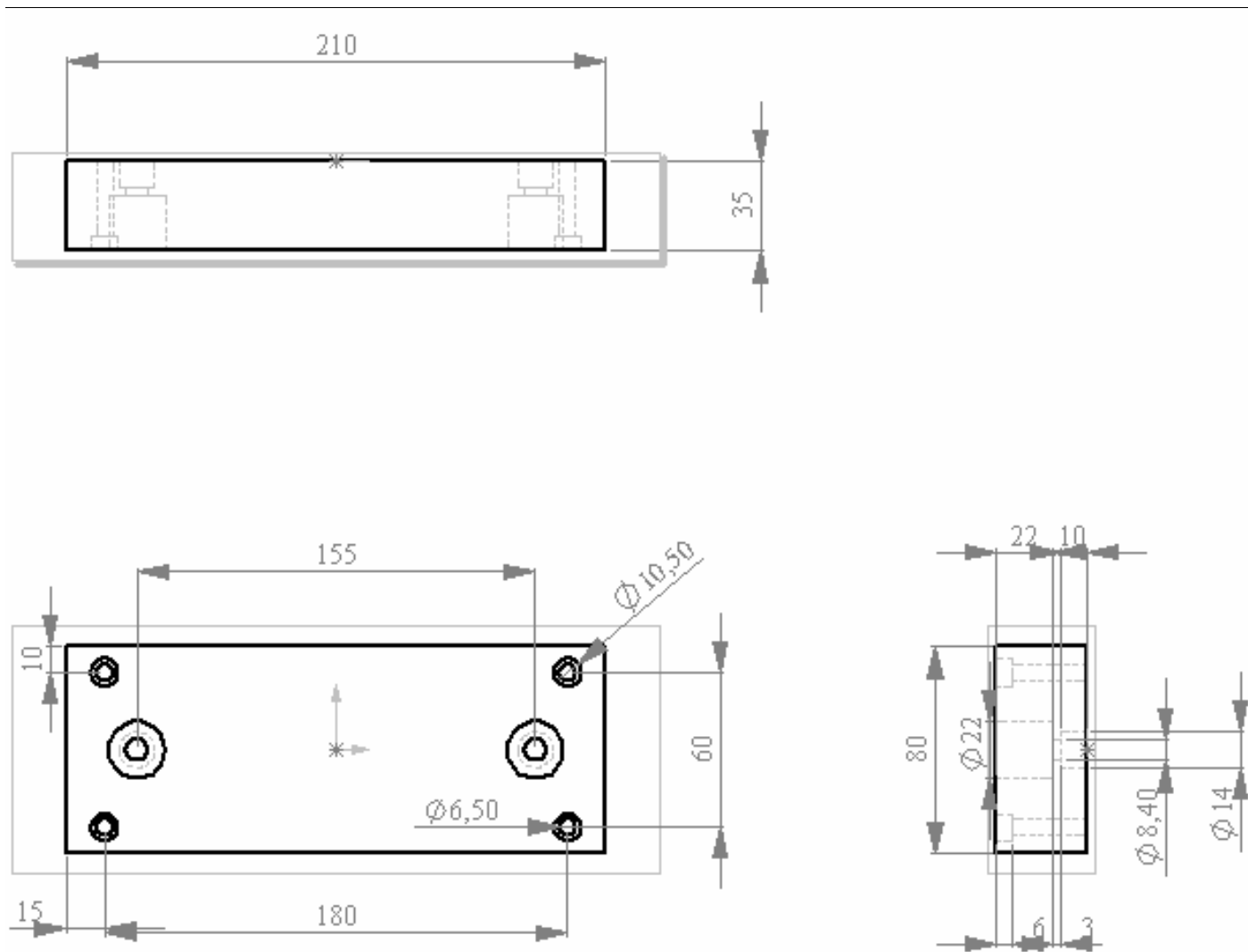


Figure 9.2. Orthographic projection of the upper base plate

9.2. Lower Base Plate

Lower base plate, first of all, must be heavy and large enough. Heavy weight is a necessity, because it must be motionless during the elements that it carries are moving and sliding. That is why the material is not important that much, but the best preference was a low carbon steel.

This lower base plate (Figure 9.3 and Figure 9.4) has the main characteristic that it contains a lot of holes which are spaced closely, but with equal intervals. The upper base is designed with 180×60 mm intervals. 20 mm is the most appropriate interval which divides both 180 and 60 mm. So the closely distributed bolt holes are 20 mm distant from each other by center.

The holes have 6 mm diameter with M6 threads. The overall dimensions are thought to be $400 \times 160 \times 25$ mm. From this point of view, the upper plate has a 180 mm freedom to move left and right with a minimum 20 mm steps. At the same way it can easily be calculated that it has besides a 60 mm freedom to move forward and backward again with minimum 20 mm steps. As a result the plane has $19 \times 7 = 133$ bolt holes totally. These holes are cut for thread with a 12 mm top length. The rest is threadless $\text{Ø}6$ hole.

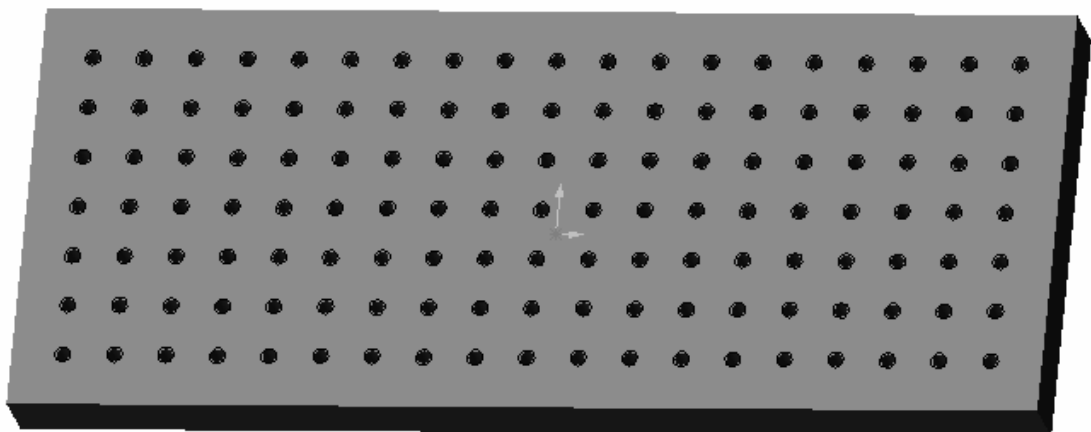


Figure 9.3. 3D view of the lower base plate

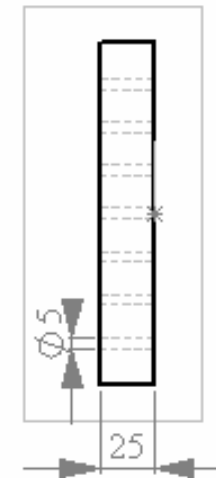
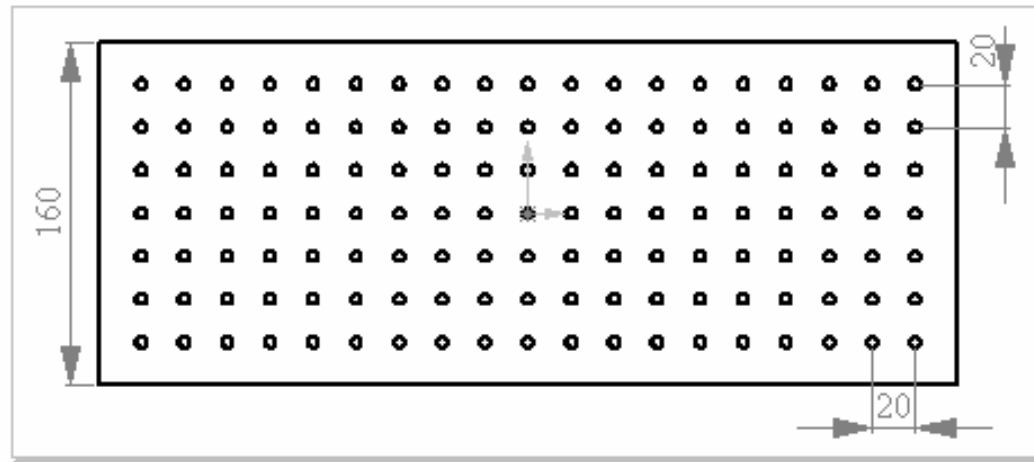
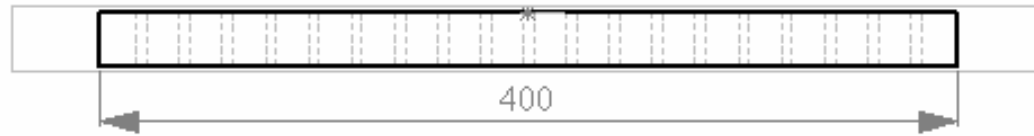


Figure 9.4. Orthographic projection of the lower base plate

The volume of the plate: $400 \times 160 \times 25 = 1600000 \text{ mm}^3$ (holes are excluded)

Density of low carbon steel $\cong 7.8 \text{ g/cm}^3$

Weight of the plate: $1600 \text{ cm}^3 \times 7.8 \text{ g/cm}^3 = 12480 \text{ g}$

12 kg of weight seems to be enough for the block to serve a motionless behavior.

9.3. Cap Plate

The most and only essential job of the cap plate (Figure 9.5 and Figure 9.6) is to hold the shafts straight and parallel to each other to provide a smooth motion for the moving plate. Two shafts need attachment to upper base plate from its base and are supported from top by a similar but narrower type plate. This plate only contains a couple of diametrically stepped holes. These holes are only to join the cap plate to two shafts and to sink the bolt caps. Bolts are again identical with the ones used with the upper base plate. The shaft side diameter is 22 mm with a 5 mm depth this time. Since there is no friction with another surface, and in order to get rid of excess weight; aluminum, not a steel based material, is preferred.

The overall dimensions are $190 \times 35 \times 20 \text{ mm}$. 35 mm is enough only to hide the shafts from top. 20 mm is appropriate for sunken bolt heads and shaft tops. The distance between the shafts from center to center is identical as at the upper base plate to supply two complete shaft axes.

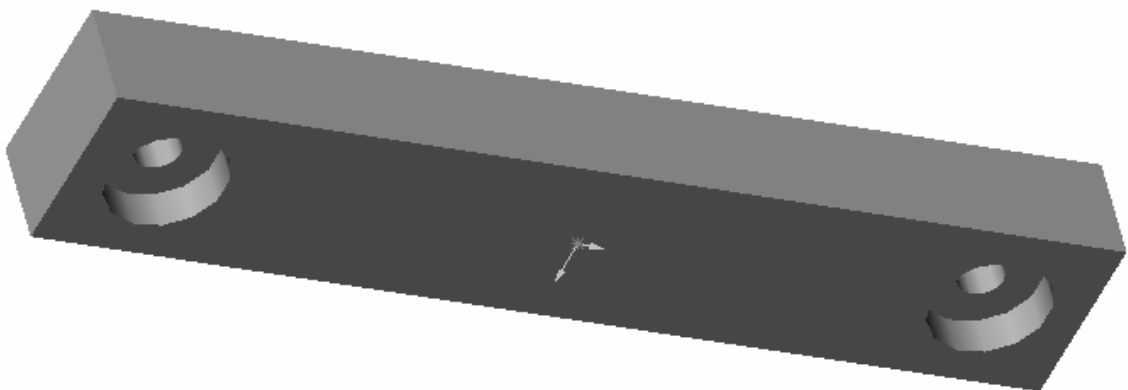


Figure 9.5. 3D view of the cap plate

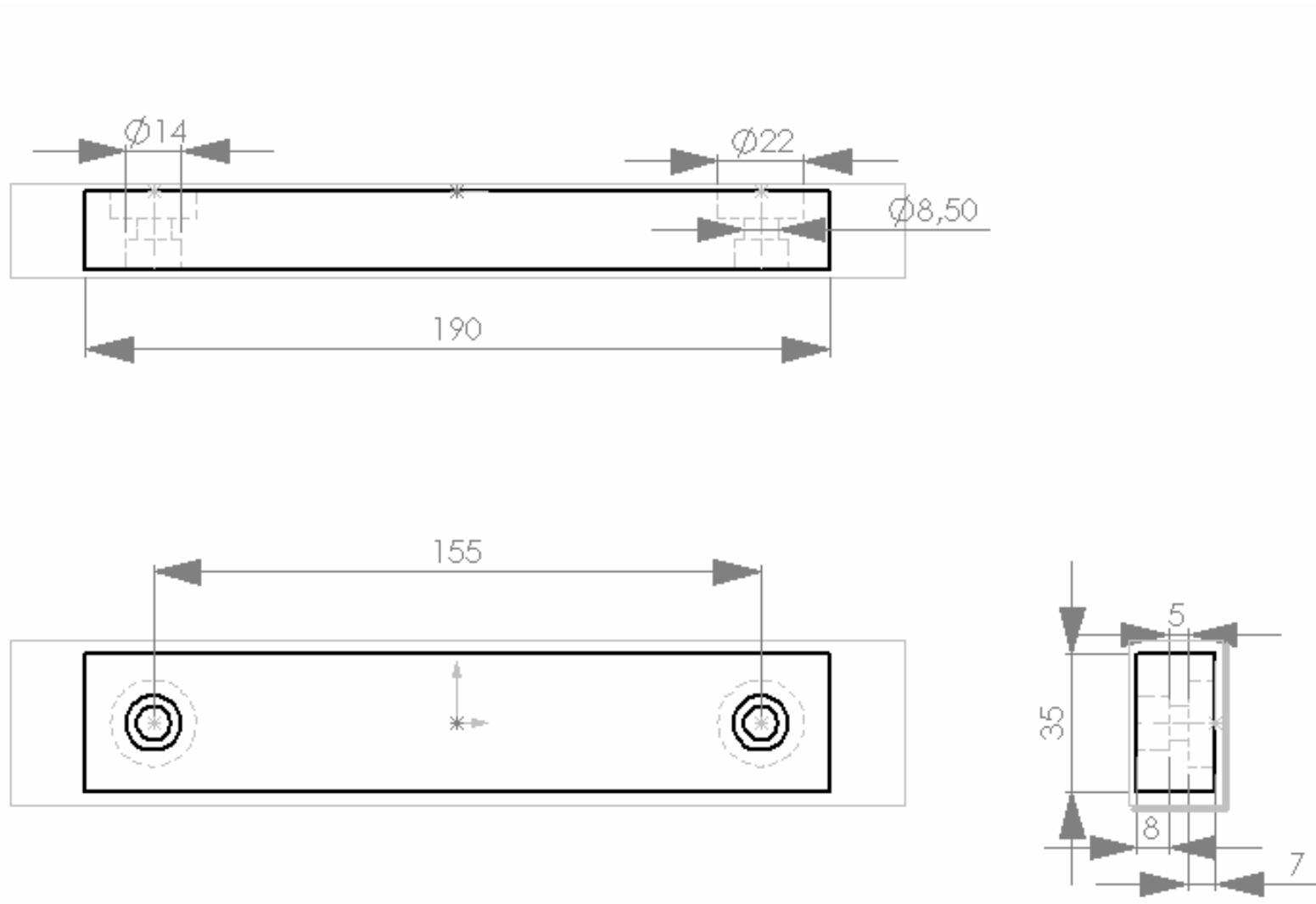


Figure 9.6. Orthographic projection of the cap plate

9.4. Shafts

Shafts (Figure 9.7 and Figure 9.8) are serving as the elevating system's track along which the moving plate is taking the extensometer up and down. The lower base plate and the cap plate are designed with a diametrically stepped hole and one and the biggest step is 22 mm. As the same way, the shafts have a diameter of 25 mm, except it has diametrical decrease with 3 mm at both ends, one with 15 mm length to be released inside the upper base plate and one with 5 mm length to be released inside the cap plate.

Both ends have a bolt hole with M8 thread and length of 20 mm for each. The overall dimension of each shaft is $D25 \times 820$ mm.

Since it is facing with friction as a result of possible repetitive displacement of the moving plate, the material must be resistive against wear and hard enough. 1.2210 [115CrV3, K510 (Böhler)] is a good alternative among cold worked tool steels.

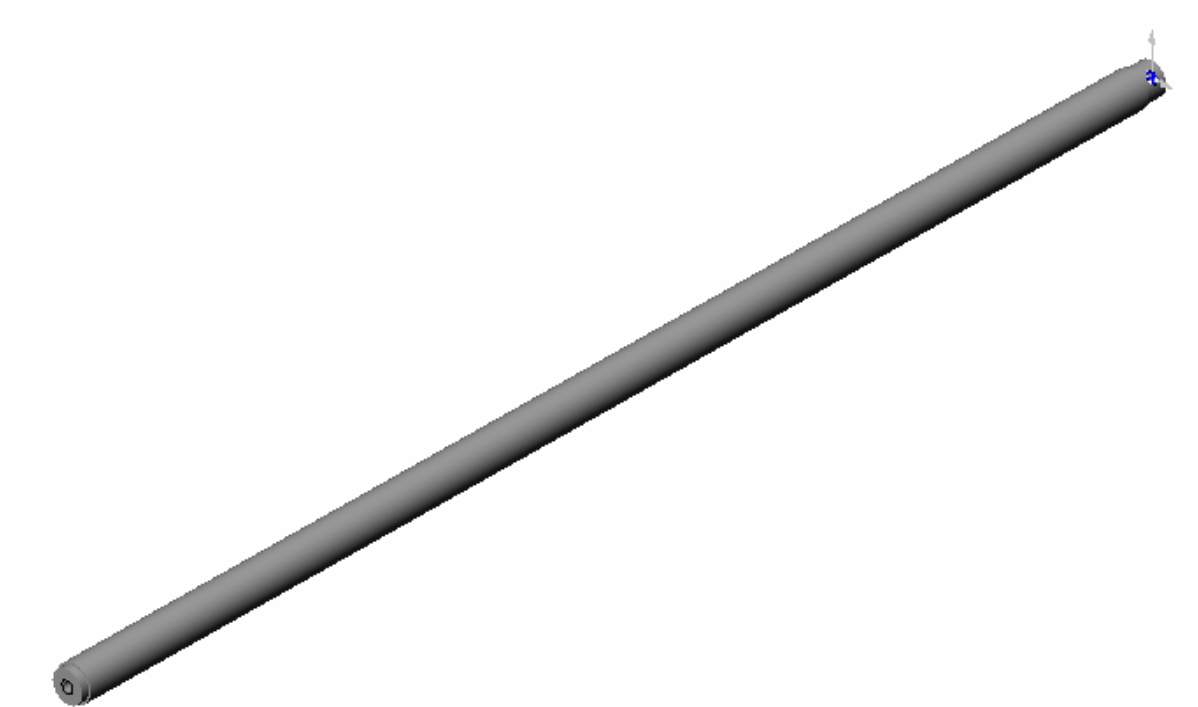


Figure 9.7. 3D view of the shaft

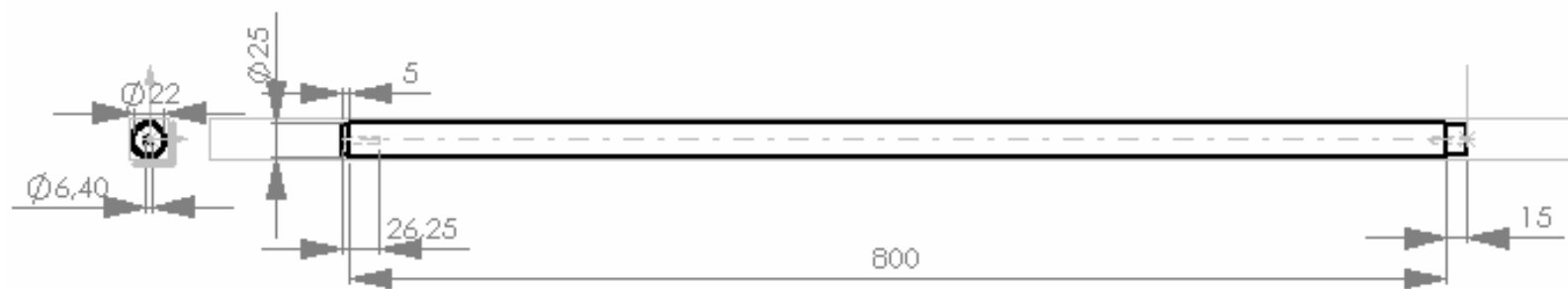


Figure 9.8. Orthographic projection of one shaft

9.5. Moving Plate

Moving plate (Figure 9.9 and Figure 9.10) is the element in the elevating system, which takes the extensometer up and down, also which only contacts with the extensometer. In other words, it is the connecting element between the elevating system and the extensometer. This part has a female structure of the two shafts with two holes with the diameter of 25 mm. The outer sides of these holes contain one slit along whole depth to fix the moving plate and consequently the extensometer by one bolt, when the appropriate height is adjusted. One side of the slit has the hole with M8 thread.

Roughly the dimensions of the part are $210 \times 70 \times 27.5$ mm. But the outer sides of the shaft holes are narrowed to 45 mm to provide an easier and more flexible fixing by M8 bolts which are sunken in the part with their heads.

Another case is that there are seven bolt holes in a row with threads in the midst of the moving plate to join the extensometer to the most appropriate position.

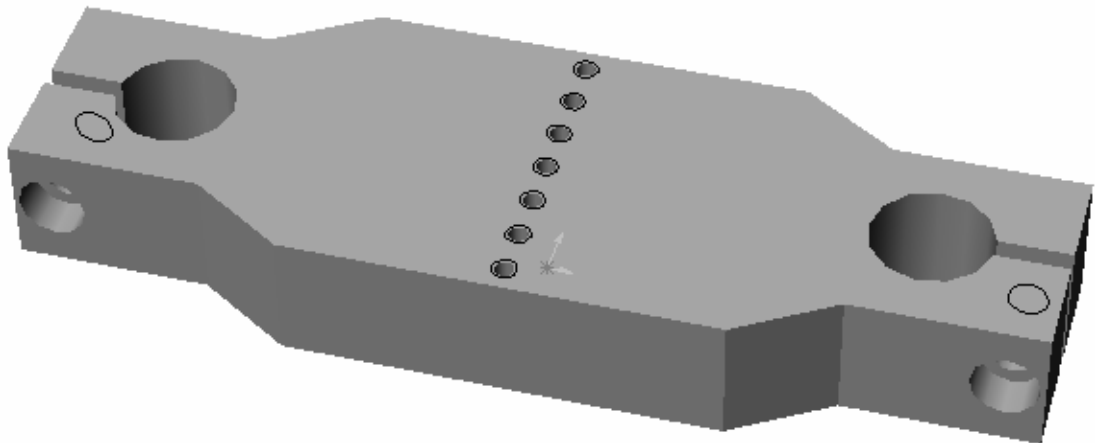


Figure 9.9. 3D view of the moving plate

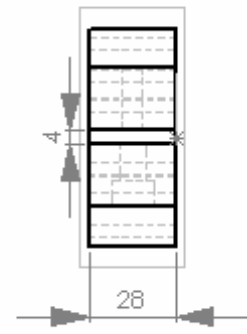
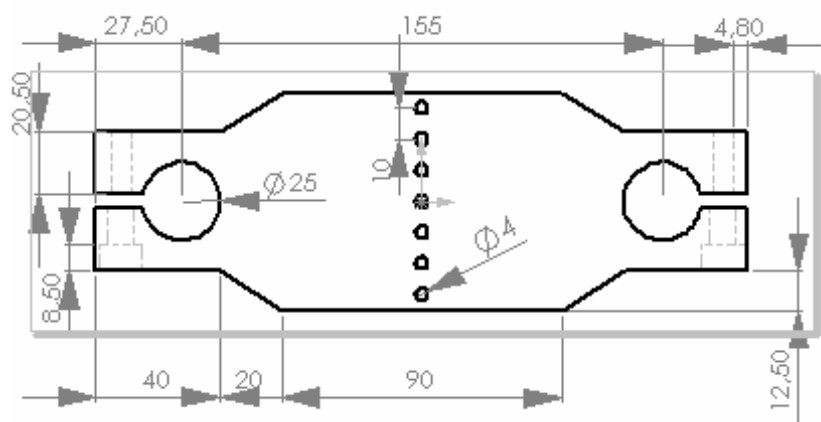
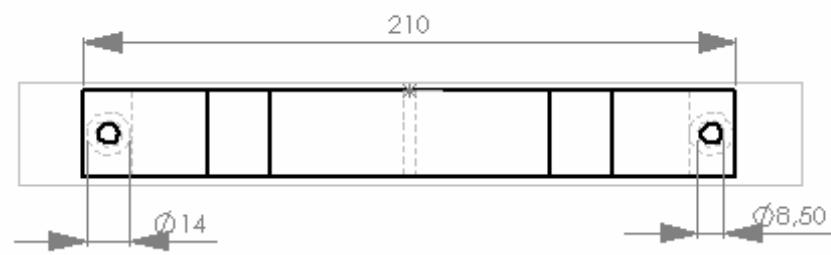


Figure 9.10. Orthographic projection of the moving plate

10. FINAL DESIGN OF THE EXTENSOMETER

The whole measurement system excluding the elevating system is the extensometer itself, which must be designed and manufactured with much more care and much more sensitively.

The extensometer is the combination of the extensometer body and LVDT and its accessories. The whole construction of the extensometer body includes two brackets and its supporting rods forming a ladder like structure, a rectangular chassis carrying the two lever arms with the assistance of plunger type joining elements which will be discussed and informed about in the following section, the two lever arms holding the LVDT and its core that cooperates with a core connecting rod and a bolt which is specially manufactured, the two contact elements which are fixed at the front side of the arms, and finally the base plate of the extensometer which is the only connection to the other main system, the elevator.

All member of the extensometer, except the LVDT with its core, core connecting rod, contact elements and of course the special bolt, have a rectangular sectioned design. Each member of this construction is represented one by one.

10.1. Brackets

The two brackets' (Figure 10.1 and Figure 10.2) main functions are to

- carry the chassis, so the lever arms too, and let it rotate around the plungers to get it positioned vertical to the ground,
- serve as the element to be attached to the base plate again with plungers to adjust the target inclination angle concerning the contact force.

It is also supported by the supporting rods to obtain a strengthen construction under the arms within the chassis.

The overall dimensions of the part is roughly $200 \times 16 \times 12$ mm. Since it is translating the elements on its upper side by inclining forward, it needs to have an enough length to reach by the specimen. It is designed with a rectangular section of 16×12 mm against the tendency to an unwanted bending behavior. The regions are shaped considering the supporting rods to penetrate within 16×12.1 sockets.

These regions are also containing holes for bolting the supporting rods to the brackets, and holes with threads to attach the plungers inside to press on the chassis and lower plate of the extensometer from both sides.

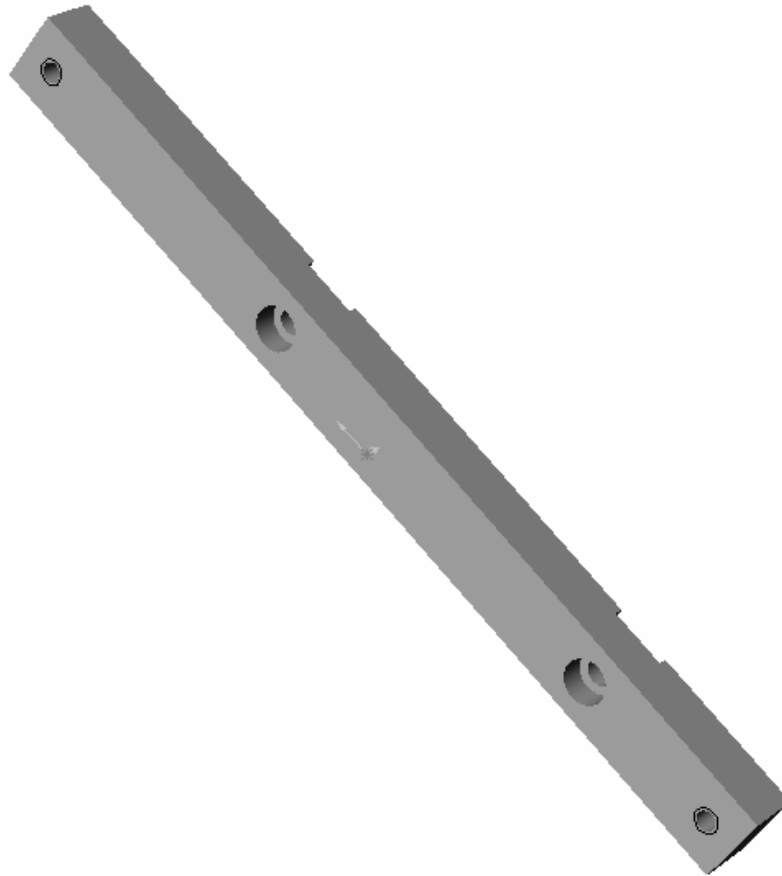


Figure 10.1. 3D view of one bracket

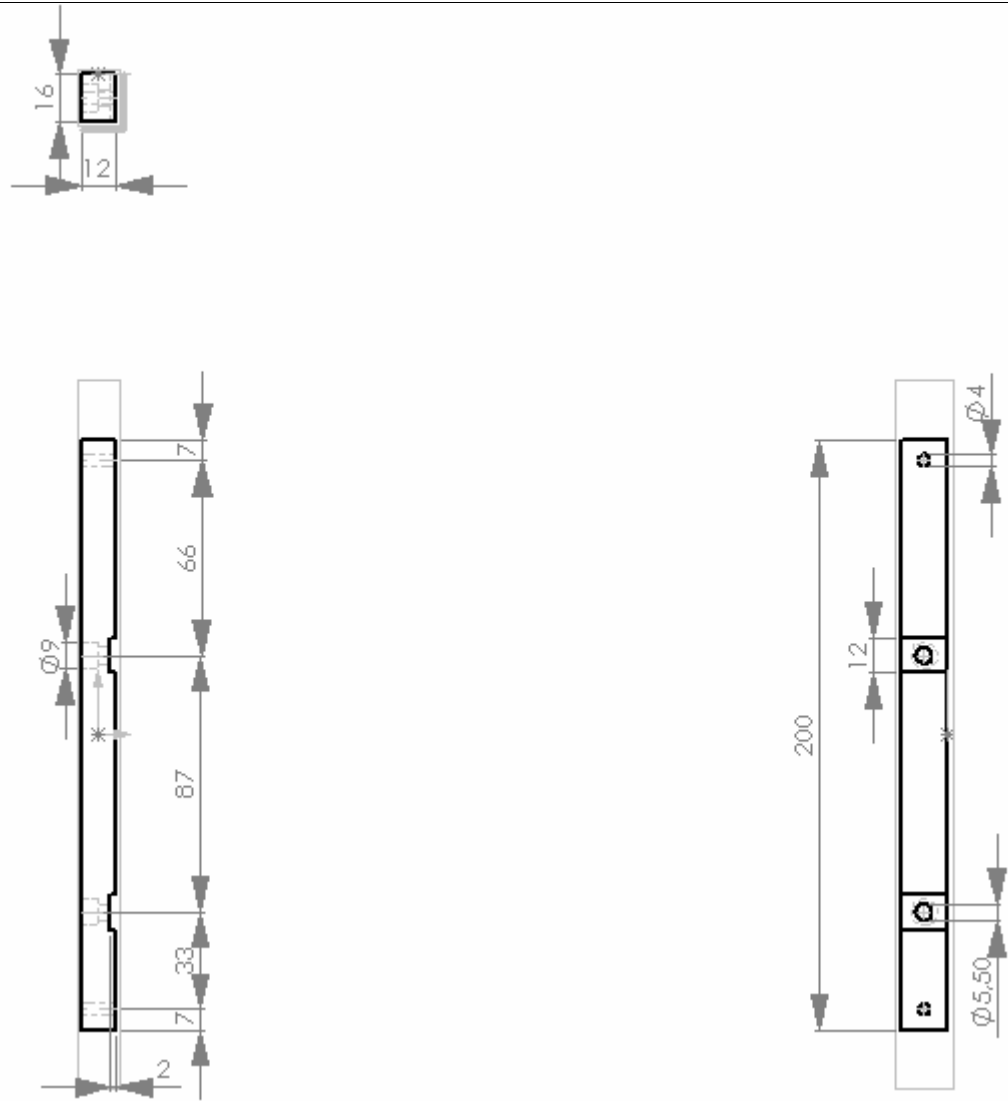


Figure 10.2. Orthographic projection of the bracket

10.2. Chassis

Chassis (Figure 10.3 and Figure 10.4) is the part on which the two lever arms are positioned between the plungers to be suspended and rotate independently. On the other hand, it is rotating around other two identical plungers. So that it is carried by the brackets.

At first view, it was designed to be a narrow rectangular shape. But the chassis and the plungers are cooperating. That is why, the dimensions of the most suitable plunger is taken into account before rearranging the chassis design. The total length is 20.5 mm for the plunger which is discussed in the following section. From this point of view, it was obvious that the best way was to enlarge the width to make the plunger fit longitudinally.

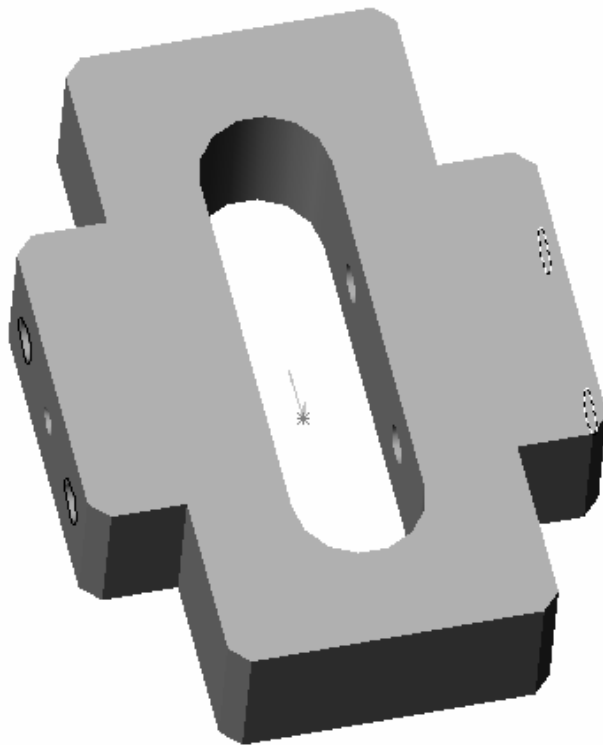


Figure 10.3. 3D view of the chassis

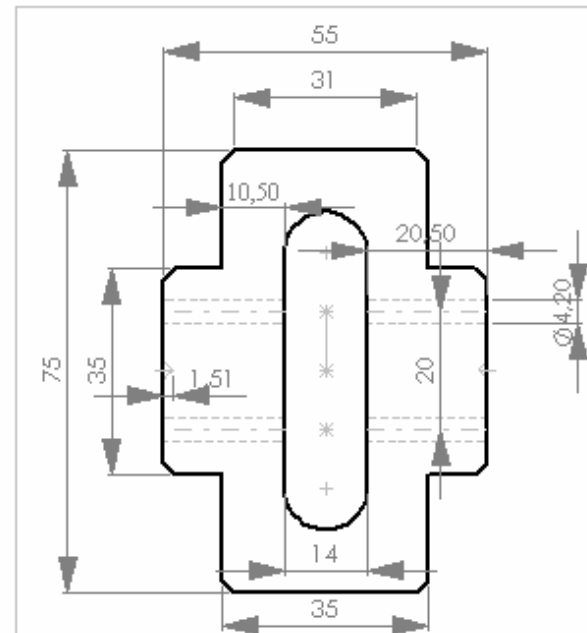
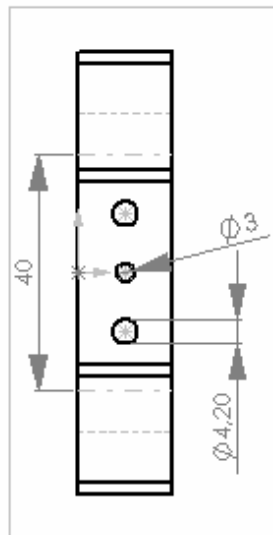
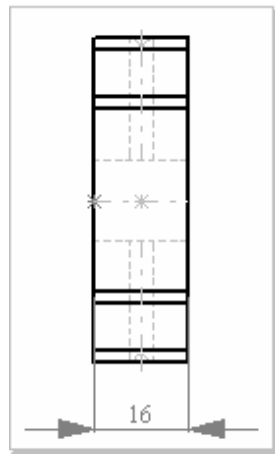


Figure 10.4. Orthographic projection of the chassis

For these reasons, the overall dimensions of the chassis are $75 \times 55 \times 16$ mm. It has a rounded cavity on its longitudinal central axis with a length of 54 mm. The outer edges are all chamfered. It has two holes with M5 threads to bolt the plunger and one cone-shaped hole for the tip of the plunger at each side.

The excess material would be shaved at four corners with 10×20 rectangles. The thickness of the plus-shaped chassis is also 16 mm which coincides with the lateral thickness of the brackets.

10.3. Base Plate

Base plate (Figure 10.5 and Figure 10.6) is the part which functions first to make the two brackets rotate around and second to attach the extensometer construction to the elevating system through the moving plate.

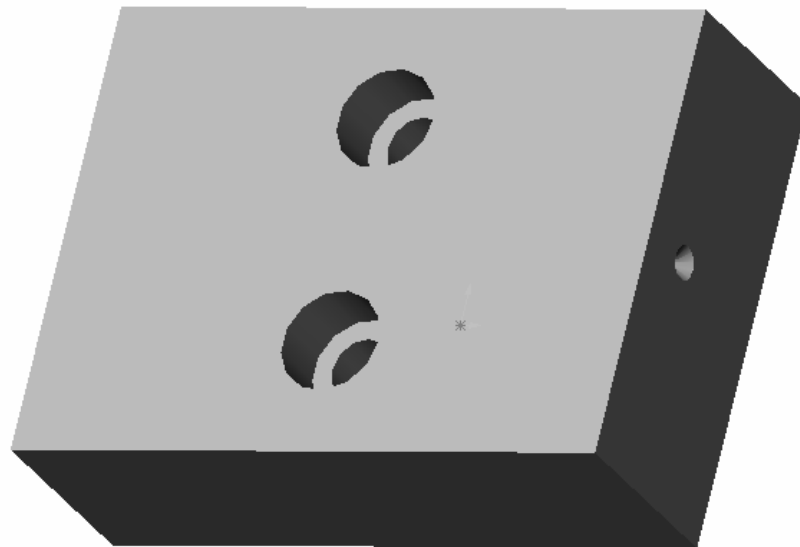


Figure 10.5. 3D view of the base plate

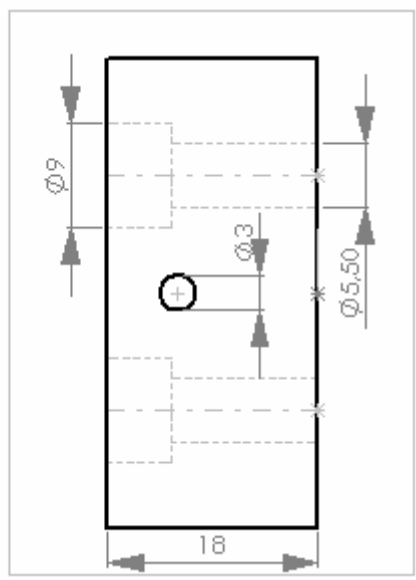
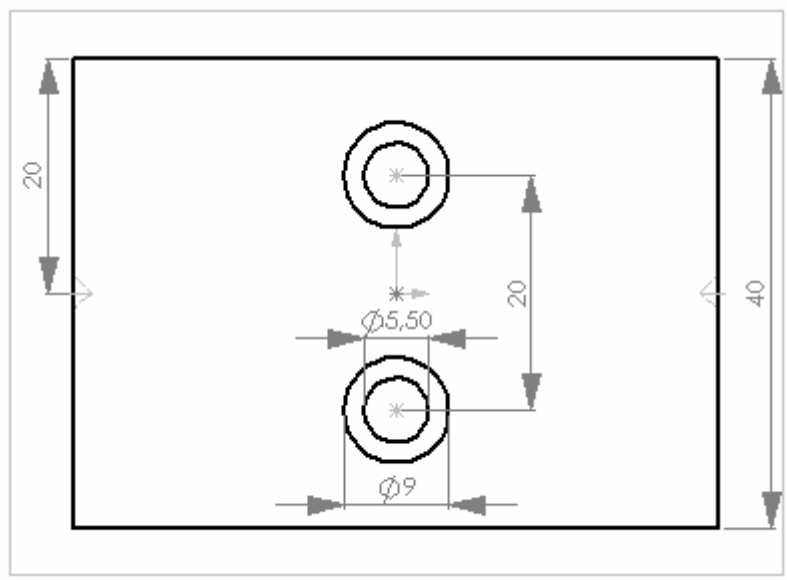
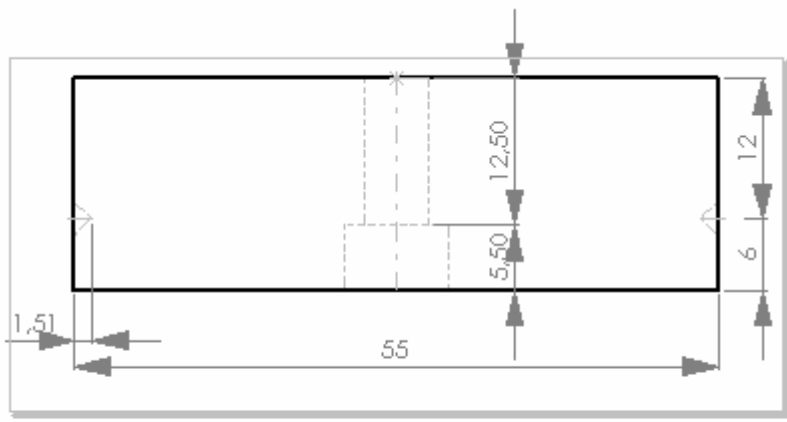


Figure 10.6. Orthographic projection of the base plate

It is a rectangular part with overall dimensions of 55×40×18 mm. 55 mm is chosen to be as the same as the width of the plus-shaped chassis. In 40 mm, attachment is possible by two M5 bolts. The two imbus M5 bolt holes are placed with a spacing of 20mm and are arranged to make the bolts sunken and to reach to the threads on the moving plate. The threaded holes on the moving plate give a freedom of 50 mm to the part to move forward and backward with 10 mm steps.

The cone shaped holes which contact with the spherical edges of the plungers are placed at an appropriate height that the edges and the corners of the brackets are not touching the moving plate of the elevator when it rotates.

10.4. Supporting Rods

As its name makes it clear, the function of the supporting rods (Figure 10.7 and Figure 10.8) is to support the brackets from within to construct a rigid and strong assembly together with the brackets.

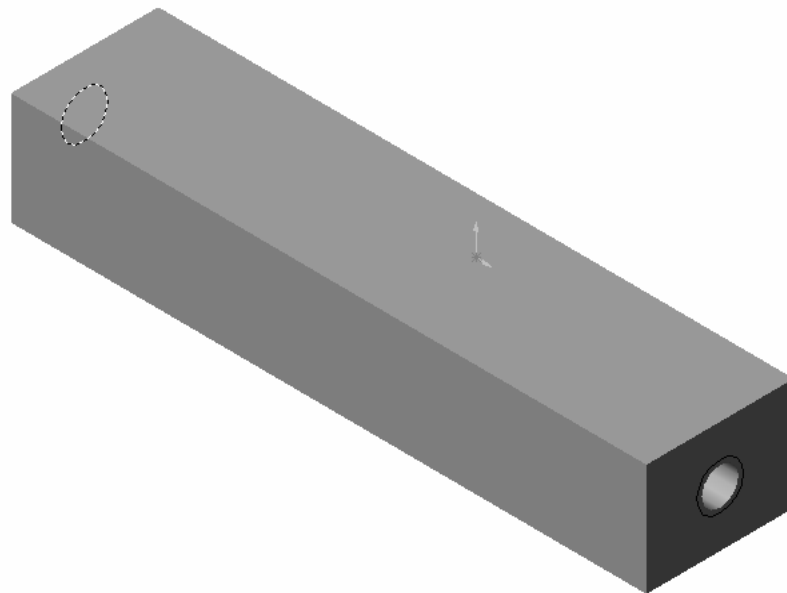


Figure 10.7. 3D view of the supporting rod

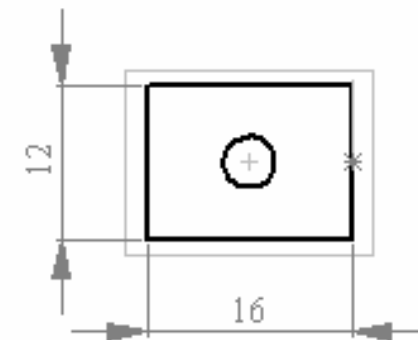
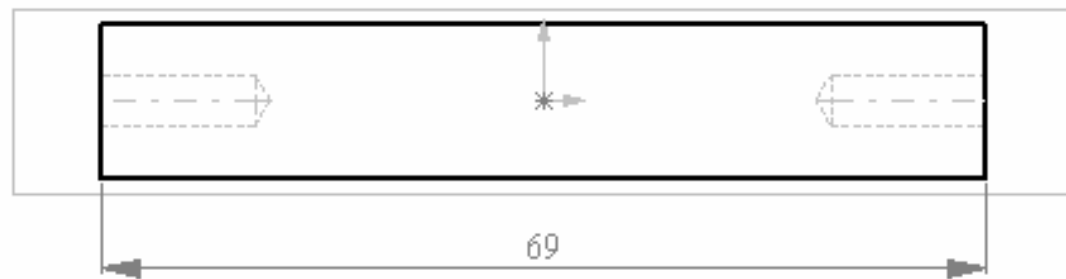
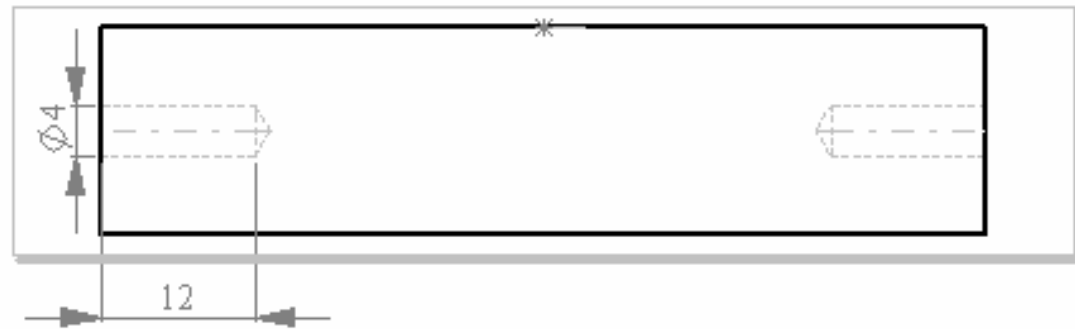


Figure 10.8. Orthographic projection of the supporting rod

The sectional dimensions are identical with the brackets (16×12) and the vital dimension is the length of the supporting rods. Because this determines the equal clearances between the couples, brackets-chassis and brackets-base plate. The clearances are composed to be 5 mm from each side of the chassis and the base plate to the brackets. That makes a 10 mm length addition and also the 2 mm deep sockets on the brackets make 4 mm length addition. That is why the overall dimensions of the two supporting rods are 69×16×12 mm.

It needs one hole with an M5 thread on its both sides to make the assembly with the brackets.

10.5. Upper Arm

As it was stated in the arm design section, the most essential part of the whole system is the arms. The upper arm's functions are to

- contact the specimen indirectly with the presence of the contact element,
- provide a space to fix the contact element,
- carry the specially manufactured bolt with a very low pitch value at the rear side,
- ensure a constant position for that bolt,
- rotate around the plungers freely, and finally
- sense the displacement at the target point on the specimen and translate it directly to the point on the center of the special bolt.

The upper arm (Figure 10.9 and Figure 10.10) has overall dimensions of 167×16.5×16 mm roughly. But mostly it has a cross-section of 10×8 mm along the arm. The exceptional regions are the front and rear end of the arm. The front end's cross-section is 13.5×8 mm with a 15 mm height. This portion is strengthened to be able fix the contact element inside and press on it with a set-screw. The rear end's cross-section is 13×16 mm with a 20 mm height. This portion is thickened to provide an appropriate placement of the low pitched bolt which controls the release of the core connecting rod which is bonded with this bolt from one side and with the core from the other side.

The cross-sectional change is straight at front, but rounded at the rear end. The bolt hole has got also thread and slot to fix the position of the special bolt by again another smaller bolt at the very rear end. That is why one side of the slot contains a hole with thread.

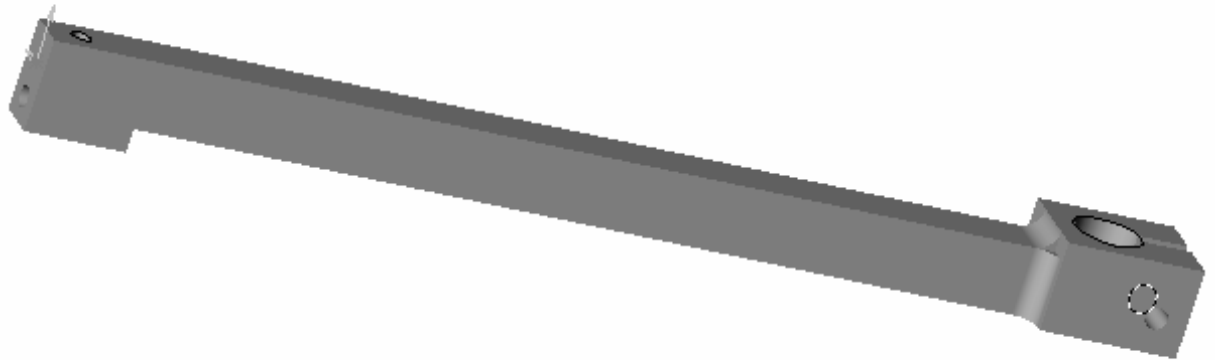


Figure 10.9. 3D view of the upper arm

The upper arm contains also a cone shaped hole to supply its own rotation. The coordinate of this hole is adjusted as the midpoint of the 10 mm height and the midpoint of the overall length from the tip of the contact element, after it is mounted on the arm, to the central axis of the hole of the special low pitched bolt.

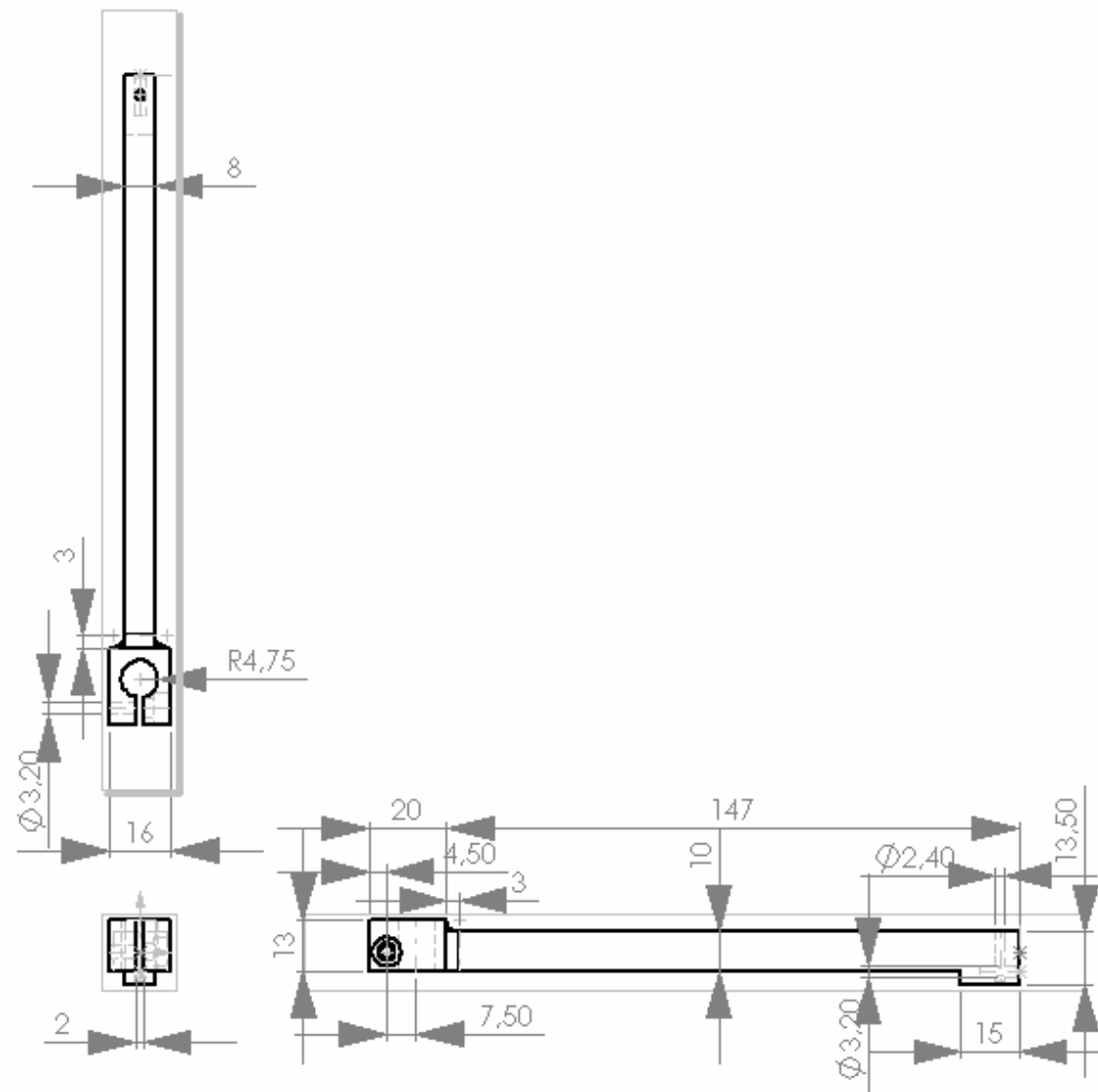


Figure 10.10. Orthographic projection of the upper arm

10.6. Lower Arm

The lower arm (Figure 10.11 and Figure 10.12) is also joined to a contact element as the upper arm is and also it is rotating around another plunger to translate the displacement of the other target point of the reference gage length to the center of the bore of the LVDT body. But the difference from the upper arm is that it carries the LVDT body in which the core moves up and down at the rear side and holds it tight not to let the body move.



Figure 10.11. 3D view of the lower arm

It has overall dimensions of $167 \times 16.5 \times 16$ mm roughly too like the upper arm and mostly has a cross-section of 10×8 mm along the arm. It has the same cross-section as the upper one has, 13.5×8 mm with a height of 15 mm for the contact element. At the same way, a set-screw is applied. The rear end's cross section is 16×16 as a differentiation with a 20 mm depth. This zone has a similar function like the upper arm has. But its duty is to hold the LVDT body at a desired level which is projected to be the midlevel of the rear end. In the same manner, a slot with a small bolt hole is available.

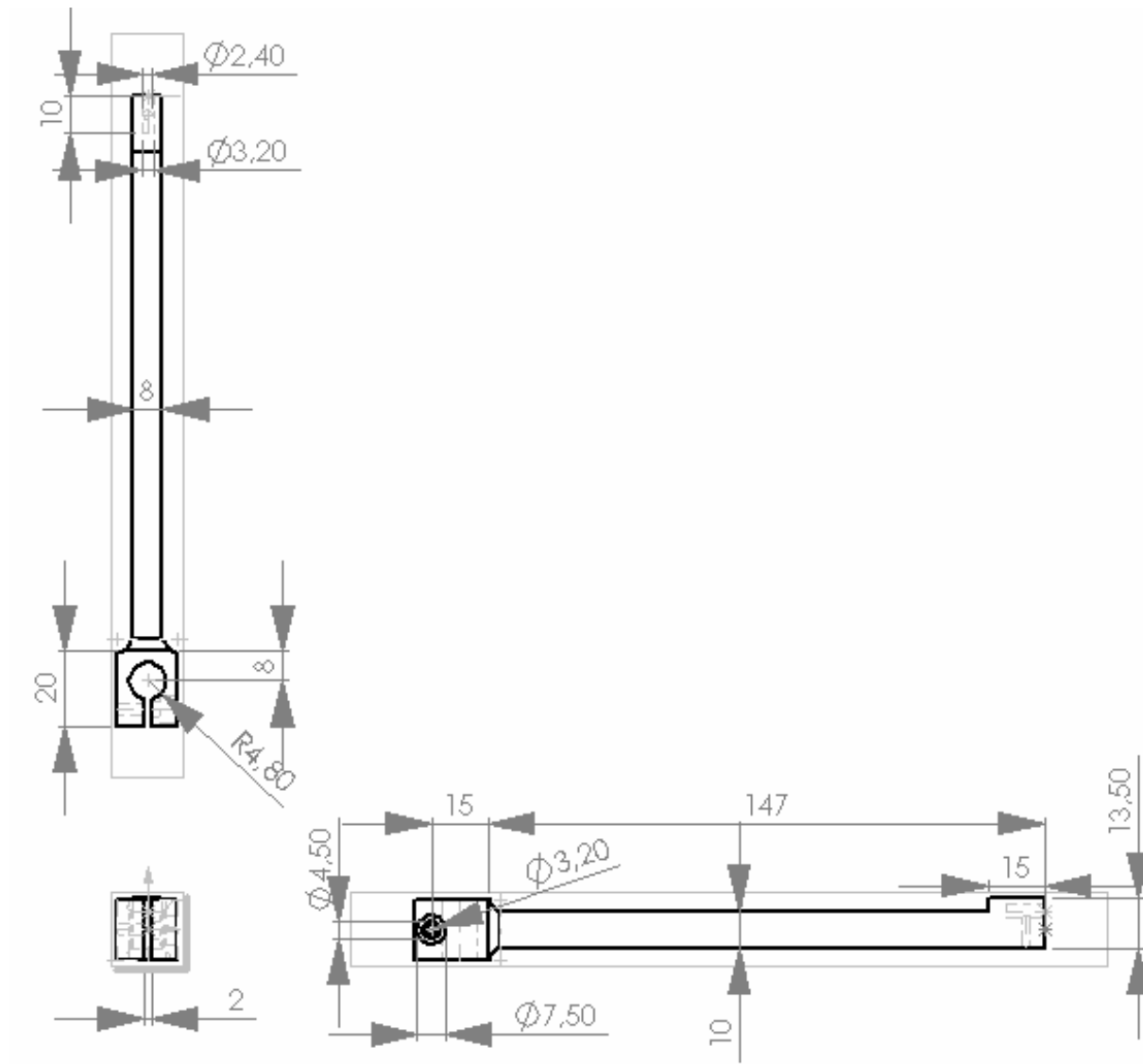


Figure 10.12. Orthographic projection of the lower arm

10.7. Special Bolt with Low Pitch

The only reason for using a specially manufactured bolt (Figure 10.13 and Figure 10.14) is that it has to be moved up and down sensitively while it is holding the core by a rod. That is why there is a need for a small pitched bolt which would also be used practically by handling. The advantage of this utilization is that it is possible to know the amount of bolt's release by a scaled bolt head. The bolt head also contains a nerved part for the ease of handling.

Pitch of this special bolt is 0.75 mm and the head contains 30 divisions which make a 0.025 mm displacement upwards and downwards by a rotary motion within only one division. It is expected from the bolt that it would serve a good behavior during calibration processes and to find the exact midpoint of the LVDT bore.

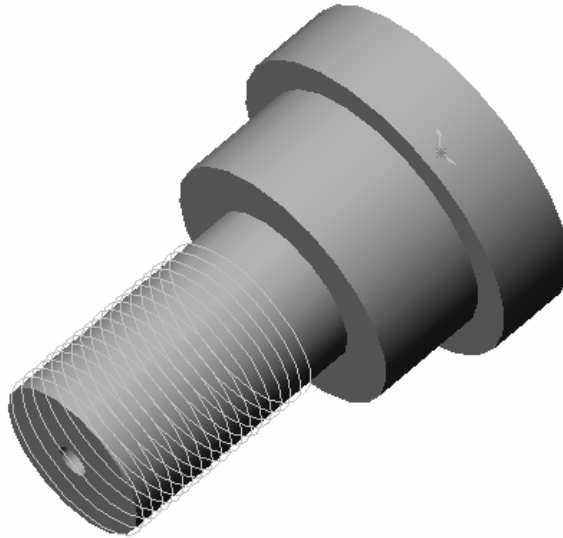


Figure 10.13. 3D view of the special bolt

The overall height of the bolt is 28 mm. It is not a metric bolt. A standard metric M10 bolt has a 1.5 mm pitch. Diameter of the base circle for threads is 10 mm and with the threads included 10.5 mm. Head height is 12 mm, scaled lower portion is 7 mm and the nerved portion is 5 mm of height.

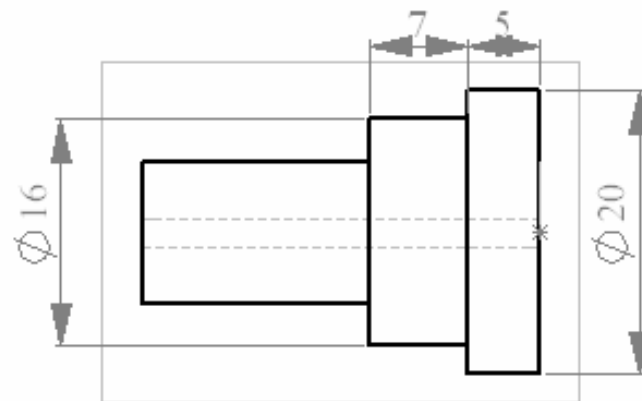
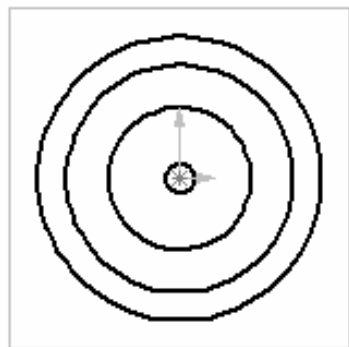
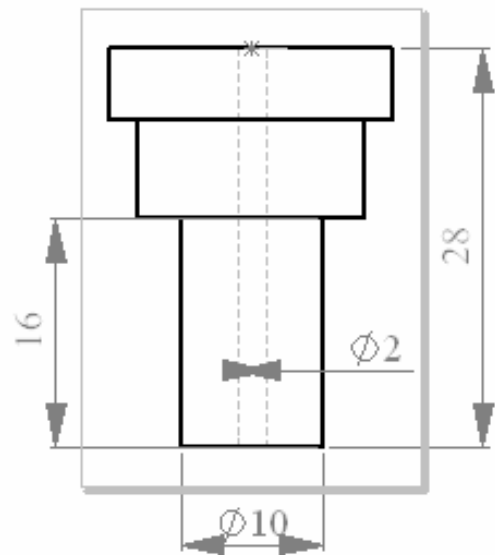


Figure 10.14. Orthographic projection of the special bolt

It contains a hole from top to bottom with a 2 mm diameter to cover the core connecting rod and a radial hole at the scaled portion to attach a set-screw which is pressing on this rod.

10.8. Core Connecting Rod

Core connecting rod (Figure 10.15 and Figure 10.16) is a very thin with a 2 mm diameter which has a function of carrying the core with the help of the M2 thread on its lower tip and reaching to the specially manufactured bolt and being held by a set-screw on the bolt.

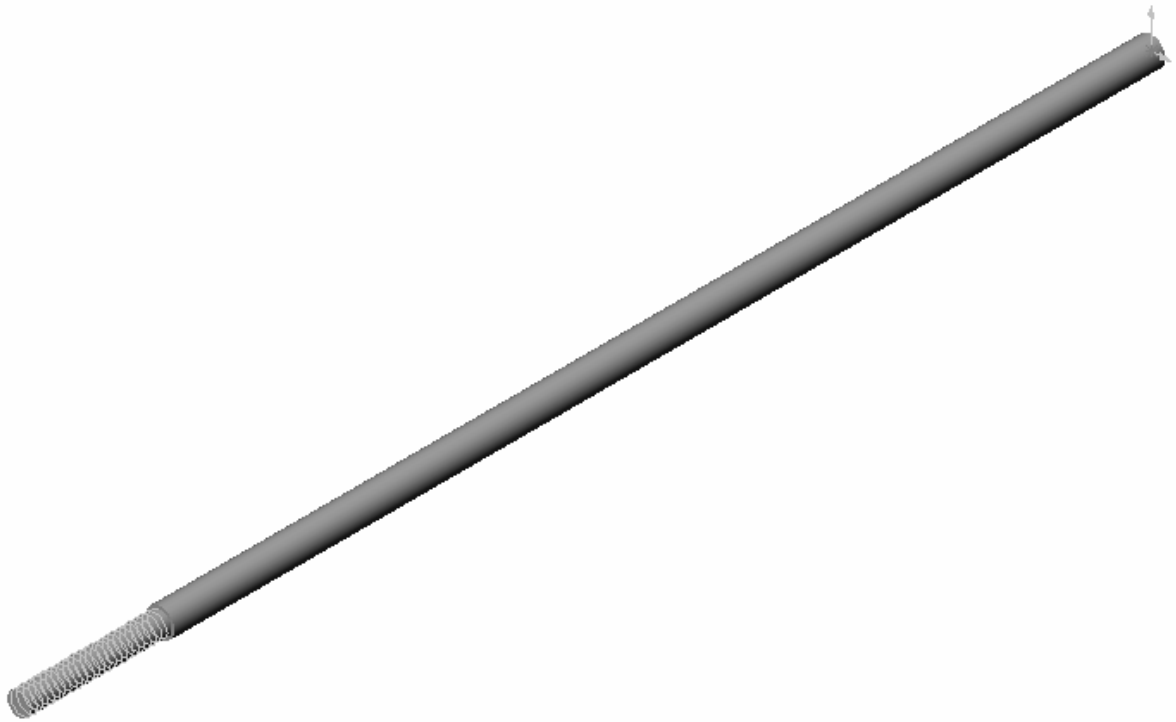


Figure 10.15. 3D view of the core connecting rod

Its overall dimensions are $D2 \times 80$ mm and the height of the threaded zone is 10 mm which is to be attached to the core hole.



Figure 10.16. Orthographic projection of the core connecting rod

10.9. Connecting Elements

Connecting elements (Figure 10.17 and Figure 10.18) are the only parts which touch the target specimen from one point for each. So it must be a spiky and sharp pointed tool and this top and sharp point must be concentric with the axis of the overall connecting element. This is the most important point for this part.

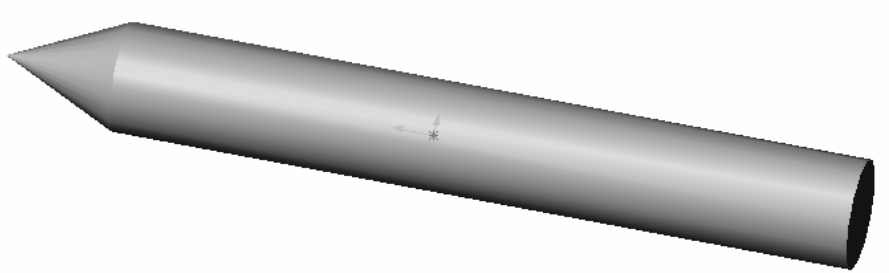


Figure 10.17. 3D view of the connecting elements

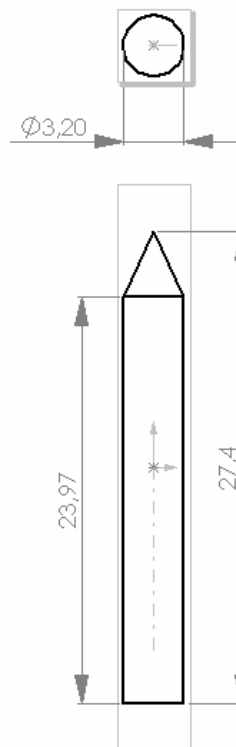


Figure 10.18. Orthographic projection of the connecting elements

The length of the element is 27.4 mm with a diameter of 3.2 mm and its top angle is 60°.

10.10. Additional Weights

Those are the parts to balance the lower and the upper arms in Figure 10.19 and 10.20, because the LVDT side and the special bolt side respectively for each make the arms turn preventing the balance.

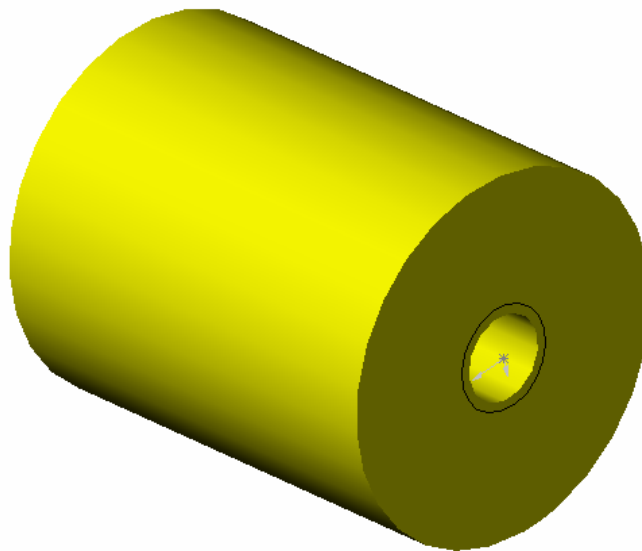


Figure 10.19. 3D view of additional weight of the upper arm

So a brass cylindrical weight for each arm which has overall dimensions D14x17.5 mm and D14x12.5 mm is joined by a set-screw on each arm from upper surface for the upper and lower surface for the lower arm respectively to ensure a low volume as much as possible.

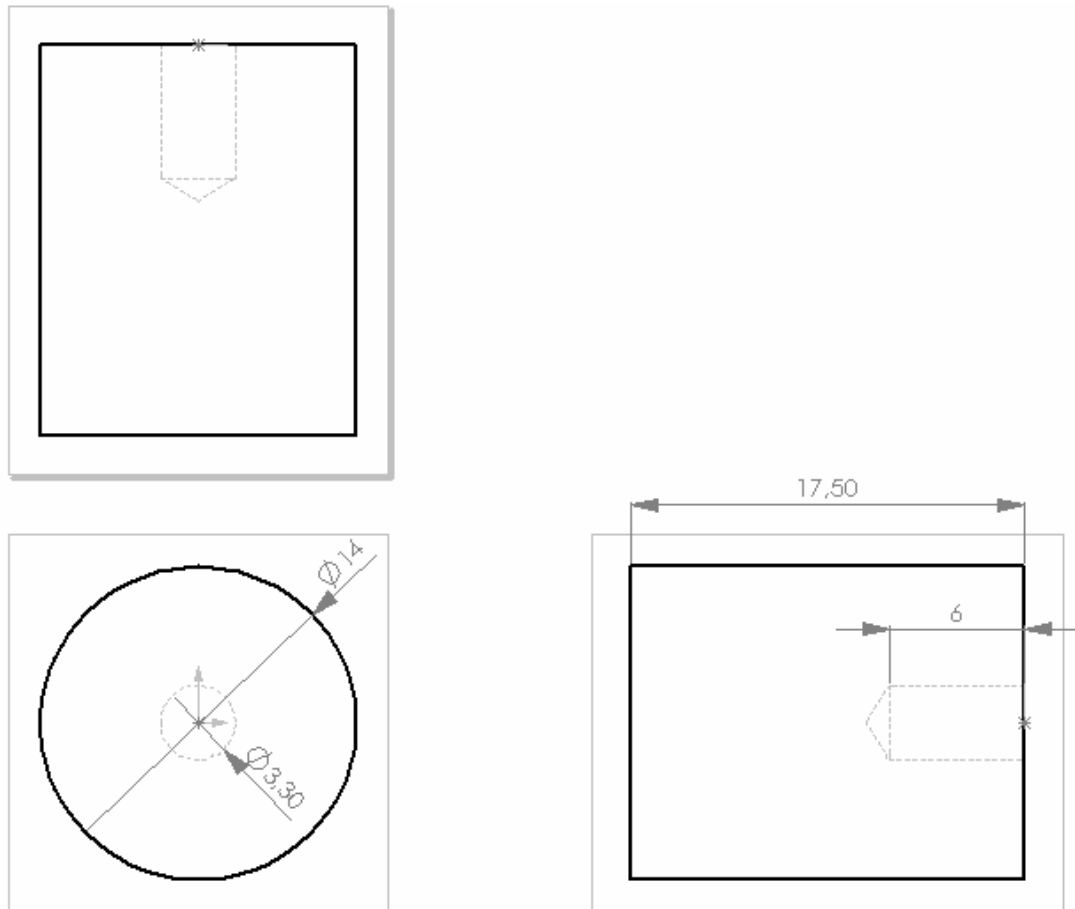


Figure 10.20. Orthographic projection of additional weight of the upper arm

The main body of the extensometer is shown in Figure 10.21 after the assembly without the secondary elements.

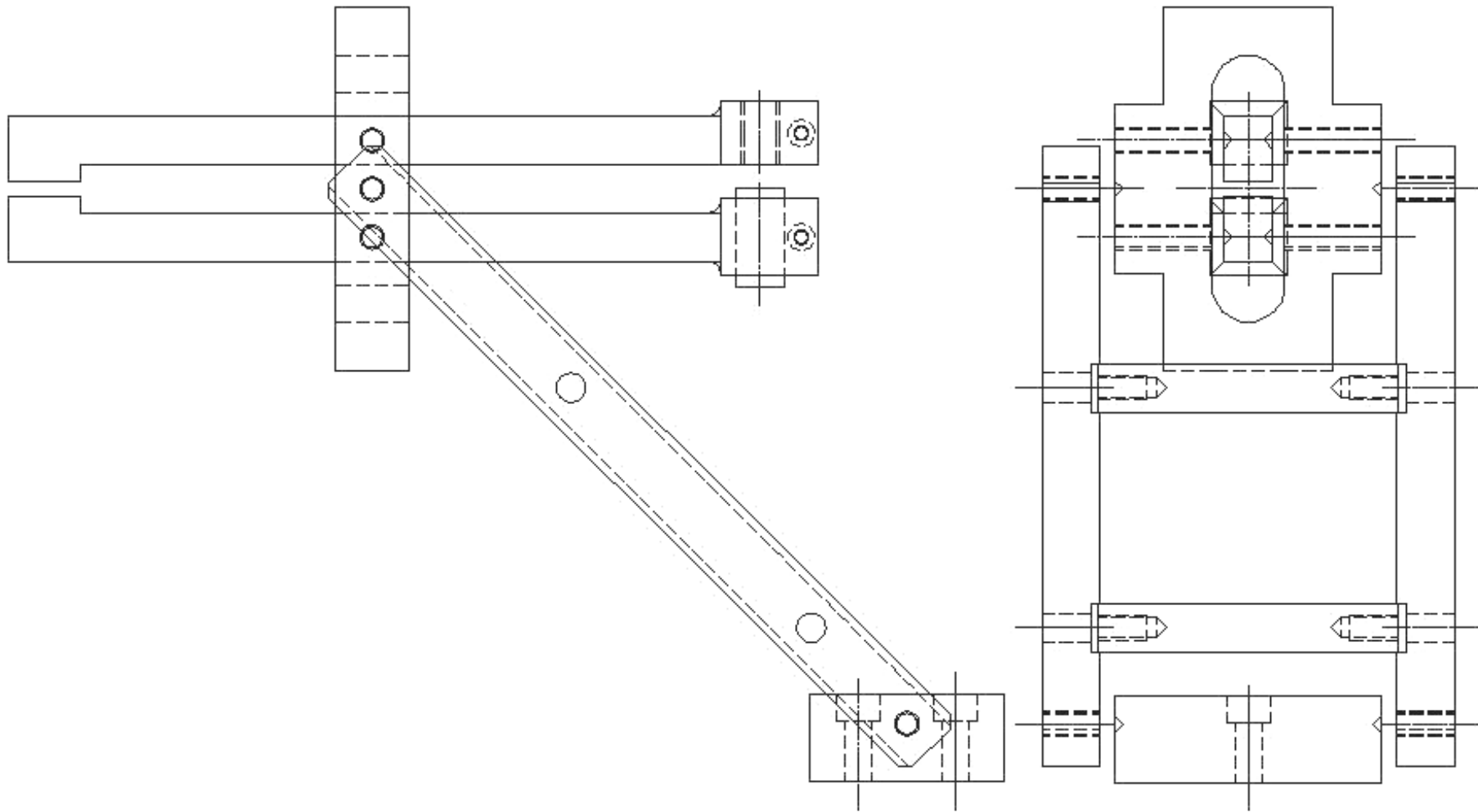


Figure 10.21. Assembly of the main extensometer body

11. FINAL DESIGN OF THE CALIBRATION UNIT

The calibration unit serves to

- carry the micrometer up and downwards,
- supply a base to hold the unit straight with the elevating system,
- fix the micrometer at a particular height,
- carry a rooted track for vertical linear motions
- have a specialty to let the unit come closer to or go further from the extensometer according to different purposes,
- prevent independent motions joining itself to the elevating system.

The calibration unit lets the user calibrate the extensometer as it is called and observe the performance of the system before a test with a specimen, by the help of reference lengths and displacements that are supplied by a micrometer on it.

The micrometer has got two jaws and each arm of the extensometer contacts with one jaw after a sufficient and convenient face to face placement of the whole system. Thus the extensometer measures the displacements and lengths which have been already known with the help of the micrometer to understand how reliable the measurement system is.

The calibration unit is a combination of a base plate that is joined to the lower base plate of the elevating system, a shaft to form a vertical track for the micrometer, a micrometer carrier and finally a micrometer, of course with several joining elements.

11.1. Base Plate

Base plate of the unit (Figure 11.1 and Figure 11.2) contains three holes on a line that the shaft is rooted and two bolt holes to join itself to the heavy lower base plate of the elevator.

The part has overall dimensions of 224.5x80x38 mm. The three shaft holes are 50 mm apart from each and have diametrical steps, 17 mm for shaft, 8.5 mm for M8 bolt and 14 mm for bolt head. The three holes are to change the place of the shaft, so the micrometer, forward and backward.

The section on which the two bolt holes available is thinner to get the plate from its one side on the lower base of the elevator and to use the M6 threaded holes on it in order to join the base plate of the calibration unit. Those two bolt holes are 60 mm apart from each. That makes it possible to use every threaded holes which are 20 mm apart from each and the edges.

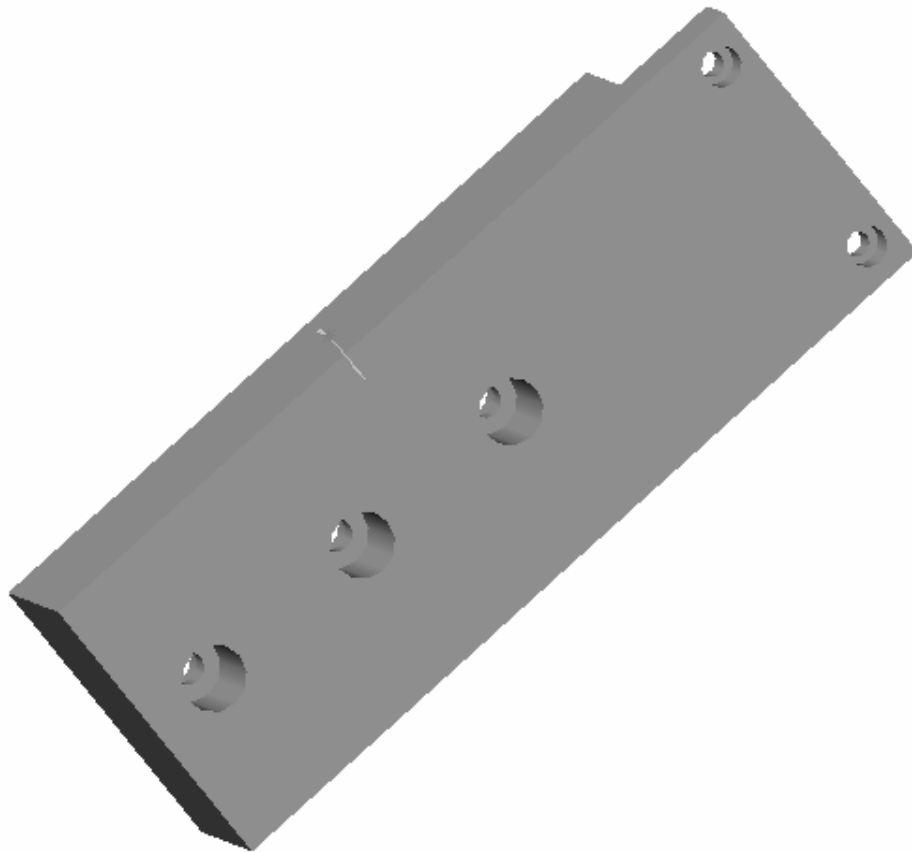


Figure 11.1. 3D view of the base plate

Part material is aluminum as usual. So that weight of the lower base plate, which is made of low carbon steel, supplies a sufficiently well and joinable base by itself.

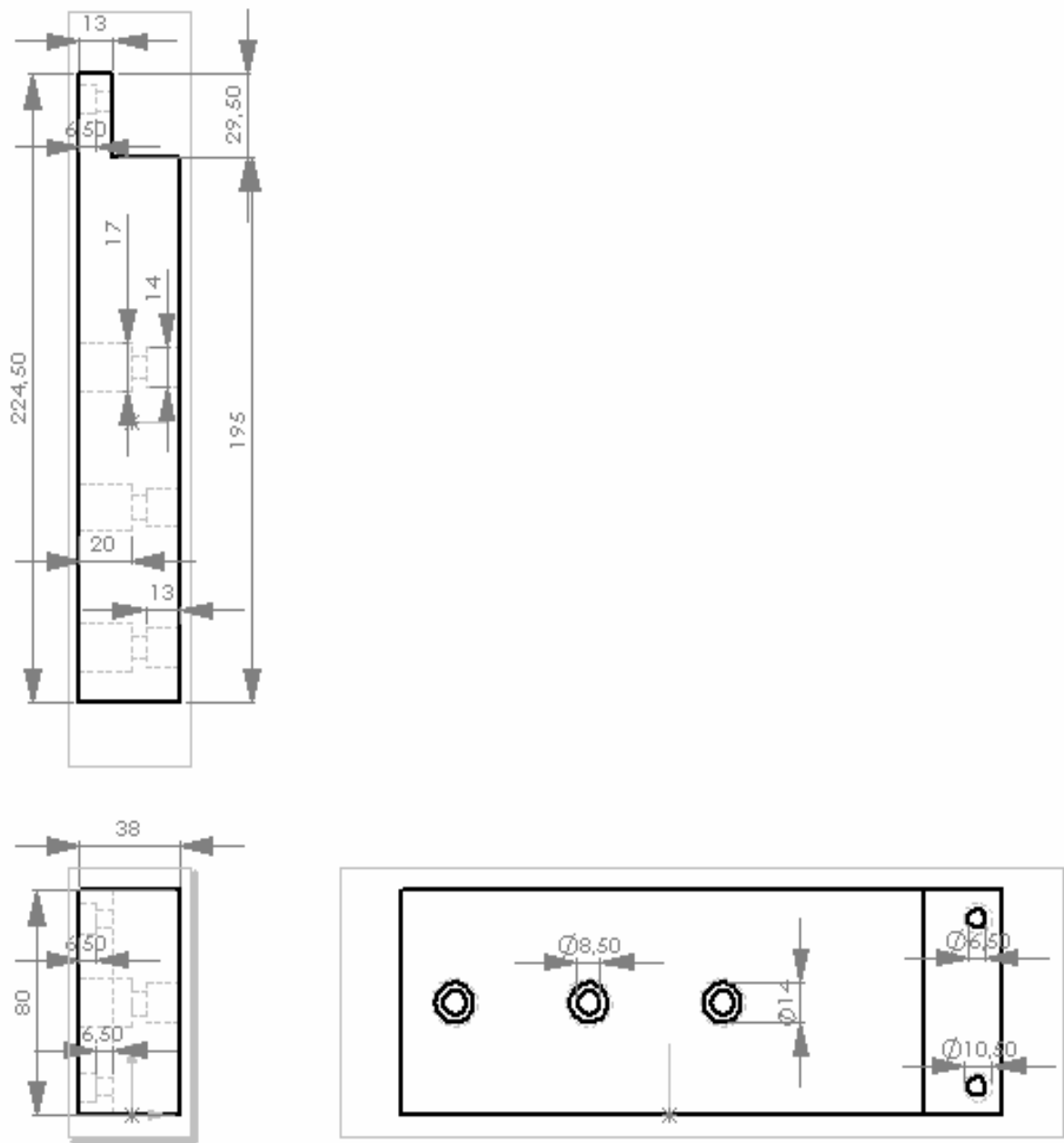


Figure 11.2. Orthographic projection of the base plate

11.2. Shaft

Shaft material is the same as the shafts in the elevating system, 1.2210 [115CrV3, K510 (Böhler)]. Another part, micrometer carrier, takes the micrometer up and down along this shaft. Shaft (Figure 11.3 and Figure 11.4) has a diametrical decrease by 3 mm at the bottom end with 15 mm length to be released inside the base plate of the unit.

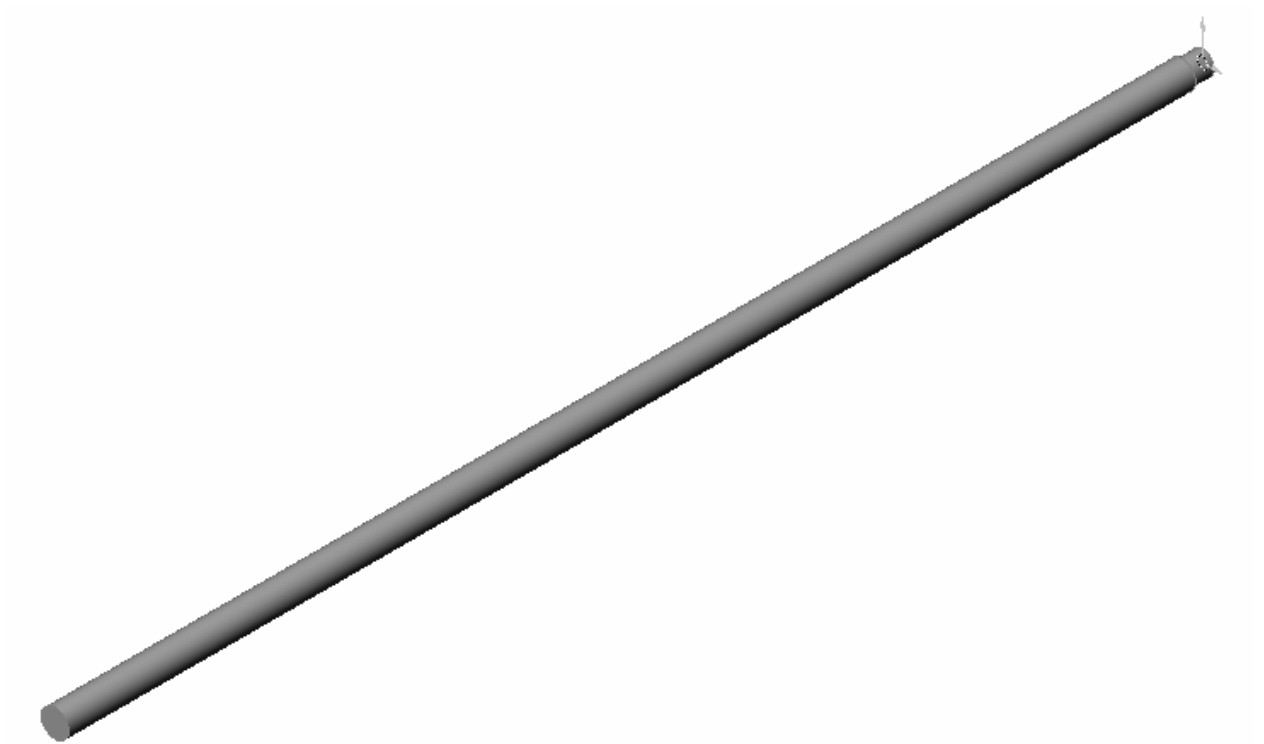


Figure 11.3. 3D view of the shaft

It has a bolt hole with M8 thread at its bottom to make the joining with the base plate. The overall dimension is D20x835 mm to reach to the same height with the other two shafts of the elevator.

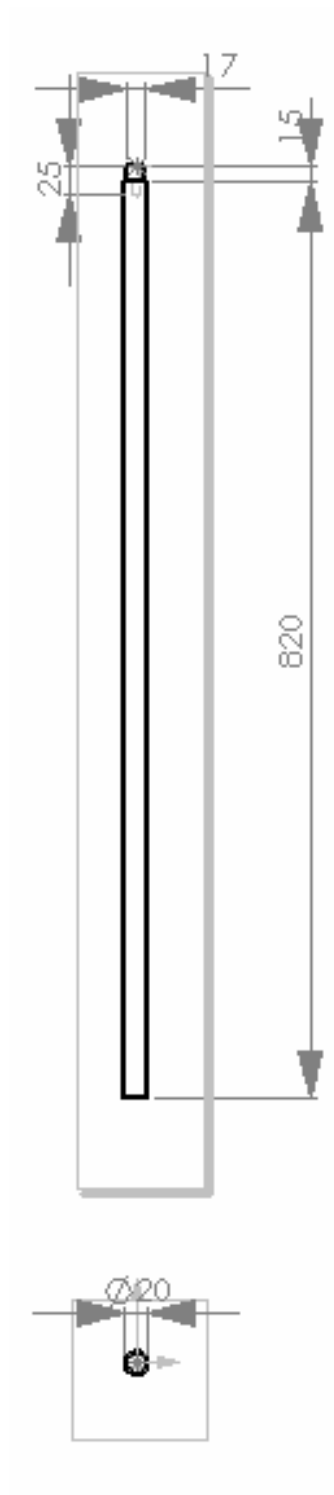


Figure 11.4. Orthographic projection of the shaft

11.3. Micrometer Carrier

The micrometer is mounted on this carrier shown in Figure 11.5 and Figure 11.6 and it takes the micrometer up and down along the shaft. It has two holes with M5 threads to join the micrometer by the use of its two holes. This is the female part of the shaft with its hole with a diameter of 20 mm. The slit at the rear end of this part is arranged to fix the micrometer with its carrier at a constant height by two M6 bolts. There are two holes with M6 threads at one side of the slit, and two holes for bolts which are sunken in the part with their heads at the other side.

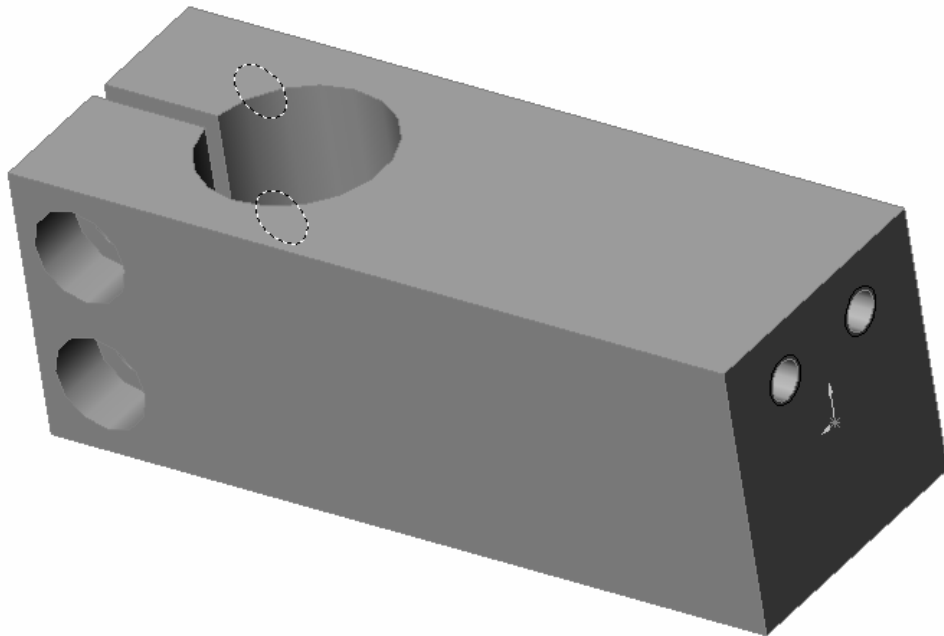


Figure 11.5. 3D view of micrometer carrier

Roughly the dimension of the part is 83x30x30 mm.

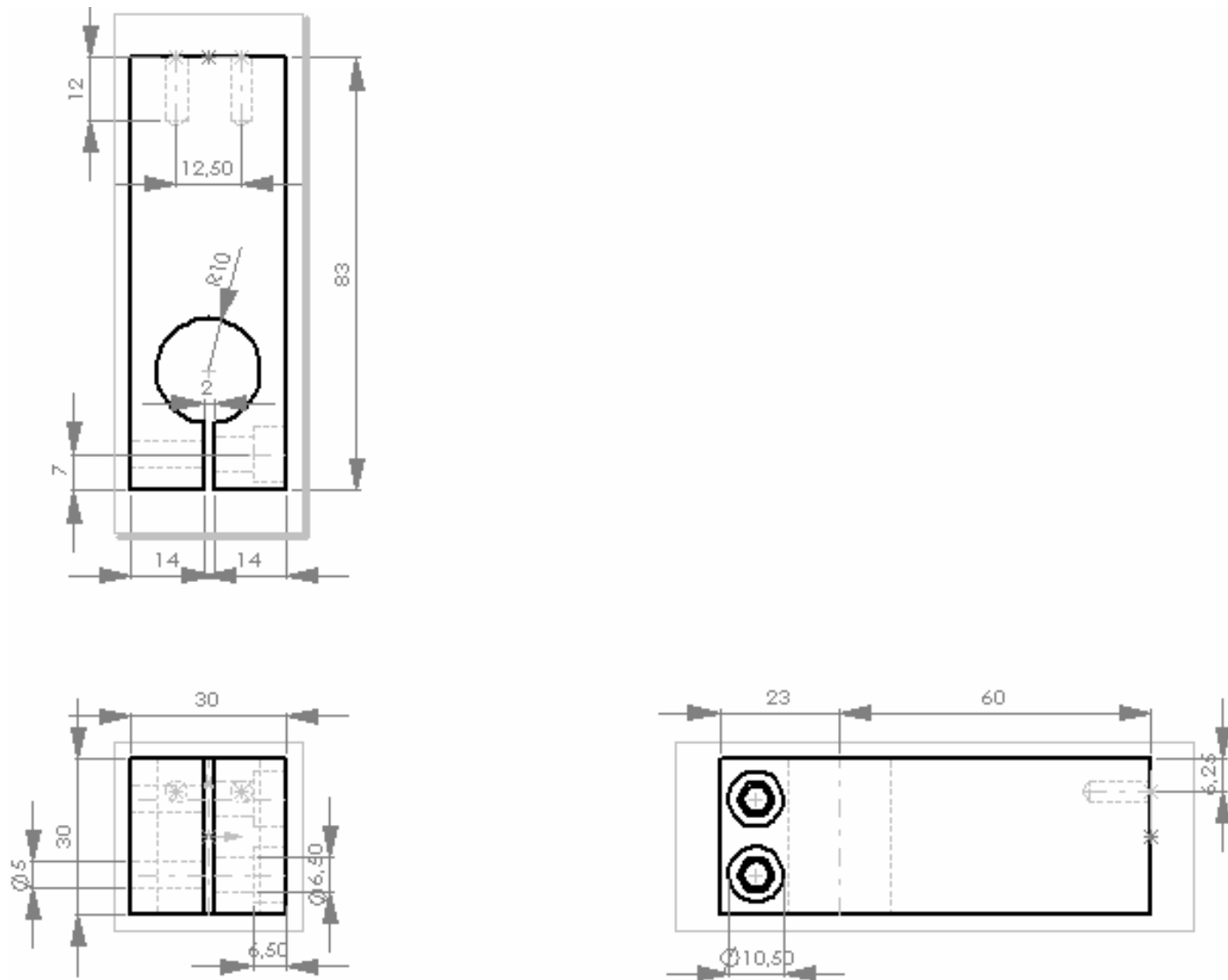


Figure 11.6. Orthographic projection of micrometer carrier

11.4. Micrometer

Micrometer, as shown in Figure 11.7, has got two jaws, one is stationary and the other is active and it moves. It has got a stroke range of 0.5 inch (12.7 mm). The necessary stroke range for a 10 mm gage length is ± 0.5 mm, as it is determined before. LVDT on the extensometer has got a nominal stroke range of ± 0.5 inch (± 1.27 mm). As a result, the micrometer is convenient and acceptable to use.

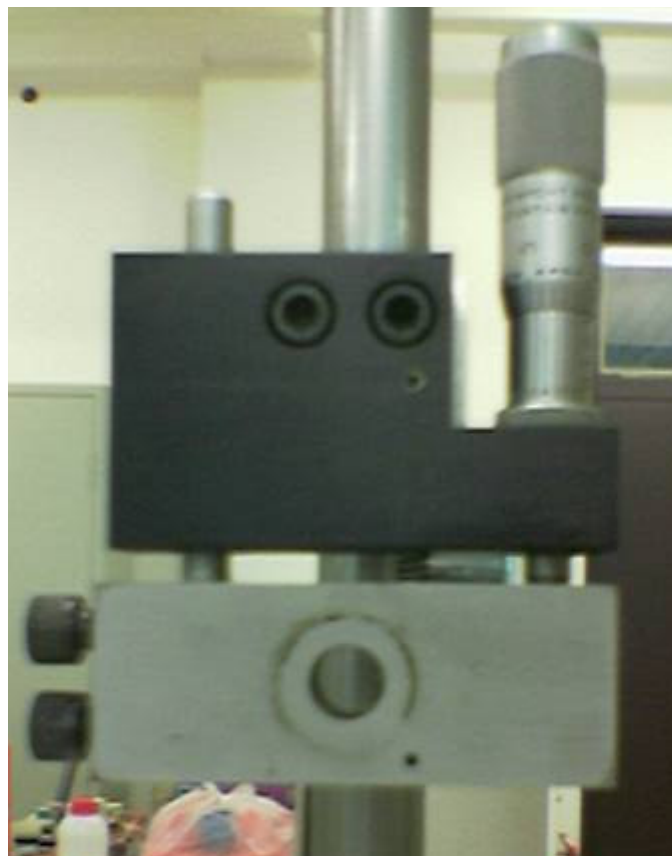


Figure 11.7. A photograph of the micrometer while it is on the shaft

Micrometer contains 5 divisions and 20 subdivisions which make a 0.005 inch (0.127 mm) unit displacement upwards and downwards within one division.

12. JOINING ELEMENTS

Three types of joining elements are used in the whole construction of the measuring system.

- 1) Bolts at different sizes (M8, M6, M5, M4)
- 2) Set-screws (M3, M4)
- 3) Spring Loaded Plungers (SLP with M5 thread size)

Six pieces of M8, four pieces of M6, six pieces of M5 and two pieces of M4 imbus bolts are used in the overall construction. Three pieces of M3 set-screws, two for contact elements and one for the core connecting rod, are available in the design. These are the most common elements.

The third joining element is a little bit more complex. A spring loaded plunger in Figure 12.1 consists of a sleeve, pin and a spring basically. They are categorized according to their pin or ball design, their spring force value, materials of the subparts and finally their sizes. In the extensometer design the essential thing is more about smooth and tangent pin tips and a harder spring, or in other words a spring with an increased force would be the best preference. The model with a longer pin length out of the sleeve with the smallest body size and a high force as much as possible are exactly the only necessities. From this point of view, the best choice was Fibro's spring plungers, which are reachable in Istanbul by the distributor, with spring loaded pin, M5 thread and increased spring force type.

It has burnished free-machining steel sleeve, hardened and burnished ball bearing steel pin, and a nirosta spring.

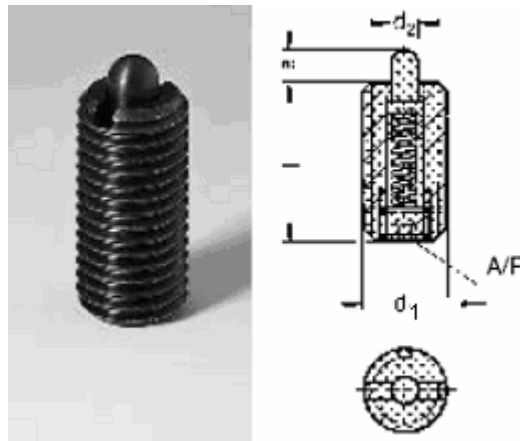


Figure 12.1. Spring Loaded Plunger (SLP) [26]

For the preferred model (2472.02.005), it has 11 to 40 N average spring force, 2.3 mm pin projection, 18 mm sleeve length and 2.4 mm pin diameter.

A suitable type of spring loaded plunger could not be found, because there is no production of it in Turkey, except a few at unfortunately not an ideal quality and type. However, they have quite weak springs. So the only way was to order 15 pieces of this product specially from Germany through the distributor in Turkey which did not have this product in its stocks.

13. MANUFACTURING

While the parts were being manufactured at the intended shape, several types of machining processes were applied on them. The intended manufacturing, more specifically the intended machining processes were made in the workshop at Boğaziçi University for the aluminum alloy parts and all small sized parts and applications. The two steel plates, the upper and lower base plates, were machined in an outer workshop in IMES (Figure 13.1 and Figure 13.2).



Figure 13.1. The lower base plate during milling process

Manufacturing of the whole construction started with the elevating system. This system is relatively much larger than the rest of the system. The starting points were the lower and the upper base plates. The appropriate materials were obtained with the marginal additions to all edges. All six surfaces which were rough and oxidized were milled gradually to achieve the final sizes. All other processes were made in the workshop at Boğaziçi University, except one about the contact elements. The lower base plate in Figure 13.3 and Figure 13.4 was later drilled by a milling machine and its 133 holes were threaded

by a tap at the appropriate length. The upper surface was then chamfered with a 2 mm depth at the edges.



Figure 13.2. The upper base plate during milling process for its lateral faces

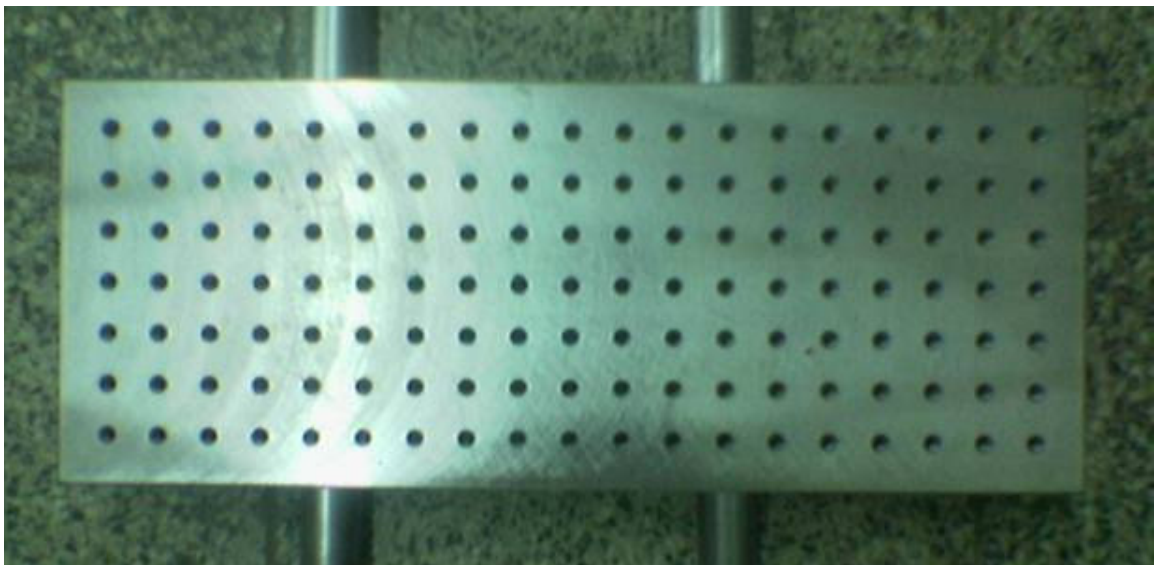


Figure 13.3. The lower base plate after drilling and tapping processes

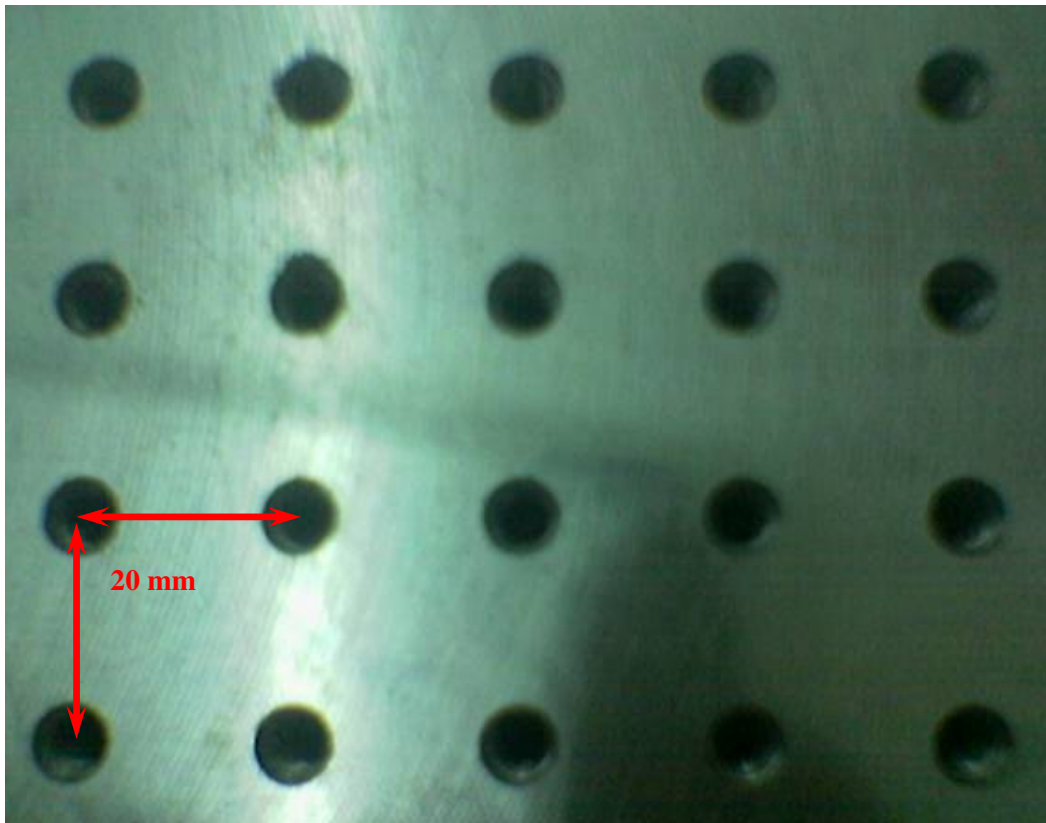


Figure 13.4. The distances between the threaded holes on the lower base plate

The upper base plate in Figure 13.5 includes four straight and two stepped holes without threads. These holes were prepared by the milling machine and then its upper surface was chamfered like the lower plate and it is observed the holes of the lower and the upper bases overlap serving the need.

Shafts were obtainable with a 1 m length for each of 1.2210 (Böhler K510) and first cut for its intended length, then machined to make a diametrical step as shown in Figure 13.6 and this was followed by drilling applications on the two tips of both shafts. These applications were made by lathe and the holes were tapped for M8 at an appropriate length.



Figure 13.5. The upper base plate after machining processes

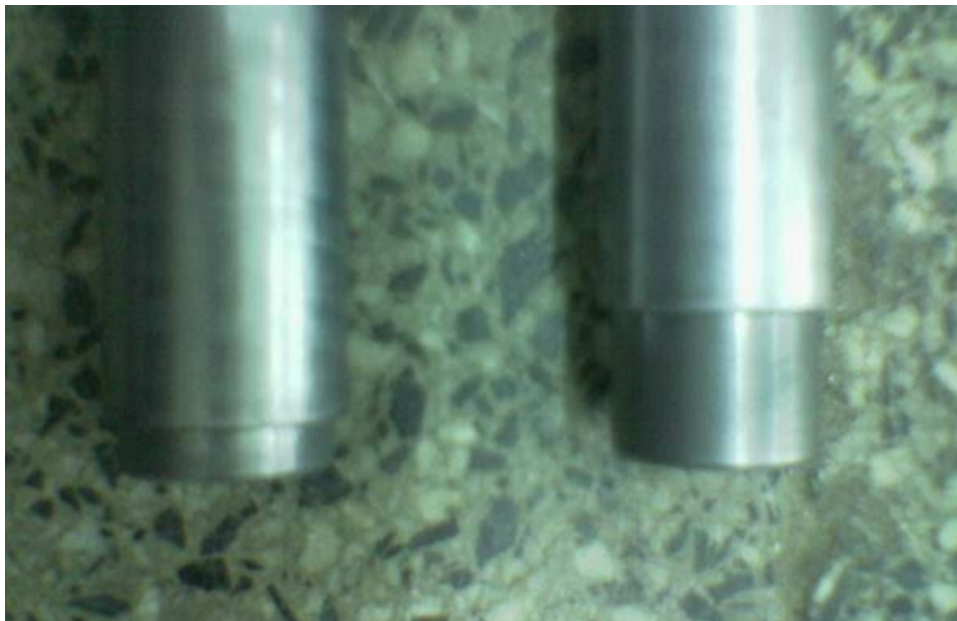


Figure 13.6. Shafts of the elevator

The following applications were on the moving plate as shown in Figure 13.7. Aluminum 7075 material was first machined with the milling machine and this went on

with the same machine to drill the two shaft holes, seven bolt holes and the slots near the shaft holes. Bolt holes were then tapped for M5 threads.

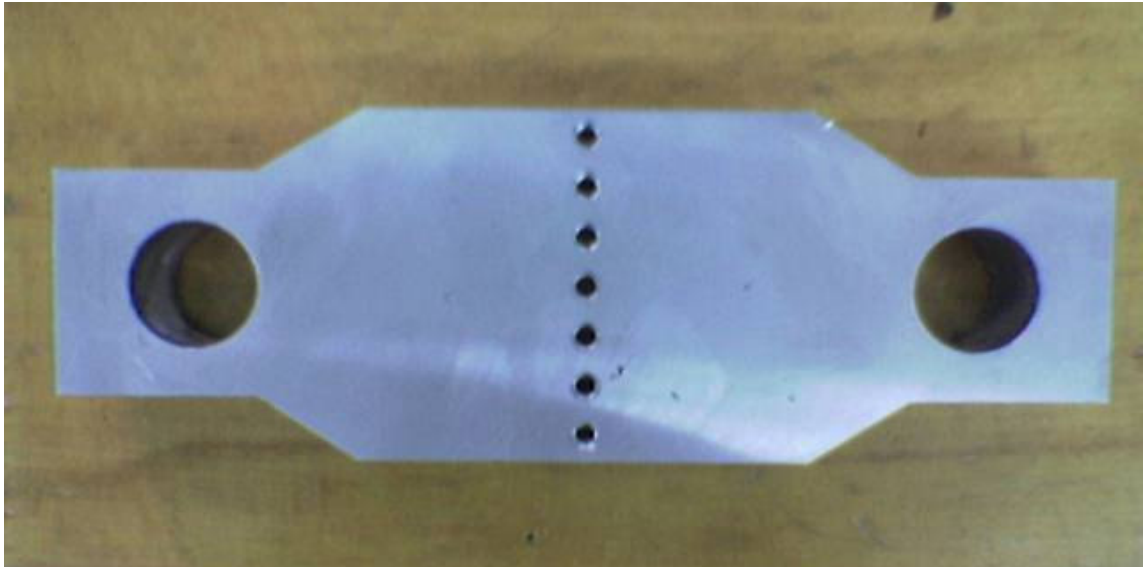


Figure 13.7. Moving plate before the slots are cut

The cap plate in Figure 13.8 is also aluminum 7075 and required milling and drilling processes by milling machine to make the material thin, narrow and to form the shaft and bolt holes respectively.



Figure 13.8. Cap plate

As a result of these processes, the elevating system in Figure 13.9 below was finished in order to make the joining of these parts.



Figure 13.9. Assembly of the elevating system

Extensometer construction started with the brackets in Figure 13.10. Rods with square section were cut, milled to give the final shape and to prepare the sockets for the supporting rods. Two M5 bolt holes without threads inside the sockets and two M5 threads were prepared for the spring loaded plungers by drilling on the milling machine and tapping.

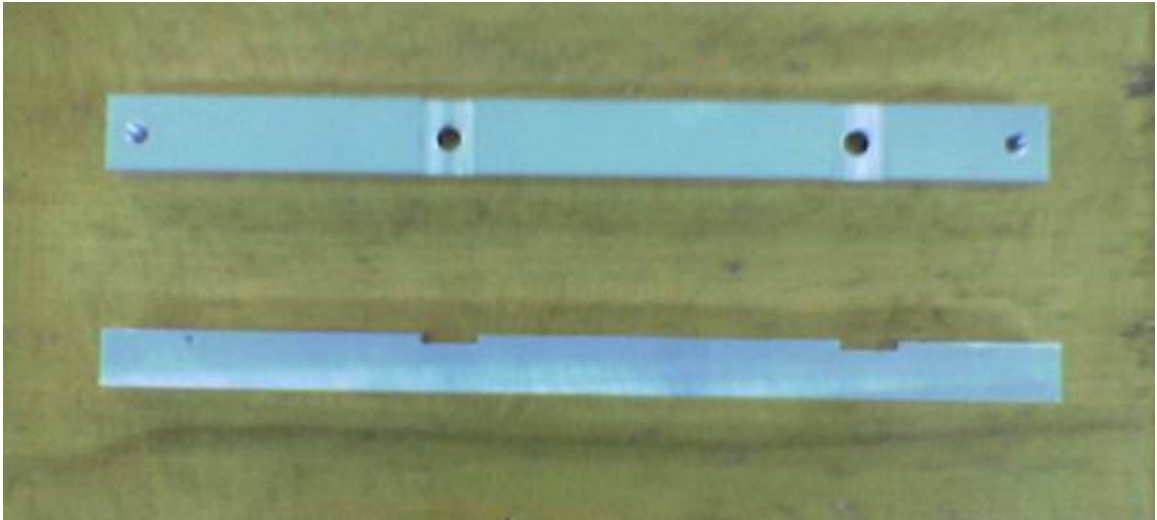


Figure 13.10. The brackets

After the brackets appeared, two supporting rods' machining took place (Figure 13.11). The only work to do was providing a rectangular sectional rod with the planned length. Milling machine made the whole work including the holes before tapping process for M5 threads.

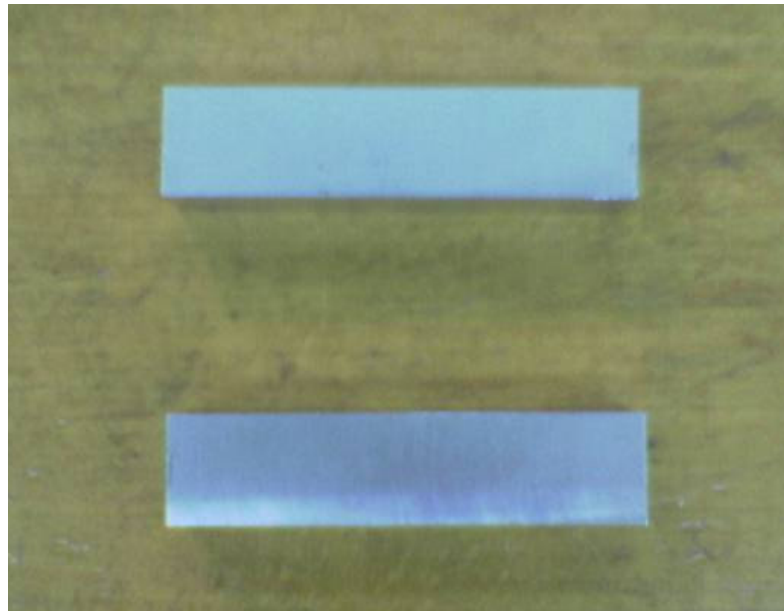


Figure 13.11. The supporting rods

Then it was the base plate's and the plus shaped chassis' turn which are at the same width. The base plate in Figure 13.12 was manufactured by milling and bolt hole drilling

and the chassis in Figure 13.13 required milling processes to form the desired central cavity and to get rid of the excess material on the corners. These followed by four M5 threads with the use of milling machine to drill the holes and tap for threads. Finally the outer edges were chamfered.

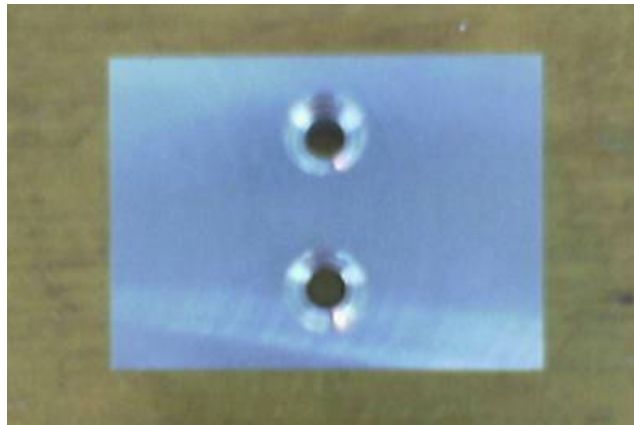


Figure 13.12. Base plate of the extensometer

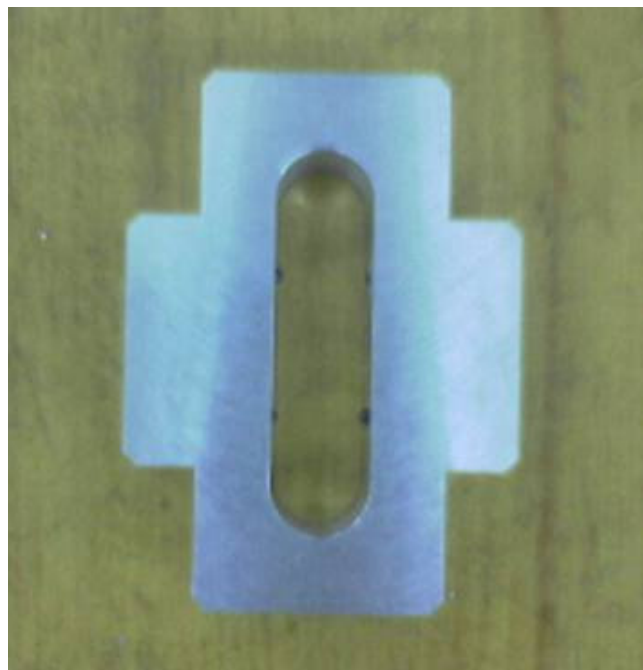


Figure 13.13. Chassis

The upper in Figure 13.14 and the lower arm in Figure 13.15 have the most complex structures for machining in the whole system. Because they consist of different three sections along the whole their lengths. That made the machining, milling, a bit difficult. The arms, its holes for the special bolt, LVDT body, contact elements and set screws were all prepared by the use of the milling machine. These followed by tapping for the set-screws with M3. Lathe made the thread for the special bolt with 0.75 mm pitch. Finally bolt holes were made; the slots and threads were cut.



Figure 13.14. Upper arm of the extensometer

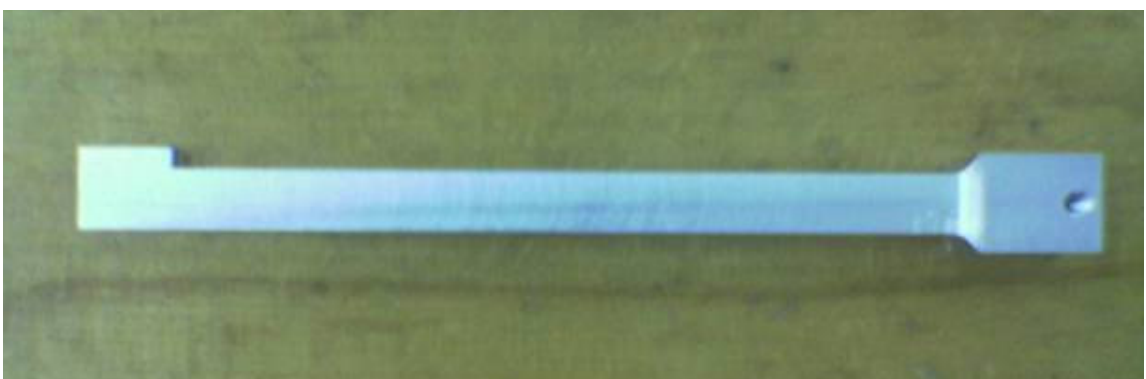


Figure 13.15. Lower arm of the extensometer

The contact elements in Figure 13.16 and Figure 13.17 are manufactured in an outer workshop by a pantograph machine to ensure the expected top angle and the concentric sharp point.

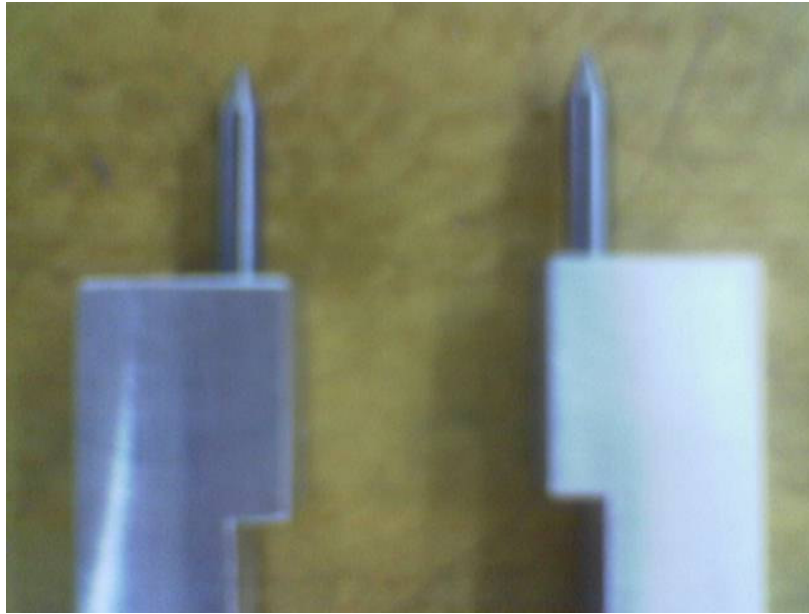


Figure 13.16. Arms tips after the contact elements are mounted

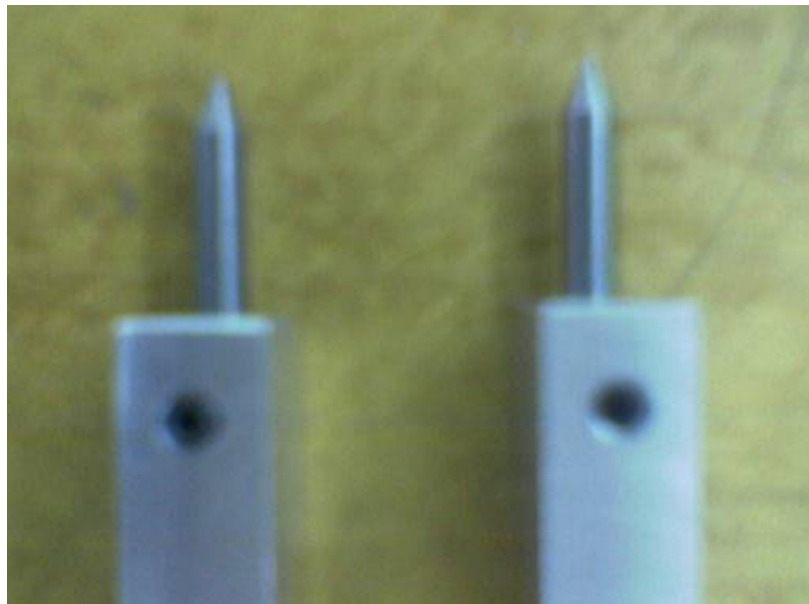


Figure 13.17. Contact elements are mounted by set-screws

The special bolt in Figure 13.18 with a scaled and nerved bolt head and a pitch of 0.75 mm was another part to be manufactured. The thread, the nerves and the hole of the connecting rod are made by the lathe. The scaled bolt head and the hole of the head were

made by the milling machine. A divisor coupled the milling machine during the drawing of the scale marks. Finally there was a tapping process for the set-screw.

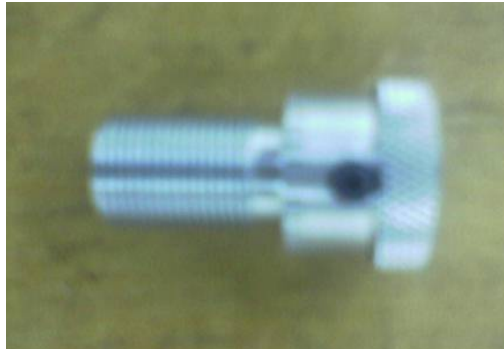


Figure 13.18. The special bolt

Another part is the core connecting rod, which was an accessory of the LVDT which was selected before. However, it could not be reached during the LVDT purchase. The necessity for the core is a non-ferromagnetic stainless steel which must have an austenitic structure [27]. So it must be a special stainless steel not to influence the LVDT signals. AISI 310 and 308 are the best solutions with low ferrite amounts. The problem was solved by an AISI 308 welding wire without clothing. M2 thread is cut by an appropriate die-stock.

The final parts for construction of the extensometer are additional weights which are made of brass. Cylindrical weights were arranged in a manner that they would not effect the esthetics of the system and the view of the gage area of a specimen in a bad way. The intended lengths for the two weights were manufactured by cutting a rod with a diameter of 14 mm. A drilling and tapping process followed that for each to join them to lower and upper arms by set-screws.

Thus, all parts of the extensometer were ready for joining. The brackets, two supporting rods and four SLPs were the first (Figure 13.19 and Figure 13.20), and then base plate, arms, and the additional weights were the second group to come together. After all those processes the overall construction of the extensometer as shown in Figure 13.21 and its elevating system were finished.

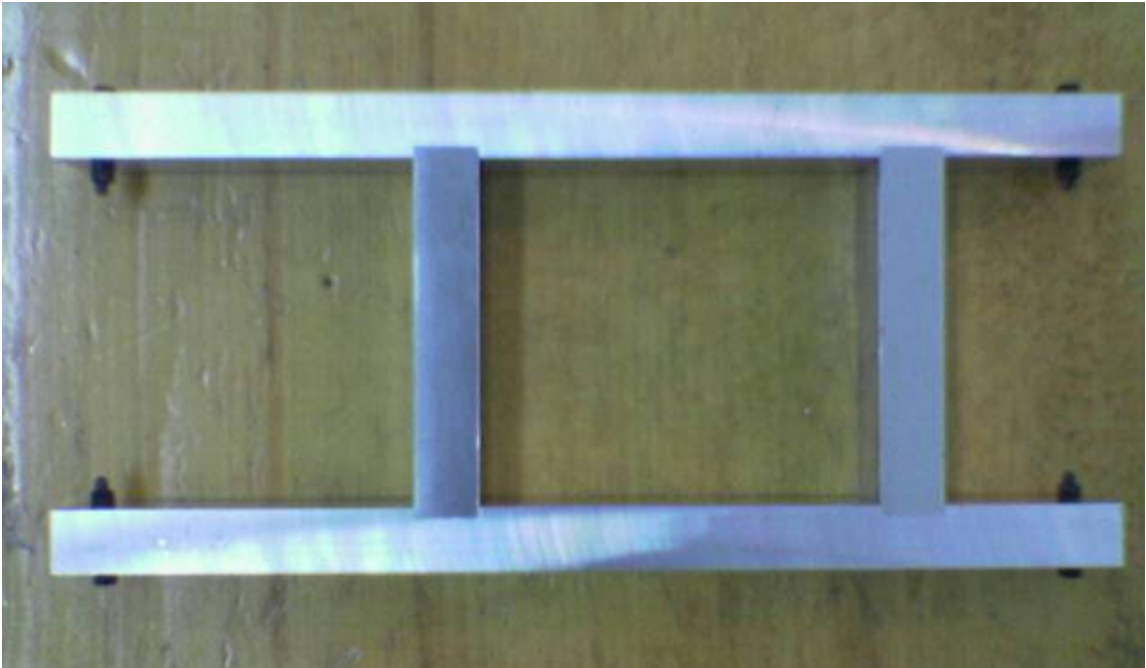


Figure 13.19. Assembly of brackets, rods and SLPs



Figure 13.20. Bracket tips after the assembly

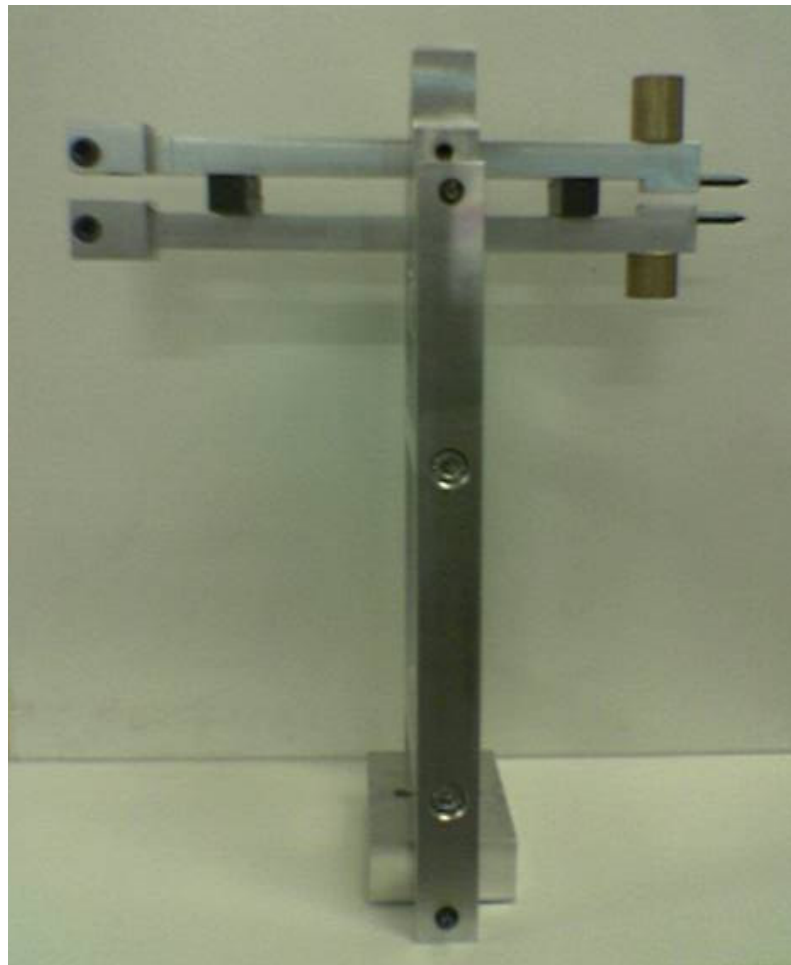


Figure 13.21. The finalized extensometer without LVDT

Manufacturing of the calibration unit started with its base plate which has three stepped holes without threads and two straight holes. Milling process for all surfaces to achieve the final sizes was followed by drilling of those holes.

Shaft was obtainable with 1000 mm length and first cut for the intended length, machined to make a diametrical step and drilled on its one tip by lathe and the holes were tapped for M8.

Finally aluminum 7075 material of the micrometer carrier was machined and drilled for one shaft hole, four bolt holes and the slot near the shaft hole by milling machine. Then necessary tapping processes were performed for those bolt holes.

Then they are assembled as seen in Figure 13.22 to finalize the whole manufacturing steps.



Figure 13.22. The calibration unit

14. ELECTRONIC INSTALLATION

Electronic equipment of this measurement system consists of;

- LVDT
- Signal conditioner board and
- Power supply

Information about the LVDT model used at this extensometer in Figure 14.1 was given in the previous sections of the thesis. However there are other specifications which essential for the relation with the signal conditioner board. First of all, excitation frequency alternatives are from 2 to 20 kHz. But 10 kHz is the recommended frequency. Nominal input voltage is 3 V rms. Sensitivity is 3.15 mV/V/0.001 in (124 mV/V/mm) [25].

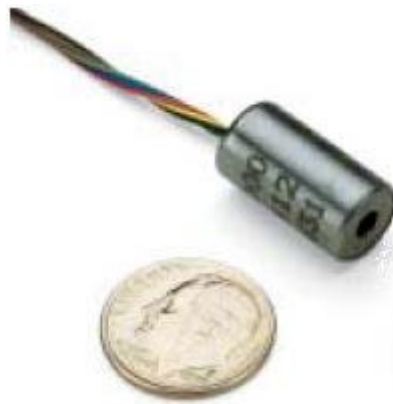


Figure 14.1. LVDT of the extensometer [25]

There are six related cables about the connection with the signal conditioner which are shown in Figure 14.2 and these are yellow and brown for primary winding and black-green and blue-red for secondary windings. Green and blue cables are connected to each other for differential output.

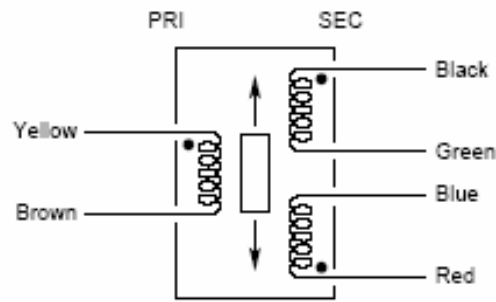


Figure 14.2. Wiring of the LVDT [25]

LVDT is Schaevitz's MHR series 050 model and the conditioner module is LVM-110, which is a compatible one, is shown in Figure 14.3 and Figure 14.4. Selectable excitations are 2.5, 5 and 10 kHz [25]. This DC powered voltage module has a 10 point screw terminal connector. The correct connections between the signal conditioner and LVDT, power supply are shown in the Figure 14.5. It has got two threaded stand-offs for mounting. A box at a suitable dimension is used to mount the board and to fit the cables inside. There are many switches which set the conditioner according to its mate, the LVDT.

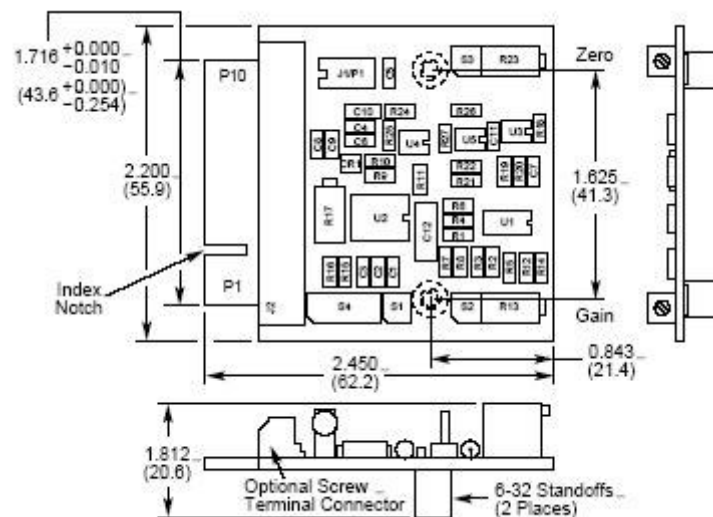


Figure 14.3. Views and dimensions of the module [25]



Figure 14.4. Signal conditioner module [25]

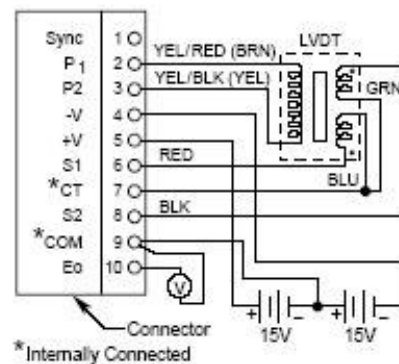


Figure 14.5. Wiring between LVDT, signal conditioner module and power supply [28]

In this set-up procedure, the recommended frequency for the LVDT, 10 kHz, is used. This means that the switches S1-C and S1-D are on. This is the operating frequency step. Since the system uses only one LVDT, this type of mode is the master mode which means that S1-B switch is on. Another step is setting the amplifier gain [28]. Full scale output of the LVDT is needed and the formula is;

$$\text{LVDT Full Scale Output} = \text{LVDT Sensitivity} \times \text{Excitation Voltage} \times \text{Full Scale Displacement} \quad (14.1)$$

According to the product manual [28],

$$3.15 \text{ (mV)} \times 3 \text{ (V rms)} \times 50 \text{ (thousandths)} = 472.5 \text{ mV full scale output}$$

Since the calibration process is for ± 10 VDC; X2, LOW is the most appropriate selection which means that S2-A is off, S2-B and S1-A are on.

Signal conditioner's output voltage is ± 10 VDC and it requires a ± 15 VDC input and a switching supply in Figure 14.6 is working in this group of equipments.



Figure 14.6. Switching power supply in the design

Another requirement is that since the extensometer could work at more than 300 mm height from base, the length of the LVDT cables would not be enough, this means that cable addition is strongly needed. So a terminal connector was used to increase the cable lengths between LVDT and conditioner module and it was hung on the lateral face of the moving plate of the elevator.

After the installation step is completed, it was time to calibrate the extensometer. This was not a part of the thesis work. However the procedure is listed below step by step [28];

- Disconnect black LVDT cable (S-2/terminal 8).
- Connect a shorting jumper between terminals 6 and 8.

- Adjust the potentiometer zero for 0 V output using terminals 9 and 10.
- Disconnect and remove the shorting jumper and connect black wire to terminal 8.
- Move the core to approximately the best center position of the coil, using the voltmeter, this point is the sensor null.
- Adjust out any remaining output signal using the zero potentiometer.
- Move the core in positive direction using the micrometer to the full scale displacement (+0.05 inches for the installed LVDT).
- Adjust the gain potentiometer for +10 VDC output between terminals 9 and 10.
- Turn back to zero position again to check zero voltage, and then move the core to minus full scale displacement to get -10 VDC output voltage.

After the entire manufacturing processes of the extensometer, elevating system and the calibration unit, and then the installation of the electronics were brought to an end, the whole measurement system which is represented in Figure 14.7 and Figure 14.8 was prepared for a test procedure to control it.

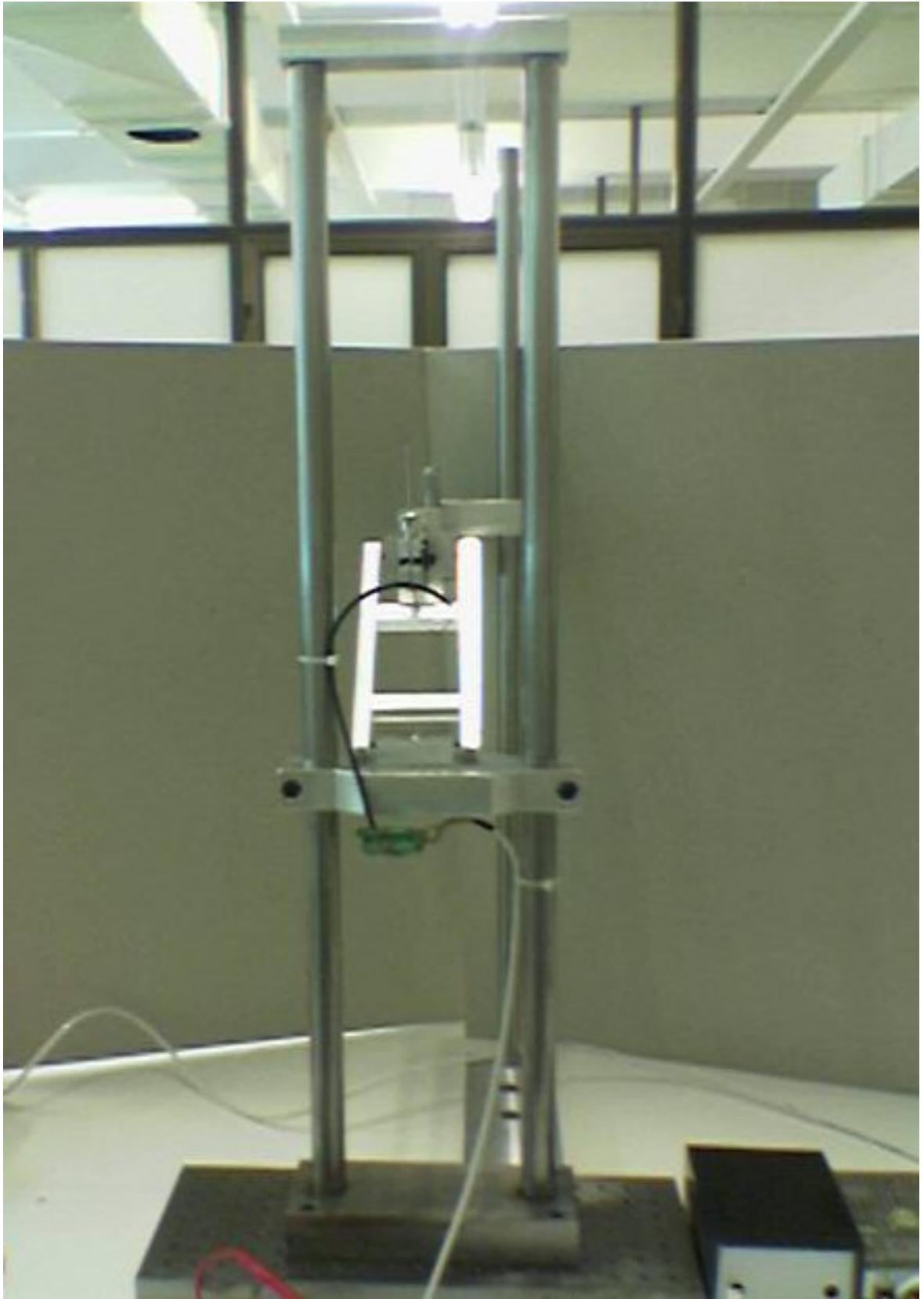


Figure 14.7. A photograph of the system from behind



Figure 14.8. A photograph of the system from left side

15. CONCLUSION

After every steps of the entire design period were completed, the extensometer within the measurement system must be examined and observed if it could meet the needs to make a displacement measurement. First of all, there were requirements which were taken into consideration before and during the design period. Basic but essential characteristics were the gage length and contact force of the extensometer.

Following the set-up of the whole system including the calibration unit, the front and rear ends of the extensometer were measured to control the distances between the arms and particularly the gage length. Exact dimensions are confirmed. It was detected that a precise 10 mm of gage length and a correct arm couple was obtained.

Contact force calculations were made in the previous chapters of the thesis. But that time it must be examined practically. The calibration unit was once more on the job. The arms through contact elements were leant against the micrometer jaws and it is essentially expected to see the following ability of the extensometer without slipping and it has passed and about 45° of inclination angles are detected to be ideally appropriate.

LVDT is mounted on the lower arm and the core with its connecting rod on the upper arm. The target was to see and feel the clearance within the necessary and evident range since the beginning of the study. All those were the controls and tests before the electronic side was switched on.

On the other hand, the results of inspections while the electronic system was featuring were positive as well. That is, zero voltage at the null point which is the initial positioning, negative and positive voltage results at equal absolute values as a result of negative and positive displacements at equal absolute values were observed with the help of a voltmeter.

As a result, a mechanical extensometer is designed and manufactured at a greatly lower price (approximately 1,100 YTL. without labor costs) including the electronic equipment compared with a standard commercially used strain-gaged extensometer at the same specialties but excluding the signal conditioning units, shipping costs, duties and taxes etc.

This extensometer and the measurement system are presently conformable to aluminum center-cracked tension specimens. But further, a wide variety of gage lengths is possible only by changing the arms making it multipurpose, probably in some cases without changing the sensor type or size and this makes it potentially functional and valuable in a broad range of materials testing.

Moreover, a target measurement set-up with a tripled extensometer or more measuring displacements from three or more different regions at the same time in a row could be designed and manufactured as a future work by achieving same number of LVDTs which is illustrated in Figure 15.1.

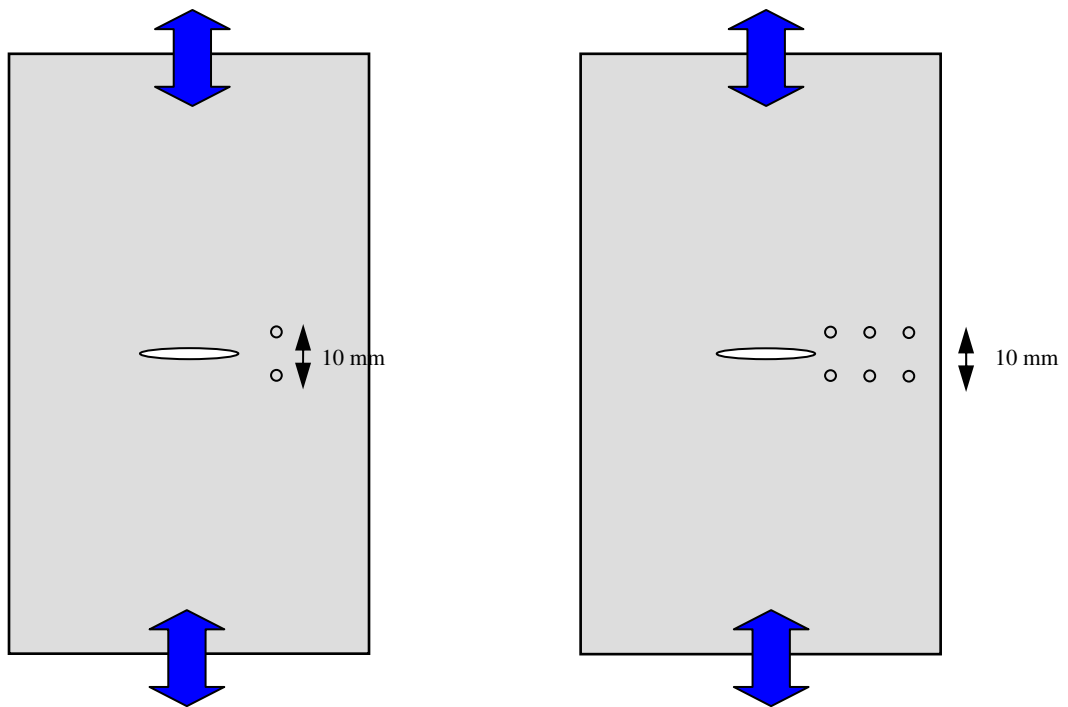


Figure 15.1. Possible gage points of the presently designed extensometer and a probable target extensometer design

REFERENCES

1. Lynch, C. S., "Strain Measurement", *The Measurement, Instrumentation, and Sensors Handbook*, 22, 6-73 CRC Press LLC, 1999.
2. Liu, K. C. and J. L. Ding, "A Mechanical Extensometer for High Temperature Tensile Testing of Ceramics", *Journal of Testing and Evaluation*, JTEVA, Vol. 21, No. 5, pp. 406-413, September 1993.
3. *EnduraTEC Ext-3542 Product Manual*.
4. Lucas, G. F. and P. C. McKeighan, Ransom J. S., *Nontraditional Methods of Sensing Stress, Strain and Damage in Materials and Structures*, West Conshohocken, PA: ASTM, 2001.
5. Zenxiang, F., S. Jize and W. Shichun, "A Theoretical Study Of The Optimum Linearity Conditions of The Structure of An Axial Extensometer", *Journal of Materials Processing Technology*, 69, pp. 152-154, 1997.
6. Barbiery, M. and A. Corvi, "An Extensometer for Fracture Mechanics Testing of Thin Composite Laminates", *Engineering Fracture Mechanics*, Vol. 30, No. 1, pp. 1-4, 1988.
7. Watson, R. B., "Calibration Techniques for Extensometry: Possible Standards of Strain Measurement", *Journal of Testing and Evaluation*, JTEVA, Vol. 21, No. 6, pp. 515-521, November 1993.
8. Liu, K. C., H. Pih and D. W. Voorhes, "Uniaxial Tensile Measurement for Ceramic Testing at Elevated Temperatures: Requirements, Problems, and Solutions", *Int. J. High Technology Ceramics*, 4, pp. 161-179, 1998.

9. Motoie, K., M. Sakane and J. Schmidt, “An Extensometer for Axial Strain Measurement at High Temperature”, *Mechanics of Materials* 2, pp. 179-182, 1983.
10. Raske, D. T. and W. F. Burke, “An Extensometer for Low-Cycle Fatigue Tests on Anisotropic Materials at elevated temperatures”, *J. Phys. E: Sci. Instrum.*, Vol. 12, Great Britain, 1979.
11. Boyd, S., N. Shrive, G. Wohl, R. Müller, R. Zernicke, “Measurement of Cancellous Bone Strain During Mechanical Tests Using A New Extensometer Device”, *Medical Engineering & Physics* 23, pp. 411-416, 2001.
12. Perusek, G. P., B. L. Davis, J. J. Sferra, A. C. Courtney and S. E. D’Andrea, “An Extensometer for Global Measurement of Bone Strain Suitable for Use in Vivo in Humans”, *Journal of Biomechanics* 34, pp. 385-391, 2001.
13. Vial, G., “Automatic Extensometers”, *Shimadzu Tech Spotlight-Advanced Materials and Processes*, September 2005.
14. *MTS Extensometer Catalogue*, 7/1995.
15. Albright, F. J. and J. Annala, “Practical Aspects of Dynamic Verification of Extensometers”, *Journal of Testing and Evaluation*, JTEVA, Vol. 22, No. 1, pp. 53-62, January 1994.
16. Eren, H., “Displacement Measurement”, *The Measurement, Instrumentation, and Sensors Handbook*, 6, 6-73 CRC Press LLC, 1999.
17. Dally, J. and W. Riley, *Experimental Stress Analysis*, Mc Graw - Hill, New York, 1991.
18. Norton, H. N., *Handbook of Transducers*, Englewood Cliffs, NJ: Prentice Hall, 1989.

19. *Proximity Sensor Lineup*, Automation Direct – Sensors Overview, 16, <http://www.automationdirect.com/proximity>, 2005.
20. Kinloch, C. D. and N. E. Waters, “Extensometer for Semi-rigid Materials”, *Journal of Scientific Instruments*, Vol. 37, pp. 93-95, 1960.
21. Churchill, J., *Accurately Measuring Ultraslow Motion*, 2006.
22. *LVDT Basics*, Macro Sensors Technical Bulletin, 01, 2003.
23. Cobbold, R. S. C., *Transducers for Biomedical Measurements: Principles and Applications*, 6, pp. 132-137, Wiley, New York, 1974.
24. *Solartron Metrology LVDT Catalogue*, <http://www.solartronmetrology.com>, 2005.
25. *Schaevitz Sensors Product Catalogue*, <http://www.schaevitz.com>, 2006.
26. *Fibro Product Catalogue*, 2006.
27. Shackelford, J. F., *Introduction to Materials Science for Engineers*, 4th SI ed., Prentice Hall International Inc., London, 1998.
28. *Schaevitz Sensors LVM-110 Product Manual*